T 388

Studies on ASE, Lasing and NLO characteristics In Certain Laser Dyes

Sr.Ritty J.Nedumpara

International School of Photonics
Cochin University of Science and Technology
Cochin – 682 022, India

Ph D Thesis submitted to
Cochin University of Science and Technology
In partial fulfillment of the requirements for the
Degree of Doctor of Philosophy

February 2007

T388

Studies on ASE, Lasing and NLO characteristics in Certain Laser Dyes

Ph D Thesis in the field of Photonics

Author
Sr.Ritty J.Nedumpara
Research Fellow
International School of Photonics
Cochin University of Science & Technology
Cochin – 682 022, India
Email : rittynedumpara@yahoo.com; rtnedumpara@cusat.ac.in

Research Supervisor
Dr. P Radhakrishnan
Professor, International School of Photonics
Cochin University of Science & Technology
Cochin – 682 022, India
Email : radhak@cusat.ac.in

International School of Photonics,
Cochin University of Science & Technology
Cochin – 682 022, INDIA

www.photonics.cusat.edu

February 2007

Front cover: Laser emission from C 540 dye doped polymer film
Back Cover: Laser emission from C 540 dye solution with well resolved equally spaced resonant modes

CERTIFICATE

Certified that the research work presented in the thesis entitled "***Studies on ASE, Lasing and NLO Characteristics in Certain Laser Dyes***" is based on the original work done by **Sr.Ritty J. Nedumpara** under my guidance and supervision at the International School of Photonics, Cochin University of Science and Technology, Cochin – 22, India and has not been included in any other thesis submitted previously for the award of any degree.

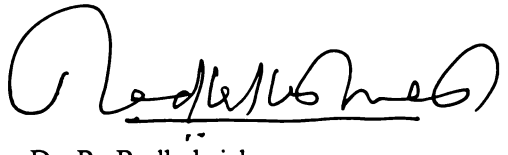

Cochin 682 022
February 14, 2007

Dr. P Radhakrishnan
(Supervising Guide)

DECLARATION

Certified that the work presented in the thesis entitled "***Studies on ASE, Lasing and NLO Characteristics in Certain Laser Dyes***" is based on the original work done by me under the guidance and supervision of Dr. P Radhakrishnan, Professor, International School of Photonics, Cochin University of Science and Technology, Cochin – 22, India and it has not been included in any other thesis submitted previously for the award of any degree.

Cochin 682 022
February 14, 2007

Sr.Ritty J.Nedumpara

Preface

The invention of lasers in 1960 marked the beginning of a new era in the fields of science and technology. Within very few years, lasers have proved their immense potential and possibilities in almost all areas of science like Physics, Chemistry, Biology, Medicine, Geology and Space Science. The advancements triggered by lasers are also remarkable in areas like communication, information technology, industry and other entertainment and consumer devices which we encounter in our day to day life.

In the search for efficient laser gain media to meet the enormous requirements of the different fields, the organic dyes came to the forefront with their ability to emit coherent radiations in a wide spectral range. With the availability of good number of organic dyes, laser emission can be tuned from near UV to near IR regions. These highly tunable sources emit radiations in a variety of regimes: from femtosecond pulses to continuous wave oscillations and from high energy pulses to high average powers. In the generation of high energy and high average powers in the visible region, the dye lasers are unparalleled. This great functional ability makes them quite attractive among laser sources. In addition to tunability and versatility, with their unique level of high performance, the dye lasers have made enormous impact in the fields of science, technology and industry.

Development of solid state dye lasers which could solve the different functional problems faced by the conventional liquid dye lasers gave a new thrust in the field of dye lasers. Intense research is going on for the effective incorporation of dye molecules into solid matrices with different host materials to get a gain medium of high optical quality and photostability. Over the years, a good number of materials have been tried as solid hosts for organic dyes and among them inorganic glasses, organically modified glasses and transparent polymers were found to be promising materials. Development of several novel organic compounds and

their derivatives which can be tailored according to the applications makes the research on dye lasers still growing.

Fluorescent dyes and fluorescence spectroscopy are attracting much interest in the areas of research and development in basic and applied sciences like molecular biology, biochemistry, genomics, bioengineering, medical diagnosis and industrial microbiology. Fluorescent based techniques are now widely used to address the fundamental and applied questions in the biological and biomedical sciences. Extreme selectivity of fluorescent labels that can target specific organisms opens new methods to resolve industrially and medically relevant problems in areas such as public health, safety of foods and environment monitoring.

Nonlinear optical characterization of organic dyes is another area which currently draws the attention of many research groups due to its widespread applications. There are different mechanisms such as two photon absorption, reverse saturable absorption and nonlinear refraction observed in organic dyes which could lead to optical limiting behaviour. On the other hand saturable absorption exhibited by dyes can have application in passive Q switching or mode locking of lasers.

The proposed thesis presents the details of the characterization studies conducted in certain laser dyes, mainly focusing on Coumarin 540, covering the different areas of applications. The thesis is organized into seven chapters.

Chapter 1: An overview of the recent developments in laser dyes and its applications is discussed in Chapter 1.A brief historical background of dye lasers and the developments in areas like pulsed dye lasers, continuous dye lasers and ultrashort dye lasers are described. The recent development of dye lasers in solid state matrix form, the dye doped waveguides, optical amplifiers and lasers for telecommunication applications and integrated optics, and the microcavity dye lasers which can be integrated with the lab-on-a chip microsystems are also briefly discussed. The importance of fluorescence studies in different biological and

related fields and the nonlinear characterization of organic dyes are also mentioned.

Chapter 2: The performance of an organic dye as a laser gain medium could be fully understood only in terms of its fundamental photophysical properties. The different decay mechanisms of the excited state of the dye molecules and their timescales have a key role in determining the lasing efficiency of the gain medium. In Chapter 2, the photophysical properties of Couamrin 540 (C 540) in different solvents which comprises of polar protic, dipolar aprotic and nonpolar are discussed in detail. The different photophysical parameters like quantum yield, lifetime, radiative and nonradiative decay rates, solvent polarity function and its control over stokes' shift are compared in these different solvent environments. The quantum yield of the dye is found be significantly high, even close to unity in polar and certain dipolar aprotic solvents. The features of amplified spontaneous emission (ASE) and laser emission observed in C540 dye solution are also discussed in this chapter. The role of pump energy and the excitation length of the gain medium on the observed ASE are also presented. At sufficiently high pump energies, laser emission with well resolved, equally spaced resonant modes are observed even in the absence of any external mirrors. These modes are found to originate from the subcavities formed by the parallel walls of the cuvette containing the high gain medium. The observed mode patterns highly varied with the different solvents used for the study. While the quantum yield remains a decisive factor, a clear correlation between the refractive indices of the solvents and the number of lasing modes exhibited by the emission spectra of the respective samples has been demonstrated. A detailed discussion of the solvent effect, which determines the reflectivity at the end faces of the cuvette, in the lasing characteristics of C 540 is also given in this chapter.

Chapter 3: Many of the functional drawbacks met with liquid dye lasers could be effectively handled by solid state dye lasers. For this reason, solid state dye gain

media have attracted considerable interest in recent years. Here, in Chapter 3 the light amplification of C 540 dye, doped in different polymer matrices like PMMA, polystyrene and polyvinyl chloride (PVC) is studied. Different solid state polymer matrices are prepared both by the bulk polymerization and free cast evaporation techniques .The ASE and lasing behavior are studied both in the bulk and thin film dye doped samples. In free standing films of micrometer thickness, laser emission and mode structure with equally spaced, well resolved resonant modes are observed in the absence of any external mirrors. The partial reflections from the broad lateral surfaces of the free standing films provided the optical feed back for the laser emission. The occurrence of the well –resolved equally spaced resonant modes is due the Fabry- Perot like optical cavity formed between the film surfaces. The mode spacing is related to the thickness of the film.

Chapter 4: The main concerns with the solid state dye lasers are their photochemical and thermal stability and a high damage threshold for laser radiation. In chapter 4 we present a very sensitive and accurate photothermal method to study the photostability of the dye (C 540) doped polymer samples. The photostability of the different dye doped polymer samples is compared with the photoacoustic technique using a minimum volume open cell configuration. In this method, the quantity measured is the nonradiative part of deexcitation. The photostability is studied under different pump powers, various concentrations of the dye, different excitation wavelengths and different chopping frequencies. The excitation radiation used is 488 nm taken from an Argon-ion laser.

Chapter 5: The investigations made on the ASE and fluorescence energy transfer phenomenon from the donor Coumarin 540 to the acceptors Rhodamine 6G and Rhodamine B in different solvent environments under pulsed optical excitation are reported in chapter 5. Study of fluorescence energy transfer is a powerful technique to unravel the photophysical processes and this method has acquired increased acceptance in recent years with its applications in the fields like

biological analysis, biochemistry, diagnostics etc. This method is highly being used for the measurement of nanometer scale distances and investigations of molecular interactions. The energy transfer mechanism is also proved to have significant applications in the area of laser materials to control light emission. Energy transfer studies of both d-a pairs are performed in four different solvent environments. Efficient transfer of energy is observed in all the donor-acceptor (d-a) pairs, with the solvent medium profoundly influencing the energy transfer process. While an efficient transfer of ASE intensity to the acceptor is observed in one solvent, the acceptor is found to act as a dark quencher for the same d-a pair, in another solvent. In the case of C 540- RhB d-a pair in methanol, a complete transfer of ASE is observed with an enhancement in acceptor emission while in dimethyl formamide environment, the donor emission is completely quenched without any emission in the acceptor side. The possible mechanism responsible for the quenching of acceptor fluorescence is also discussed. The critical transfer distance (R_0) calculated for the d-a pairs varied between 5.8 nm to 6.7 nm. This indicates the possibility of energy transfer due to long-range dipole-dipole interaction between the excited donor and ground state acceptor molecules. Due to pulsed optical excitation, the quenching rate constant is found to be significantly high.

Chapter 6: This Chapter deals with the nonlinear properties of C 540 both in the liquid and dye doped solid state polymer matrix forms. Organic molecules have not only good absorptivity but also they possess good nonlinear absorption. Polystyrene, PMMA and polyvinyl chloride (PVC) are the polymers used as solid state host materials for the dye. The open aperture Z-scan technique is employed to study the absorptive nonlinearities in the dye samples. C 540 dye, both in the liquid and polymer thin film forms exhibits reversible saturable absorption. The nonlinear absorption coefficient, the irradiance for exhibiting nonlinearity and the imaginary part of $\chi^{(3)}$ are calculated for different dye doped polymer samples. One of the very important applications of reverse saturable absorption is in

optical limiting. Details of the optical limiting property of the dye doped polymer films are also discussed in this chapter.

Chapter 7: A brief summary of the experimental results and important findings are included in Chapter 7. Further areas in which the work can be extended are also discussed.

Most of the results included in this thesis have been published or communicated for publication.

Lists of publications

Journals

1. "Photoacoustic investigations on the photostability of Coumarin 540 doped PMMA"**Ritty J. Nedumpara**, Santhi.A, Binoy Paul, P. Radhakrishnan, V.P.N.Nampoori,C.P.G.Vallabhan Spectrochimica Acta Part A, 60 (2004) 435-439.
2. "Light amplification in dye doped polymer films"**Ritty J.Nedumpara**, Geetha K, Dann V.J, V.P.N Nampoori, C.P.G Vallabhan and P Radhakrishnan; J. of Opt. A: Pure and Appl. Opt. 9 (2007) 7-14
3. "A Study of Solvent Effect in Laser Emission from Coumarin 540 Dye solution"

   Ritty J.Nedumpara, Thomas K.J, Jayasree V.K, C.P.G.Vallabhan, V P N Nampoori and P Radhakrishnan ,Applied Optics (under revision)
4. "Rhodamine B as a dark quencher in dye mixtures"

   Ritty J Nedumpara, Manu P J, C.P.G.Vallabhan,V P N Nampoori and P Radhakrishnan (Communicated)
5. "Amplified spontaneous emission and energy transfer studies in dye mixtures under pulsed laser excitation" **Ritty J.Nedumpara,** Manu P J, C.P.G.Vallabhan, V P N Nampoori and P Radhakrishnan (Communicated)
6. "Thermal lens technique to evaluate the fluorescence quantum yield of a schiff base"Santhi.A, U.L. Kala, **R.J.Nedumpara**, A. Kurian, M.R.P. Kurup, P. Radhakrishnan, V.P.N. Nampoori, **Applied Physics.B, Springer**, UK, 79, (2004) p.629-633
7. "Enhancement in Thermal lens signal from molecules of Rhodamine 6G Dispersed in Silver sol and its Effect on Quantum yield Measurements" Santhi.A, **Ritty J Nedumpara**, V S Abraham,V Ramakrishnan, P Radhakrishnan,C P G Vallabhan and V P N Nampoori; **Proceedings of SPIE**, APOC 2003, Nov 4-6, Wuhan, China, p.661

Seminar/conference presentation

1. Laser emission from random nanosize scattering media. **Ritty J. Nedumpara**, Bindu Krishnan, V.P.N Nampoori, P. Radhakrishnan, Proceedings of International Conference on Optoelectronic Materials and Thin Films for Advanced Technology (OMTAT) Oct. 2005
2. Investigations of the Random Lasing from a Gain Media with Nanosize Scatterers,**Ritty J.Nedumpara**, Bindu Krishnan, V.P.N.Nampoori, P.Radhakrishnan, Proceedings of International Conference on Optics & Optoelectronics, Dehradun-2005
3. Photo-acoustic diagnostics of laser- induced processes in leaves **Ritty J.Nedumpara**, Asha Susan Varghese, Joe Susan Mathew ,Liji Varghese, Achamma Kurian V.P.N Nampoori , Proceedings of International Conference on Optics & Optoelectronics, Dehradun-2005
4. Spectral Narrowing of Light Emission from a Laser Dye in a Solid-State Polymeric Host, **Ritty J. Nedumpara**, Manoj V. Mathew, V.P.N.Nampoori, P.Radhakrishnan, Proceedings of National Laser Symbosium,Vellore -2005
5. Nonlinear Absorption in Dye Doped Polymer Matrices, **Ritty J. Nedumpara**, Litty Mathew, V.P.N. Nampoori, P.Radhakrishanan. Proceedings of International Conference on Photonics 2006
6. Nonlinear optical characterization of Nd doped solgel films,Lyjo K Joseph, **Ritty J Nedumpara**, Thomas K J,V P N Nampoori and P Radhakrishnan , Procee. of International Conference on Photonics 2006
7. Energy Transfer and dark quenching in dye mixtures,**Ritty J.Nedumpara**, Manu P J, C.P.G.Vallabhan, V P N Nampoori and P Radhakrishnan Proceedings of International Conference on Photo-radiochemistry, M.G.University ,Kottayam, Feb 2007
8. Rhodamine B as a dark quencher in dye mixture,**Ritty J.Nedumpara,** P.Radhakrishnan, International conference on Materials,MatCon 2007

Acknowledgement

**"My soul magnifies the Lord,
and my spirit rejoices in God my saviour"(Lk 1: 46-47)**

Mother Mary had well expressed the state of a mind who receives bounteous blessings from the Lord. Nothing else I would like to say at the outset of completion of my thesis work, but to add; my heart delights in the company of people of great heart and good will.

While I step down to submit my thesis, looking back, a group of people are in front of me, before whom I would like to fold my hands to say a 'Big Thank You' and to keep them in my heart to remember them in my prayers.

I express my heartfelt gratitude to my guide and supervisor Dr.P.Radhakrishnan for accepting me as research student. Gratefully I acknowledge the constant support, able guidance, valuable suggestions, approachability and freedom of work extended to me throughout the period. The meticulous care he bestowed and the time he set apart for the final formation of the thesis is really commendable. Besides the guidance of a thesis work, he guides through the light of his life. There are a lot of things to imbibe from him for the quality of life. He is a person of righteousness who loves simplicity, hardwork and perfection. He upholds sincerity in thought and action.

I would like to thank Dr.V.P.N. Nampoori, the director, for providing me all the facilities at ISP for the successful completion of my work. Director or not, he always stands for the best. He is a person who surprises people by the way he manages hundred things together. I express my deep sense of gratitude for all the constructive suggestions ,encouragement and constant support he rendered to me .

I am extremely grateful to Dr.V.M.Nandakumaran, the then director of ISP, for accepting me as a research student of ISP. A simple man with a pleasant nature, but well versed in the theories of physics - he always was a source of inspiration and encouragement .I was fortunate enough to attend a few of his

outstanding classes and to understand his in -depth knowledge. I also gratefully remember the friendly support of Mr.Kaislasanath and the timely help.

I am deeply indebted to Dr.C.P.Girijavallbhan, the founder father of ISP, who is still a pathmaker for research. The genuine interest he had taken in my work was really a push for me. At all stages of my work, his valuable suggestions and critical comments led me through the right way. For paper communications, the guidance and personal interest taken by him was really a big help for me.

The long years at ISP granted me the company of a good number of people whom I gratefully remember while I leave ISP. Binoy Paul, Pramod Gopinath, Unnikrishan, Dr.Deepthy, Pravitha, Bindu, Sajan, Rajesh S, Thomas Lee, Aneesh, Prasanth, Suresh Sir who welcomed me to the family of ISP with their gracious mind and enlightened visions and taught me to walk with them upholding the scientific culture of ISP and the pleasant world of humaneness. I specially thank Binoy, Pramod and Sajan for making me acquainted with the different laser systems and equipments in the Lab. I remember with love all my contemporaries, Sreeja, Rekha, Dilna,Samuel and specially Geetha, Santhi, Rajesh M and Jayasree teacher for the fruitful discussions and timely help rendered to me in many different ways and for their loving companionship. I was fortunate enough to walk with a group of very talented and highly enlightened youngsters- Manu, Jijo, Vinu, Abharaham, Saritha, Thomas, Lyjo, Dann, Litty, Sheeba, Parvathi, Saritha, Sajeev,Prabhathanand Nithyaja. Oh, my good friends, I remember you all with love and sincerely thank you for the timely help graciously rendered to me and for all your kind deeds. A special thanks to Manu, for helping me with simple Matlab programs needed for my work and making the atmosphere of our sitting room humorous. My sincere thanks to my companion Litty, who wholeheartedly rendered all possible help in various ways.

I owe a debt of gratitude to Manoj Mathew our former M.Tech student for the timely installation of the Acton monochromator with CCD with which I could complete a major part of my work. Vinu also needs a special mention for the automation of the different equipments and for the modifications of the cover

page. I would like to place on record the help of Dr.Deepthy regarding the preparation of some manuscripts and for the many fruitful suggestions regarding my work.

I extend my sincere thanks to the non-teaching staff who were extremely helpful in office matters. I am also grateful to the librarians of ISP as well as the dept.of Physics and central libraries for all assistance. I would like to thank Dr.T.V.Antony, Dr.Manoj of Chemistry Dept, Dr,Sr.Mable and Dr. Honey of Polymer Dept.for the discussions regarding the chemistry part. I gratefully acknowledge the help rendered to me by RRL Thiruvanthapuram regarding the lifetime measurements.

I cherished the warmth and love of many good friends in the hostel. Gratefully I remember the good company of Kochurani, my roommates Sunitha and Nisha, Beena, Feeba ,Radhika ,Maya, ,Jitha, Biby, Reena, Gleeja and many more.

I'm grateful to University Grants Commission for awarding me the teacher fellowship. At the completion of my thesis I'm deeply indebted to many in my institution,Vimala College,Thrissur. With a great sense of gratitude I remember my former principals, Dr.Sr.Omer and Sr.Dheera and present principal Sr.Lekha for their loving support and encouragement. Gratefully I acknowledge the loving support and encouragement extended to me by my colleagues and non teaching staff of the Department of Physics and other teaching and non teaching staff of the college.

The genuine interest, the loving consideration and deep understanding I experienced from my superiors Sr.Pulcheria and Sr.Daisy Paul and sisters of my community was a great encouragement for me. With much gratitude I acknowledge the kind support and encouragement always extended to me by my provincial superiors Sr.Nirmala , Sr.Nilus and the councillors throughout my research period.

I know, in the back of all my success in me life, my loving parent's incessant prayers which pierces the heavens and their love and support have a

unique role. All my family members were always there with me to give constant mental and spiritual support. Cherishing all the love, care and support from all around me, I bow my head in thanks and raise my heart in prayer.

All glory is to the Lord Almighty.

Sr.Ritty J.Nedumpara

Contents

1 Laser Dyes and Their Applications: Recent Developments

Abstract 1

1.1 Introduction 1

1.2 Laser dyes 2

1.3 Development of dye laser: A brief historical background 5

1.3.1 Laser pumped pulsed dye lasers 5

1.3.2 Continuous wave dye lasers 7

1.3.3 Ultrashort pulse dye lasers 8

1.4 Recent advancements in dye lasers 9

1.4.1 Introduction: Solid state dye lasers 9

1.4.2 Inorganic sol-gel glass matrices 10

1.4.3 Polymer matrices 12

1.4.4 Hybrid materials 13

1.4.5 Dye doped waveguides 14

1.4.6 Dye doped optical fibers: Lasers and Amplifiers 15

1.4.7 Microcavity Lasers 17

1.5 Fluorescence related applications 18

1.6 Nonlinear properties of organic dyes 20

1.7 Conclusion 21

1.8 Present work 21

References

2 Photophysical, ASE and Lasing Properties of Coumarin 540

Abstract 29

2.1 The Photophysics of Laser dyes 29

2.1.1 Energy level diagram 30

2.1.2 Absorption and fluorescence spectral characteristics 33

2.1.3 Solvent effect on fluorescence spectra 33

2.1.4 Stoke's shift and solvent polarity function 34
2.1.5 Fluorescence quantum yield 35
2.1.6 Fluorescence Lifetime 36
2.2 Structure of Coumarin 540 (C 540) 37
2.3 Experimental details 38
2.3.1 Absorption and fluorescence spectra 38
2.3.2 Quantum yield measurements 40
2.3.3 Lifetime measurements 44
2.4 Photochemical effect 46
2.5 Amplified spontaneous emission (ASE) 49
2.5.1 Introduction 49
2.5.2 Features of ASE 50
2.5.3 Experimental details to study ASE 50
2.6 Laser Emission from dye solution 53
2.6.1 Solvent effect on laser emission 57
2.6.2 Efficiency of the laser gain medium 64
2.7. Frequency up-conversion emission 65
2.8. Conclusions 66
References

3 Light Amplification in Dye Doped Solid State Polymer Matrices

Abstract 69
3.1 Introduction 69
3.2 Solid State Dye Lasers 70
3.3 Dye doped polymer matrices 71
3.4 Optical gain studies in dye doped polymer matrices 73
3.4.1 Amplified Spontaneous Emission 73
3.4.2 Gain coefficient 74
3.5 Experimental details 76
3.5.1 Fabrication of dye doped polymer matrices 76

3.6 Dye doped PMMA matrices 76
3.6.1 Gain studies 77
3.7 Solid State Thin Films:Preparation 79
3.7.1 Gain studies 79
3.7.2 Laser Emission 83
3.7.3 Laser resonant modes 86
3.8 Dye Doped Polystyrene Matrices 88
3.9 Dye doped Polyvinyl chloride films 94
3.10 Conclusions 96
References

4 Photostability of Dye Doped Polymer Matrices -A Photoacoustic Study

Abstract 101
4.1 Introduction 101
4.2 Photodegradation measurements 103
4.3 Photoacoustic method 104
4.4 Rosencwaig-Gersho Theory 105
4.5 Photostability investigations using PA technique 108
4.6 Experimental Details 109
4.6.1 PA studies in bulk samples 111
4.6.2 PA studies in dye doped polymer film samples 117
4.7 Conclusion 121
References

5 ASE and Energy Transfer Studies in Dye Mixtures

Abstract 125
5.1 Introduction 125
5.2 Different Energy Transfer Mechanisms in a d-a Pair 126
5.2.1 RadiativeTransfer 127

5.2.2 Radiationless Transfer Due to Electron Exchange Interaction 127
5.2.3 Radiationless Transfer due to Coulombic Interaction 128
5.3 Importance of Fluorescence Resonance Energy transfer 129
5.4 Theory of Resonance Energy Transfer 130
5.5 Experimental Details 134
5.6 Results and discussions 135
5.6.1 ASE in C 540 – Rhodamine 6G d-a pair 138
5.6.2 C 540-Rhodamine B as d-a pair 141
5.7 Conclusions 153
References

6 Nonlinear characteristics of Coumarin 540

Abstract 157
6.1 Introduction 157
6.2 NLO properties of organic molecules 160
6.3 Nonlinear absorption (NLA) 161
6.4 Open aperture Z-Scan to Study NLA 163
6.5 Theory of open aperture z-scan technique 164
6.6 Experimental setup 166
6.7 Nonlinear absorption in C 540 dye solution 167
6.8 Nonlinear absorption in Dye doped polymer films 171
6.9 Optical limiting 173
6.10 Optical limiting in dye doped polymer films 174
6.11 Conclusion 175
References

7 Conclusions and future prospects

7.1 General conclusions 178
7.2 Future prospects 182

Chapter 1

Laser Dyes and Their Applications: Recent Developments

"This most beautiful system could only proceed from the dominion of an intelligent and powerful being". Issac Newton

Abstract

An overview of the recent developments in laser dyes and their applications is concisely discussed. A general introduction to organic dyes, a brief historical background of the development of dye lasers and the modifications and advancements made over the years to meet the widespread applications in diverse fields of science and technology are presented in this chapter. The importance of fluorescence dyes in the fields of biochemistry, molecular biology and nonlinear optics are also included.

1.1 Introduction

The invention of lasers has added a new era in the fields of science and technology. The applications and possibilities they have generated in the fields of physics, chemistry, biology, medicine, industry, technology and for applications we encounter in the day to day life are enormous. In the search for powerful and tunable

sources which cover the entire visible, near ultraviolet and near infrared red regions, the dye lasers have proved to be quite promising. The dye lasers have come into the forefront with its versatility and ability to emit variable frequency coherent radiations in the above ranges. In addition to tunability and versatility, the high performance of the dye lasers in areas such as spectroscopy and photochemistry make them unique among the laser sources. These sources emit radiation in a variety of regimes from femtosecond pulses to continuous wave oscillations ,from high energy pulses to high average powers and from near ultraviolet to near infrared regions. This unique operational flexibility has made the dye laser an essential tool in numerous fields of applications like physics, spectroscopy, photochemistry, biology, medicine and communication [1].

With the almost unlimited number of dyes available and the ease with which the structure of organic compounds and its derivatives can be modified ,the field of dye lasers is still not matured and the intense research is going on to develop new organic materials and to tailor them to suit different applications.

1.2 Laser dyes

Laser dyes are organic compounds defined as hydrocarbons and their derivatives. Schafer explains the unique properties of large absorption and emission exhibited by organic dyes in terms of their bond structure [2]. Among the saturated and unsaturated organic compounds, organic dyes come under the unsaturated groups which contain at least a double or triple bond. These multiple bonds use π electrons for bonding. A π bond is formed by the lateral overlap of the π electron orbital, which is maximum when the symmetry axes of the molecules are parallel. In this position, bond energy is minimum giving a planar molecular structure of high rigidity. If two double bonds are separated by a single bond, the two double bonds are called conjugated bonds.

Chapter 1

Compounds with conjugated double bonds absorb light at wavelengths above 200 nm. All the dyes having a high absorption in the visible region of the spectrum possess several conjugated double bonds. Dye molecules are planar in structure with all the atoms of the conjugated chain lying in a common plane and linked by σ bonds. The π electrons have a node in the plane of the molecule and form a charge cloud above and below this plane along the conjugated chain.The position of the absorption band of the dye is determined by the chain length L and number of π electrons N and is given by the relation;

$$\lambda_{max} = \frac{8mc_0}{h}\frac{L^2}{N+1} \qquad (1.1)$$

where h is the Planck's constant, m is the mass of electron and c_0 is the velocity of light. Stable dye molecules have an even number of electrons in the π electron cloud [3]. Since the π electrons are free to move over a distance roughly equal to the chain length L, dyes have a very large dipole moment (μ) according to the relation $\mu = eL$. Correspondingly the absorption cross section σ_a, which is proportional to μ^2 is also large (10^{-16} cm^2). The stimulated emission cross section is also found to be large which is again proportional to the dipole moment.

Laser dyes are generally classified into three groups:(1) Coumarins- the most common blue – green laser dyes.(2) Xanthene dyes which have emission in the 600 nm region among which the most studied members are Rhodamines and (3) the Cyanines with emission in the red and near IR region. All these classes of structure share the property of conjugation of π bonds to carbon. Chemical structure of a representative of these 3 classes is given below [3].

(a)

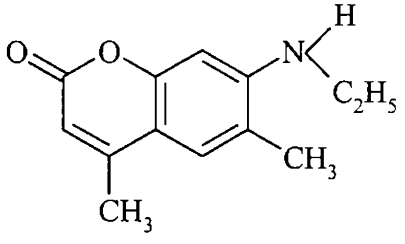

(b)

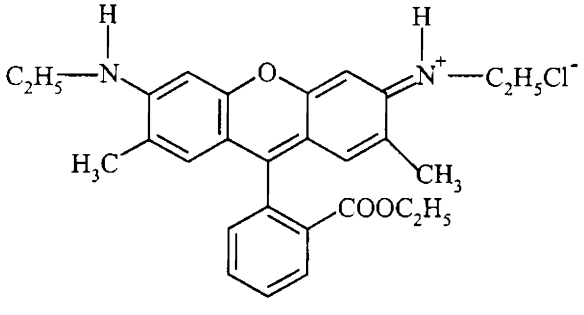

(c)

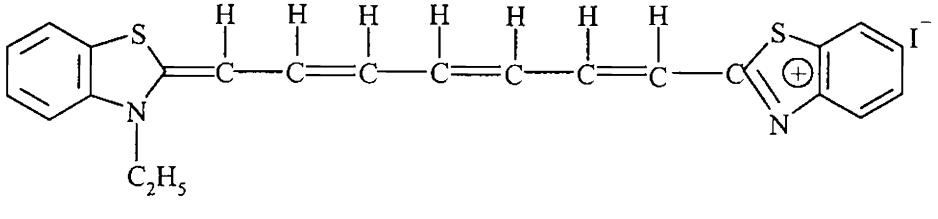

Fig 1.1 Chemical structure of some common dyes.(a) Coumarin 2
(b) Rhodamine6G (3)3,3' diethyl thiatricarbocyanine iodide

1.3 Development of dye laser: A brief historical background

The observation of stimulated emission from chloro-aluminum phthalocyanine by Sorokin et al. in 1966 marked the entry of dye lasers into the scenario of lasers. Stimulated emission of spectral width of $5cm^{-1}$ at 755 nm was observed when the phthalocyanine solution was excited by a powerful beam from a giant-pulse ruby laser [4].Within a short period, different research groups could attain promising results with advancements in different parameters like spectral width, tunable range, output power, excitation sources, experimental arrangements etc.[5-7]. With its versatility, wide range of tunability and high performance, the organic dye lasers are usually classified into three main categories namely the pulsed dye lasers, continuous wave (cw) lasers and ultrashort pulse dye lasers [1].

1.3.1 Laser pumped pulsed dye lasers

Following the development of first dye laser, Schafer et al. reported a liquid dye laser with emission ranging from 730-870 nm with megawatt peak power and beam divergence angle of 5 mrad.[8]. Efficient spectral narrowing and tunability over a wide spectral range had been demonstrated in solid and liquid organic dye lasers using diffraction grating as cavity reflectors by Soffer et al. [9]. Wavelength tunability being the attractive parameter in dye lasers, great interest was shown in developing dye lasers with wide spectral range. The operation of dye lasers in the wavelength range 440-700 nm was reported by Schafer in 1967 [10]. In all the early works on dye lasers, the pumping sources were giant-pulse or Q-switched ruby lasers.

It was Kotsubanov who had experimented the potentiality of xanthene dyes as a laser gain medium [11]. He had reported the laser emission from solid and liquid dye solution of xanthene dyes in the wavelength range 570-640 nm which later

became the most efficient dye laser gain media. Pumping was accomplished by means of second harmonic of a neodymium laser. A versatile high spectral energy density pulsed dye laser suitable for lidar application and high resolution spectroscopy was reported by Franscis Bos et al. in1981 [12]. Such experiments need very high power lasers with narrow linewidth and low divergence. An efficiency of 55% was achieved providing 165 mJ in a single longitudinal mode. A spectral range varying from 565-880 nm was achieved from different dye solutions.

The use of N_2 laser as a direct UV excitation source for dye laser was reported by J. A. Myer et al. [13]. The system was capable of repetitive rate as high as 100 Hz with reasonably good efficiencies. A N_2 laser pumped dye laser system is described by Itzkan et al. which uses an oscillator-amplifier arrangement and fast flow dye cells in order to achieve spectral narrowing and spatial coherence [14]. The resulting system was capable of producing 50 kW, 0.5 ns pulses with a spectral width of 0.02 Å. This is found to be a useful tool for studying atomic systems at visible wavelengths. Tunable dye lasers have proven to be very useful in the fields of spectroscopy and chemical kinetics. For many photochemical experiments including isotope separation, a simple tunable source capable of shorter-wavelength operation is highly desirable. A dye laser which could be used for applications in high resolution atomic and molecular spectroscopy and generated power of 50 kW at a linewidth of about 6×10^{-4} Å and tunable up to 230 nm had been efficiently generated by frequency doubling in a crystal of lithium formate monohydrate [15].

The pulsed dye lasers are now used as sources of tunable coherent radiation in the visible, near ultraviolet and near infrared region. Although reliable high power lasers like excimer and Nd:YAG lasers etc are now common, the dye lasers are still characterized by a general group of parameters including efficiency of energy

conversion from the pump source, tunable spectral range, spectral purity and narrow spectral width.

1.3.2 Continuous wave dye lasers

Many spectroscopic, photochemical and biological studies require a coherent tunable source in the UV wavelength regime. In numerous applications for which high peak powers are not necessary, a tunable cw source may be more advantageous than a pulsed radiation source. A cw laser source offers better amplitude stability and beam quality. Another unique feature of cw dye laser is its ability to provide tunable single -frequency oscillation. First cw dye laser using Rhodamine 6G in water was described by O.G.Peterson [16]. Power output was 30 mW at 577 nm when excited with a 1-W argon ion laser. A tunable dye laser operating continuously in the range 570-620 nm was demonstrated with a single prism and an intracavity etalon [17]. They could achieve single mode operation with a bandwidth less than 35MHz. Blit et al. had reported the generation of broadly tunable UV radiation from 285- 400 nm by SHG and sum frequency generation [18].

Though single mode laser is an extremely useful device for many scientific and industrial applications, the output power has been limited to 200-300mW. The limited output power of single mode(SM) dye lasers is predominantly due to the fact that most of the lasers were operated as standing wave lasers. In standing wave SM lasers, spatial hole burning occurs. To suppress all modes but one, dispersive losses are inserted into the cavity by prisms, Fabry-Perot etalons etc. which mainly restrict the efficiency of SM lasers. Being non-ideal elements, they produce higher losses not only for the undesired modes but also for the prime modes. In a traveling wave cw laser, spatial hole burning does not exist, thereby eliminating the need for high selectivity. A traveling wave cw laser was realized by unidirectional operation of a

ring laser, yielding single mode output powers of 1.2 W at 595 nm and of 55 mW in the UV region with intracavity frequency doubling [19].

1.3.3 Ultrashort pulse dye lasers

Since the introduction of femtosecond laser systems in 1981 much progress has been made towards the reductions of laser pulsewidths. Significant developments have also been made in the generation of ultrashort dye laser pulses. Subtle changes in cavity configuration resulted in dramatic variations in laser operation. W.Schmidt et al. had reported mode locking in a dye laser using an organic dye as a saturable absorber and a commercial flash lamp as pumping light [20]. Later a direct production of pulses as short as 0.3 ps by employing a cavity configuration, incorporating an optically contacted saturable absorber was achieved by Ruddock et al. [21].

It is generally believed that the introduction of dispersive elements will produce significant pulse broadening. But Dietel et al. had reported the generation of short pulses of width 53 fs with a 2 mm thick BK7 glass inserted in the cavity [22]. Advances in the generation of ultrashort pulses have used either passive mode locking in a colliding pulse laser or soliton like shaping in a laser containing an optical fiber. Some groups had shown that a combination of an optical fiber and a diffraction grating can be used to generate ultrashort optical pulses. Fork et al. could achieve ultrashort pulses of duration 8 fs by a combination of prism and diffraction grating [23].

Distributed feedback dye laser (DFDL) was found to be a convenient tool to generate ultrashort pulses in a wide spectral range. For their operation, they need a perfect high-visibility interference pattern to be created in the dye solution. In the earliest DFDLs this was achieved by using a beam splitter in a laser beam to obtain two interfering partial beams, a method which necessitates a laser beam of high spatial and temporal coherence. In a later version, a grating was used as a beam splitter. Here,

the period of the interference pattern can be made independent of the pump wavelength, decreasing considerably the requirements for the temporal and spatial coherence; but the position of the interference pattern is still wavelength dependent. Later it was shown that this drawback could be avoided by introducing a second grating to create an image of the first grating. With the latter arrangement, subpicosecond pulses could be generated. Szatmari et al. had reported widely tunable distributed feedback dye laser which made use of a microscopic objective which images a transmission grating into the active medium to generate subpicosecond pulses [24]. N.Takeysau et al. had designed a distributed feedback dye laser with a quenching cavity which generated tunable picosecond pulse of 60 ps with a narrow spectral linewidth of 9.4 pm [25].

1.4 Recent advancements in dye lasers

The outstanding potentials of dye lasers necessitate the modifications of these systems in order to be used in practical applications. From the early days of development of dye lasers, attempts were carried out to miniaturize the laser system so that it can effectively be used to meet the requirements of different fields. A brief discussion of the developments is given below.

1.4.1 Introduction: Solid state dye lasers

The various technical and handling problems faced with the conventional liquid dye lasers prompted intensive research to replace the liquid dye lasers by their solid counterpart. Solid state lasers have obvious advantages such as compactness, low cost and they are non-flammable and non toxic. The first solid state dye lasers were reported in the late 1960s by Peterson and Snavely [26]. They demonstrated stimulated emission from polymeric materials doped with organic dyes. Though the attractions of solid state dye lasers were many, the work on solid state dye lasers was

not pursued much due to their low lasing efficiency and fast degradation [27]. The incorporated dye had a limited lifetime due to photo-degradation. It was in 1980s, efforts to incorporate the organic dyes in solid matrices regained momentum. Intensive research was done by different groups for the synthesis and development of new and efficient solid state host materials for dyes to attain laser gain media of high optical quality and photostability. The other basic requirements imposed on a solid matrix to be used as a host for lasing dye molecules are a low level of scattering and a wide range of transparency covering both pump and lasing wavelengths. They should have high thermal conductivity, good thermal and chemical stabilities and a high damage threshold such that it can withstand high power laser radiations. The high thermal conductivity provides an efficient mechanism for uniform heat distribution and dissipation within the sample. In addition, the technology of incorporating the various organic dyes to different host materials is also simple [28]. Over the years, a good number of materials have been experimented as solid hosts and among them inorganic sol-gel glasses, organically modified silicates (ORMOSILS), silicate nano composites and transparent polymers were found to be promising materials. In recent years the synthesis of new high performance dyes and the implementation of new ways of incorporating the organic molecules into the solid matrices have resulted in significant advances towards the development of practical tunable solid state dye lasers. Exploring the physics and chemistry of various organic and inorganic materials, enormous research is going on to develop high performance solid state dye lasers to implement them in various fields of applications.

1.4.2 Inorganic sol-gel glass matrices

In the search for efficient materials with good optical quality and high laser damage resistance threshold, the inorganic glasses gave the first promising results. They present better thermal properties and a higher damage threshold than polymers. Lots

of work have been done in silica based inorganic polymers such as aluminosilicates, titania-silica and silica –zirconia materials. Zirconia is found to be a suitable material as solid host for laser dyes with its high damage threshold, superior mechanical strength and high refractive index which is barely affected by thermal expansion [29]. By the combination of silica-zirconia hosts the refractive index of the material can be varied.

In 1990s, work with silica gels had indicated that sol-gel materials show higher photostability and better thermal properties than that based on organic polymers [30]. D.Lo et al. had demonstrated narrow linewidth laser emission in the yellow, blue and near UV region from three dyes incorporated with sol-gel silica [31]. These dye doped sol-gel samples were chemically stable under repetitive laser excitation. These results show the versatility of sol-gel derived materials as solid hosts for dyes. Very limited choice of blue or UV emitting laser dyes was found to be chemically compatible with polymer matrices. Inorganic glasses of silica gel present better thermal properties and a higher damage threshold than polymers and the incorporation of dyes into inorganic materials by the sol-gel process has allowed one to obtain relatively photostable materials with acceptable laser efficiency[32].

The high porosity of sol-gel derived glass is an undesirable factor for lasers. Eli Yariv et al. had demonstrated that organically modified silicates (ORMOSILS) could be better solid host materials than porous glasses. Compared to inorganic glasses ormosils are characterized by improved mechanical and optical properties due to relatively high flexibility and low porosity [33]. Ormosils modified by different organic compounds were studied by many groups and the conclusions drawn were that the incorporation of organic chains in the porous glass could increase the laser efficiency. By using organically modified silica which is less polar compared to pure

inorganic silica, the monomeric form of incorporated dye is favoured which will increase the lasing efficiency [29].

1.4.3 Polymer matrices

Among the variety of materials experimented as solid state matrices, transparent polymers are found to be the most promising materials both from the economical and technical point of view though the first results were not so attractive. They have high optical transparency, superior homogeneity, good compatibility with organic dyes, inexpensive fabrication technique and control over medium polarity and viscosity. There are vast possibilities in polymer synthesis by which the structure and the chemical composition of the polymers can be modified which allows one to introduce controlled changes to optimize their properties [34]. The polar characteristics of a given polymer can be changed by introducing the appropriate groups directly into the polymeric chain, for instance, by copolymerization of methyl methacrylate with hydroxy–methacrylic polymers [28]. Understanding the advantages of polymers, extensive work has been done to explore the potential of polymers as host materials for laser dyes [35]. In general the polymers used are polyacrylics, polyurethanes (PUA), polycarbonates etc. In polyacrylic class the most commonly used polymeric hosts are polymethylmethacrylate (PMMA). These polymers have excellent optical transparency in the visible region. They possess high optical homogeneity and have relatively high laser damage threshold [34].

Although the polymer matrices are found to be quite attractive with its unique properties, they have the limitations of low damage threshold and limited lifetime [36]. Polymers are poor thermal conductors and have large time of heat dissipation .A large number of laser dyes are insoluble in PMMA .The laser damage of polymeric materials are found to be energy dependent and the matrix viscoelastic properties

determine the damage threshold resistance. Out of the conclusion that the laser damage resistance can be significantly improved by changing the viscoelastic properties of the medium in an appropriate way, a great amount of work was done by many research groups. Costela et al. have done extensive work in this line by the co-polymerization of different monomers. They have incorporated different dyes like Rhodamine 6G,Coumarins and Pyrromethene in homopolymer PMMA or in a variety of co-polymers of methylmethacrylate with monofunctional monomers 2-hydroxyethyl methacrylate (HEMA), 2-hydroxyethyl acrylate (HEA) ,2-phenoxyethyl acrylate (PEA) and 2,2,2 –trifluoromethyl methacrylate (TFMA). They have also tried cross linking monomers like ethyleneglycol dimethacrylate (EGDMA) trimethylolpropane trimethacrylate (TMPTMA),pentaerythritol triacrylate (PETA) etc. These modifications resulted in solid state dye lasers which lase efficiently and have remarkable photostability [34].

1.4.4 Hybrid materials

The sol-gel based silica showed superior mechanical, thermal and optical properties. Nevertheless, these solid state dye lasers have limited lifetime due to photodegradation of the incorporated dye caused by the high local intensity of the pumping light. As the photostability of dyes embedded in a solid matrix is dependent on the dye as well as on the host, the problem may be solved by changing either the dye structure or the host structure [27].

The methods of sol-gel chemistry have represented a real breakthrough in the use of molecular chemistry to design new materials. They allow the synthesis and development of hybrid organic-inorganic matrices based on Si-O-Si networks, which are very attractive mainly due to the relative high stablility of the Si-C bond. The quality of Si-O-Si network is excellent in terms of transparency, thermal and chemical

stabilities resulting in stable materials with chemical and physical properties well defined and which can be modified by choosing suitable organic-inorganic components. Synthesis of new materials of hybrid character in which excellent thermal properties of the inorganic glasses and the excellent optical properties of the polymeric materials could be combined was reported [36].

Laser action of Rhodamine 6G is reported which is incorporated into a hybrid matrix of poly(2-hydroxyethyl methacrylate) (HEMA) with different weight proportions of TEOS and TMOS. Costela et al. has incorporated Rh6G dye into1:1 v/v copolymer of MMA and 2-hydroxyethyl methacrylate (HEMA) with different weight proportions of tetraethoxysilane (TEOS) and tetramethoxysilane as inorganic component. Significant enhancement of the laser action of Rh6G has been reported by the incorporation of the above mentioned hybrid materials and lasing efficiency of upto 28% and high stabilities were demonstrated [37].

1.4.5 Dye doped waveguides

The advances in the fields of fiber optics communication and integrated optoelectronics increased the interest in guided wave optics in which optical waveguides and optical fiber are the significant components. The demand for compact visible lasers has accelerated the research in the field of planar waveguides. Due to the long gain length and optical confinement, waveguide structures can reduce the lasing threshold which is a requirement for efficient lasing. The ease of fabrication of planar waveguide makes devices based on dye doped waveguides more attractive.

Polymer waveguides doped with laser dyes rhodamine 6G, rhodamine B and coumarin dyes, which exhibited significant superradiance and amplification of guided beams, were reported in the early 1970s [38-40]. Organic polymers however have the disadvantage of relatively low refractive indices which limit the variety of suitable

substrates and high dependence of the refractive index on temperature, compared to the low value of dn/dT for inorganic glasses[41]. Considering glass substrates, the conventional method of glass waveguide preparation does not allow the incorporation of organic materials because of the high temperature involved. The sol-gel method could resolve this problem which enables the preparation of waveguiding films made of hybrid organic-inorganic glasses at ambient temperature. Sorek et al. was successful in developing planar glass waveguide at room temperature by the sol-gel method [42-43]. They have prepared several glass waveguiding films from titania and modified silica using sol-gel method doped with the laser dye, Rhodamine B. They could achieve stimulated emission and spectral narrowing of fluorescence from rhodamine B doped waveguides with a maximum gain of 54dB/cm. Xiang Peng et al. have realized ASE wavelength control and tuning in organic dye (DCM) doped polymethyl methacrylate (PMMA)/silica hybrid material planar waveguide [44]. A supernarrowing laser spectrum and mirrorless emission are reported from rhodamine B cored dendrimers at a fluence level of $2mJ/cm^2$ by Otomo et al.[45].

1.4.6 Dye doped optical fibers: Lasers and Amplifiers

Optical fibers play a key role in the fast advancing optical communication system and information technology. In communication systems conventional wire cables are being replaced by single mode silica fibers for the high speed data transmission. Though silica fibers are the first member of this class to be approved universally, the polymer optical fibers (POF) have already proved their merits and potentials to be utilized in data communication applications. The high data transmission bandwidth of POF, the low loss of the graded index POF and its large core diameter make them very promising in communication systems [46-48].

The data communication in graded index (GI) POF is carried out at visible wavelengths because they have low loss regions around 570-690 nm. Therefore optical amplifiers, couplers, and optical switches are necessary for GIPOF network. Laser dyes as a gain medium are powerful candidates for high power light amplification because of extremely large absorption and emission cross sections. The availability of different organic dyes makes light amplification possible in the above wavelength region [46]. Among the various applications possible with dye doped polymers, fiber amplifiers and fiber lasers are the most studied components.

The first report of optical amplification in dye doped polymer optical fiber was presented by Tagaya et al.[49]. In their experiment using Rhodamine B doped gradient index POF, maximum gain of 27 dB was achieved at 591 nm with a short fiber length of less than 0.5m.This was achieved with a pump power of 690 W and with a conversion efficiency of 10-15%. Peng et al. had reported the development of step index polymer optical fibers of good optical quality. Both high gain and high efficiency optical amplification have been achieved in a rhodamine B doped polymer fiber[48]. Though lots of work were done in GIPOF as fiber amplifiers, the commercially available fibers are step index POFs. Recently H.Liang et al. had developed a preform technique of fabricating step index (SI) POFs and reported optical amplification using Rhodamine B doped SI POF [50]. A high gain of 23 dB was achieved for a SI POF with 60 cm length and 400 μm diameter. The launched pump power was 10kW. The signal wavelength providing the highest gain for a 60 cm SI POF is around 630 nm which is closer to the low loss window of PMMA POF.

Providing the pump power through an optical fiber is an efficient way of utilizing it. Here the light is well confined in the core area and propagates diffraction free. Therefore, it is expected that the pump power requirement will be substantially reduced because of possible long interaction length and small core cross section. The

reduction in pump power is significant in practical applications since photostability of solid state gain media is a main concern where higher pump intensity could cause the quicker degradation of dye molecules. Fiber lasers are quite attractive in this regard. R. Gvishi et al. had demonstrated a Rhodamine 6G doped sol-gel derived fiber laser lasing at ~ 568 nm with a full width at half maximum of ~7 nm [51]. Efficient lasing from commercially available dye doped graded index polymer optical fiber was demonstrated by Kobayanshi [52]. K. Kuriki et al had fabricated a GI POF containing rhodamine 6G in poly (methyl methacrylate–co-2-hydroxyethyl methacrylate)[53]. Lasing behaviour of the fiber was studied by pumping with a frequency-doubled Q-switched Nd:YAG laser. A slope efficiency of 43 % and a lifetime of 110 000 shots at a repetition rate of 10 Hz have been observed. With a pump energy of 1.5mJ, an output energy of 640 μ J was produced.

1.4.7 Microcavity Lasers

For the high performance of lab-on-a-chip microsystem it requires the integration of lasers and other active optical components. Compact, efficient, and on-chip light sources are of considerable interest to use in these systems. In most cases fabrication of the lab-on-a-chip systems is based on silicon and polymer micro fabrication. Currently the most commonly used miniaturized laser sources in the visible to infrared wavelength regions are made from III-V semiconductor crystals. These types of devices cannot be easily integrated with the silicon or polymer based microsystems. Microcavity dye laser is a novel technique to solve this problem of integration. Dye molecules are used as the active medium dissolved in liquid solution or cast into a solid matrix. The first report of a microfluidic dye laser designed using the standard micro-fabrication technique is by Helbo B et al. They have successfully designed and realized a miniaturized liquid dye laser-a microcavity fluidic dyer laser which can be integrated with the lab-on-a-chip microsystems [54]. Rhodamine 6G dissolved in

ethanol was the laser gain medium. The micro-fluidic dye laser consists of a micro-fluidic channel fitted with mirrors forming the laser cavity. The laser dye is pumped through the channel and it is optically pumped by an external laser source. Dye laser output is emitted vertically from the device. In the design, the micro-fluidic channel structure is defined in a layer of photodefinable polymer (SU-8).

Later a tunable microfluidic dye laser was fabricated by Helbo et al. in SU-8[55].The tunability is achieved by integrating a microfluidic diffusion mixer with an existing micro-fluidic dye laser design. By controlling the relative flows in the mixer, the concentration of the dye in the laser cavity was adjusted allowing the wavelength to be tuned. In this report lasing wavelength was tuned from 568 -574 nm.

Spherical designs of microstructure resonators are also implemented for compact miniature laser devices. This combines effective coupling of the emission to the resonator modes within a microstructure and with the resonant modes being ring modes along the characteristic circumferences In the search for low cost microfabricated lasers which may find numerous applications in interference based sensors and lab-on-chip microsystems, polymers are the preferred choice of materials due to their low cost and easy way of fabrication. A variety of methods have been demonstrated for the microfabrication of dye lasers. Among the various approaches, the distributed feedback (DFB) techniques have been proven to be successful in obtaining single mode lasing. Balslev et al. had reported a solid state single mode DFB polymer dye laser fabricated by the standard UV lithography in dye doped SU-8[56]. They have obtained laser emission in the chip plane at 551.39 nm with a FWHM linewidth below 150 pm.

1.5 Fluorescence related applications

Fluorescent dyes and fluorescence spectroscopy are attracting much interest in the areas of research and development in basic and applied sciences like molecular

biology, biochemistry, genomics, bioengineering, medical diagnosis and industrial microbiology. Fluorescent based techniques are now widely used to address the fundamental and applied questions in the biological and biomedical sciences. This is due to the high sensitivity of fluorescence detection [57]. Only few biogenic substances show adequate inherent fluorescence. Therefore fluorescent dyes are used to tag the substances of interest. In this way it is possible to determine the presence of molecules such as enzymes, proteins, DNA or antibodies even in a very low concentration down to single molecules [58]. Molecular methods for the early diagnosis of malignant disease have been considerably improved by employing fluorescence.

Multicolor staining with fluorescent dyes is actively used to observe the distribution of biological materials like proteins in the field of tissue and cell research. Fluorescence lifetime imaging microscopy is a new technology which can be used to visualize the factors that affect the fluorescence lifetime of the dye molecules that is, the state of the environment around the molecule. This technique also makes it possible to obtain information on the molecules while observing a living cell. The factors that affect the fluorescence lifetime include ion intensity, hydrophobic properties, oxygen concentration, molecular binding and molecular interaction. The extreme selectivity offered by fluorescence measurement is invaluable.

Fluorescence resonance energy transfer (FRET) is another technique which has found wide applications in biological analysis and biochemistry. The transfer of energy from a donor to an acceptor is significant only over distances of a few nm. Hence it can be used as spectroscopic ruler and as a means of detecting molecular interactions and conformational changes [59]. FRET makes it possible to measure the interactions between two proteins that are labeled with a pair of fluorescent dyes. Measurement of energy transfer can provide intra or intermolecular distance data for

proteins and their ligands in the range 1-10 nm. Green fluorescence protein (GFP) based fluorescence resonance energy transfer is widely used in investigations of intermolecular and intramolecular interactions in living cells [60]. Extreme selectivity of fluorescent labels that can target specific organisms opens new methods to resolve industrially and medically relevant problems in areas such as public health, safety of foods and environment monitoring.

1.6 Nonlinear properties of organic dyes

Studies of optical materials with large nonlinearity have received increasing attention of the researchers over the last two decades due to their potential applications in the area of optical communication, optical data processing, optical limiting, optical switching and many other related fields. The search for novel materials to realize the various needs of the photonics world has gained utmost importance. Variety of materials have been investigated for different NLO applications among which molecular crystals, semiconductors, organic molecules, liquid crystals, conjugated polymers and metallic nanocluster materials have yielded good results[61].

Since there are no symmetry requirements to observe third order nonlinearity, the organic materials are mostly studied for their third order nonlinearity. An intensity dependent refractive index variation and nonlinear transmission are the signatures of third order nonlinearity. The applications of organic materials are also classified accordingly: one which depends upon two photon absorption (TPA) or multiphoton absorption and the other which utilizes the nonlinear refractive index change. Materials with large TPA cross section are important for various applications in photonics and biophotonics like frequency up-conversion for lasers, optical power limiting, two photon excited fluorescence microscopy and two photon dynamic therapy [62-63]. Different forms of organic materials are investigated for these two

applications which include organic crystals, organic dyes, dye doped polymers, organic composites etc. The dye doped materials form an important class of materials for use in low power optical devices such as optical power limiters, low power optical phase conjugated mirrors and optical logic gates. The main attractions of organic materials are the ease with which these materials can be tailored by structural modifications and their chemical and optical stabilities.

1.7 Conclusion

The enormous potentials of organic dyes as a laser media are presented in this chapter. The various laser systems developed over the years and the developments and modifications achieved in device forms to satisfy the various needs of the photonics era are briefly discussed. The availability of a good number of organic dyes, the ease with which structural modifications can be made and the compatibility of dyes with many solid state host materials make the field wide open for further research. The scope of fluorescence dyes in the fields of biochemistry, molecular biology and diagnostics is also highlighted. Yet another field, the nonlinear optical properties of dyes, which could be tailored for different photonics applications, is also discussed very briefly.

1.8 Present work

Observing the wide possibilities of fluorescent dyes, an exhaustive investigation is done in laser dyes mainly focusing on Coumarin 540 which has a very strong emission in the green region. The photophysics of the dye is studied in detail in a good number of solvent environments. The results of the amplified spontaneous emission and lasing behaviour in both dye solution and different polymer solid state matrices and the ptotostability of the these matrices are investigated using the photoacoustic

technique and the same are also included in this thesis. The energy transfer behaviour in dye mixtures which could be utilized for laser studies and bio-analysis are also presented. The nonlinear characterization of Coumarin540 forms the last part of the experimental investigations presented in the thesis.

References

1. F.J. Duarte,L.W.Hillman, *Dye laser principles*, Academic Press,New York(1990)
2. F.P.Schafer, *Dye lasers,* Springer-Verlag,Berlin (I989)
3. O.Svelto ,D.C.Hanna, *Principles of lasers* 4th ed.Plenum press,New York (1998)
4. P.P.Sorokin, J.R.Lankard, *Stimulated emission observed from an organic dye, chloro-aluminum phthalocyanine,*IBM Journal of Research and development **10** (1996)162-163
5. B.B.Snavely, O.G.Peterson, R.F.Reithel, *Blue laser emission from a flashlamp –excited organic dye solution*, App.Phy.Lett. **11**(1967)275-276
6. M.Hercher ,H.A.Pike, *Single mode operation of a continuous tunable dye laser*,Opt. commun. **3**(1971) 346-348
7. *B.* B.B.McFarland , *Laser second –harmonic induced stimulated emission of organic dyes, A* App.Phys .Lett.**10** (1967) 208-209
8. F.P.Schafer,W.Schmidt, J.Volze, *Organic dye solution laser*, App.Phys.Lett. **9** (1966)3306-3309
9. B.H.Soffer, B.B.McFarland, *Continuously tunable, narrow-band organic dye lasers*, A App.Phy.Lett.**10** (1967) 266-267
10. F.P.Schafer,W.Schmidt, K.Marth, New *dye lasers covering the visible spectrum,* AApp.Phys.Lett. **24A** (1967) 280-281
11. V.D.Kotsubanov,Yu.V.Naboikin,L.A.Ogurtsova,A.P.Podgornyi,F.S.Pokrovskaya, *Xanthene dye series laser excited by second-harmonic radiation from a neodymium laser*, Soviet Physics- Technical Physics **13**(1969)923-924
12. F.Bos, *Versatile high power single-mode pulsed dye laser*, Appl.Opt.**20** (1981) 1886-1890
13. J.A.Myer, C.L.Johnson, E.Kierstead R.D.Sharma, I.Itzkan, *Dye laser emission with a*

pulsed N_2 laser at 3371 Å, Appl.Phys.Lett. **16** (1970) 3-5

14. I. Itzkan, F.W.Cunningham, *Oscillator-amplifier dye-laser system using N2 laser pumping*, IEEE J. Quantum Electronics,.**QE-8** (1972)101-105
15. R.Wallenstein,T.W.Hansch, *Powerful dye laser oscillator-amplifier system for high resolution spectroscopy*, Opt.commun.**14**(1975)353-357
16. O.G.Peterson,S.A.Tuccio,B.B.Snavely,*CW operation of an organic dye solution laser*, App.Phys.Lett.**17** (1970)245-247
17. M.Hercher, H.A.Pike, *Single mode operation of a continuous tunable dye laser*, Opt. Commun. **3** (1971) 346-348
18. S.Blit, E.G.Weaver, T.A.Rabson, F.K.Tittel, *Continuous wave uv radiation tunable from 285 nm to 400nm by harmonic and sum frequency generation,* Appl.Opt. **17** (1978) 721-723
19. H.W.Schroder, L.Stein, D.Frolich, B.Fugger, H.Welling, *A high-power single mode cw dye ring laser*, Appl.Phys.lett. **14**(1977) 377-380
20. W.Schmidt, F.P.Schafer, *Self mode-locking of dye lasers with saturable absorbers*, Phys. Lett.. 26A (1968) 558-559
21. I.S.Ruddock, D.J.Bradley, *Bandwidth-limited subpicosecond pulse generation in mode-locked cw dye lasers,* Appl.Phys.Lett. **29** (1976) 296-297
22. W.Dietel, J.J.Fontaine, J.C.Diels, *Intracavity pulse compression with glass: a new method of generating pulses shorter than 60 fsec.* Opt.Lett. **8**(1983) 4-6
23. R.L.Fork, C.H.Brito Cruz, P.C.Becker, C.V.Shank , *Compression of optical pulses to six femtoseconds by using cubic phase compensation*, Opt.Lett.**12** (1987)483-485
24. S.Szatmari,F.P.Schafer , *Subpicosecond, widely tunable distributed feedback dye laser* Appl.Phy.B, Photophy. And Laser chem.. **46** (1988) 305-311
25. N.Takeyasu, T.Deguchi, M.Tsutsumikawa, J.Matsumoto, *A Tunable Picosecond Dye Laser for Use in Dioxin Analysis,* Analytical Science ,**18** (2002) 243-246
26. O.G.Peterson B.B.Snavely , Stimulated emission from flash lamp excited organic dyes

in polymethyl methacrylate Appl.Phy.Lett.**12** (1968) 238-240

27. A.Costela,I.Garcia-Moreno J.M.Figuera,F.Amat-Guerri ,R Sastre, *Polymeric matrices for lasing dyes: recent developments*, Laser Chem.**18** (1998) 63-84
28. A.Costela, I.Garcia-Moreno, R Sastre, *Polymeric solid-state dye lasers: recent developments*, Phys.Chem.chem.Phys.**5** (2003)4745-4763
29. S. Schultheiss,Eli Yariv,R.Reisfeld,H.D.Breuer, *Solid state dye lasers: Rhodamines in silica-zirconia materials*, Photochem.Photbiolo.Sci.**1**(2003) 320-323
30. D.Lo, J.E.Parris,J.L.Lawless, *Multi-megawatt superradiant emission from coumarin doped sol-gel derived silica*, App.Phy.B.**55** (1992) 365
31. D.Lo, S.K.Sam,C.Ye,K.S.Lam, *Narrow linewidth operation of solid state dye laser based on sol-d\gel silica*, Opt.commun. **156** (1998)316-320
32. M.Canva, P.georges, J.F.Perelgritz, A.Braun, F.Chaput, J.P.Boilot, *Perylene and pyrromethene –doped xerogel for a pulsed laser,* App.Opt. **34** (1995)428
33. E,Yariv, S.Schultheiss, T.Saraidarov, R.Reisfeld, *Efficiency and photostability of dye doped solid-state lasers in different hosts*, Opt.Mat. **16** (2001) 29-38

. Y.Yang,G.Qian, Z.Wang, M.Wang,Opt.communication.**204**(2004) 277-282

34. R.Sastre, A.Costela, Polymeric *solid-state dye lasers*, Adv.Mat. **7** (1995) 198-202
35. S.Singh, V.R.Kanetkar,G.Sridhar,V.Muthuswamy,K.Raja,*Solid-state polymeric dye lasers*, Joul.of Lumines.**101** (2003)285-291
36. A.Costela, I.Garcia-Morena, C.Gomez, O.Garcia, R.Sastre, *Enhancement of laser properties of pyrromethane 567 dye incorporated into new organic-inorganic hybrid materials*, Che.Phys.Lett.**369** (2003) 656-661
37. A.Costela, I.Garcia-Moreno, C.Gomez, O.Garcia, L.Garrido, R.Sastre, *Highly efficient and stable doped hybrid organic-inorganic materials for solid-state dye lasers,* Che.Phys.Lett. **387** (2004) 496-501
38. D.P.Schinke, R.G.Smith,E.G.spencer, M.F.galvin, *Thin film distributed feed back laser fabricated by ion milling*, App.Phys.Lett.**21**(1972) 494

39. A.Mukherjee,*Two-photon pumped up-converted lasing in dye doped polymer waveguides*, Appl.Phys.Lett.**62** (1993) 3423-3425
40. Y.Sorek,R.Reisfeld,I.Finkelstein, S.Ruschin, *Light amplification in a dye doped glass planar waveguide*,Appl.Phys.Lett. **66** (1995) 1169-1171
41. I.Federlik,*Opticalproperties of glass* ,Elsevier, Amsterdam(1983)
42. Y.Sorek, R.Reisfeld, R.Tenne, *The microstructure of titanium –modified silica glass waveguides prepared by sol-gel method*, Che.Phys.Lett .**227** (1994) 235 -242
43. Y. Sorek, R. Reisfeld, I. Finkelstein, S. Ruschin, *Sol-gel glass waveguides prepared at low temperature,* App.Phys.Lett, **63** (1993)3256-3258
44. X.Peng, L.Liu, J.Wu,Y.Li,Z.Hou,L.Xu, W.Wang, F.Li, *Wide range amplified spontaneous emission wavelength tuning in a solid state dye wave-guide*,Opt.Lett.**25** (2000) 314-316
45. A.Otomo, S.Yokoyama, T.Nakahama, S.Mashikop, *Supernarrowing mirrorless laser emission in dendrimer–doped polymer waveguides*,Appl.Phys.Lett.**77**(2000) 3881-3883
46. M.Saito, H.Ishiguro, *Anisotropic fluorescence emission of a dye doped fiber ring that is pumped by a ring laser beam,* J.Opt.A: Pure.Appl.Opt. **8** (2006) 208-213
47. A.Tagaya,S.Teramoto, T.Yamamoto, K.Fujii, E.Nihei, Y.Koike, K.Sasaki, IEEE Quan.Electro.**31** (1995) 2215-2220
48. G.D.Peng, P.L.Chu, Z.Xiong, T.W.Whitbread, R.P.Chaplin, *Dye doped step index polymer optical fiber for broadband optical amplifier*,J.Lightwave Tech.**14** (1996) 2215-2223
49. A.Tagaya, Y.Koike,T.Kinoshita, E.Nihei, T.Yamamoto, K.Sasaki, *Polymer optical fiber amplifier*, Appl.Phy.Lett.**63** (1993) 882-884
50. H.Liang,Z.Zheng,Z.Li,Jie Xu,B.Chen,H.Zhao,Q.Zhang,H.Ming, *Fabrication and amplification of Rhodamine B-doped step-index polymer optical fiber,* J.App.Polymer science, **93** (2004) 681-685
51 R.Gvishi,G.Ruland,P.N.Prasad, *New laser medium: dye doped sol-gel*

fiber,Opt.Commun. **126** (1996)66-72

52. T.Kobayashi,W.J.Blau,H.Tillmann,H.Horhold,*Blue lasing from a stilbenoid-compound –doped glass-clad polymer optical fiber*, J.Opt.A: Pure App.Opt.**4** (2003) L1-L3
53. K.Kuriki, T.Kobayashi, N.Imai, T.Tamura, S.Nishihara,Y.Nishizawa, A.Tagaya, Y.Koike,Y.Okamoto,*High efficiency organic dye doped polymer optical fiber lasers*,Appl.Phys.Lett. **77** (2000) 331-333
54. B.Helbo,A.Kristensen,A.Menon, *A micro cavity fluidic dye laser,* J.Micromech. microeng, 13 (2003) 307-311
55. B.Bilenberg,B.Helbo, J.P.Kutter,A.Kristensen, *Tunable micro fluidic dye laser*,12th International conference on solid state sensors, Boston (2003)
56. S.Balslev,A.Mironov,D.Nilsson,A.Kristensen, *Micro-fabricated single mode polymer dye laser*,Optics Express, **14** (2006) 2170-2177
57. J.R.Lakowicz, *Radiative decay engineering: Biophysical and biomedical applications,* Analytical Biochemistry, **298** (2001) 1-24
58. N.U.Kemnitzer,A.Zilles,J.A.Jacob,K.H.Drexhage,M.Gross,M.Hamers,*Fluorescent dyes –detection methods of the future*, BIO forum International,(2002)242-243
59. J.N.Miller, *Fluorescence energy transfer methods in bioanalysis*, Analyst.**130**(2005) 265-270
60. Z.Xia,Y.Liu, *Reliable and global measurement of fluorescence resonance energy transfer using fluorescence microscope*, Biophysical Journal.**81** (2001) 2395-2402
61. R.A.Gannev, *nonlinear refraction and nonlinear absorption of various media*, J.Opt.A: pure and App.Opt. **7** (2005)717-733
62. J.D.Bhawalkar, G.S.He, P.N.Prasad, *Nonlinear multiphoton processes in organic and polymeric materials*,Rep.Prog.Phys.**59** (1996) 1041-1070
63. T.Kobayashi, *Nonlinear optics of organics and semiconductors*,T.Kobayashi, *Nonlinear optics*,1,Springer –Verlag,Berlin (1991)

Chapter 2

Photophysical, ASE and Lasing Properties of Coumarin 540

"If we know what we were doing it wouldn't be research".
Einstein

Abstract

The results of a detailed investigation of the various photophysical properties of Coumarin 540 laser dye in various solvent environments are reported. The effect of solvents on the quantum yield, lifetime, radiative and nonradiative decay rates, stokes'shift etc. is analyzed. Amplified spontaneous emission exhibited by the dye solution in methanol is studied in terms of excitation length and pump energy. Coumarin 540 dye solution contained in a quartz cuvette exhibits laser emission with well-resolved, equally spaced modes which originates from the subcavities formed between the walls of the cuvette. While the quantum yield remains a decisive factor, a clear correlation between the refractive indices of the medium which determines the reflectivity at the end faces of the cuvette, and the number of modes exhibited by the emission spectra of the respective samples has been demonstrated.

2.1 The Photophysics of Laser dyes

The significant properties of organic dyes which make them very attractive in the photonics world of application are the large absorption and emission cross sections which they exhibit in the visible part of the spectrum over a wide range of wavelengths. They constitute a large class of polyatomic molecules containing long

chains of conjugated double bonds. The large absorption cross section σ_a is due to the presence of large dipole moment μ originating from the π electrons of carbon. These π electrons are free to move over a distance roughly equal to the chain length L. Since the chain length L is quite large, correspondingly μ is also large. The absorption cross section σ_a which is proportional to μ^2 is of the order of 10^{-16}cm ^{2} [1]. Compounds with conjugated double bonds absorb light at wavelengths above 200 nm. The large number of conjugated double bonds present in organic dyes also increases the absorption in the visible part of the spectrum [2]. The dyes display strong broadband fluorescence spectra under excitation by visible or UV light. With different laser dyes the overall spectral range extends from 300 nm to 1.2 μ m.

2.1.1 Energy level diagram

The photophysics of laser dyes can be well explained by considering the energy level diagram. A schematic energy level diagram for laser dyes is shown in Fig.2.1. It consists of singlet states S_0, S_1, S_2 ...etc. with total spin zero and triplet states T_0.T_1...etc. with total spin one. Each electronic level has a manifold of vibrational states due to the many internal degrees of freedom of a complex molecule. Even more finely spaced are the rotational sublevels of each vibrational state. The total manifold of states is so dense that the absorption and emission spectra of a dye forms a continuum. Following light absorption, a sequence of different processes occurs. Optical excitation occurs in the singlet manifold. A fluorophore is usually excited to some higher vibrational levels of either S_1 or S_2. From these excited states they can relax to lower energy states through internal conversion or intersystem crossing. Internal conversion is the radiationless process by which a molecule transfers itself from one electronic state to another electronic state of the same multiplicity or within the same electronic state while in intersystem crossing the energy transfer occurs between electronic states of different multiplicity. The rate of

internal conversion between excited singlet states is extremely high, of the order of 10^{11}-10^{13} s^{-1} and consequently the lifetimes of upper excited singlet states are very short (10^{-11}-10^{-13} sec.). The deactivation to the S_1 state takes place before any radiative transitions or photo-reactions involving the upper state can take place. The lowest vibrational state of S_1 decays to the ground state by radiative emission or by the nonradiative pathway of internal conversion and by intersystem crossing to the triplet manifold. Normally the radiative emission is between the lowest level of S_1 and the various levels of the S_0 state. The transition from the excited singlet state to the ground state is quantum mechanically allowed as this does not require a change of spin orientation. The lifetime of this fluorescence emission is typically a few nanoseconds. Internal conversion is generally complete before this emission.

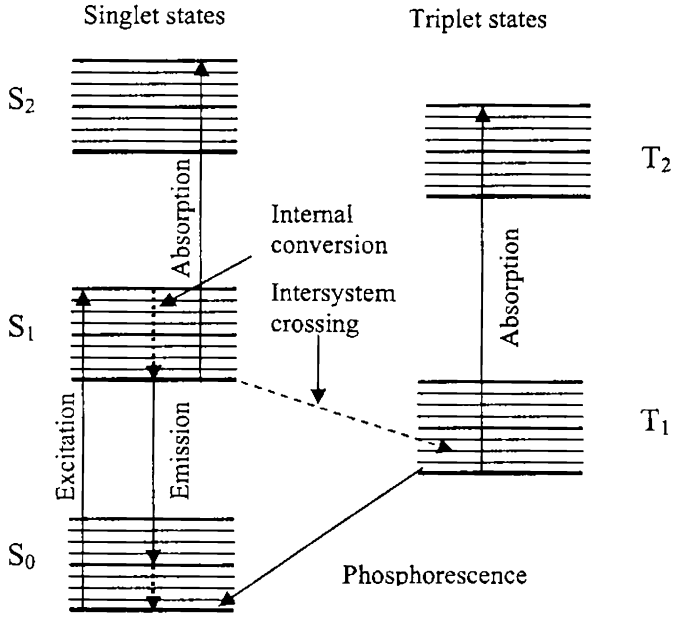

→ radiative transition - - - - - ▸ nonradiative transition

Fig.2.1 Diagram illustrating the energy levels of a dye.

Intersystem crossing between the singlet and triplet state is spin forbidden. Though the transition from S_1 to T_1 is radiatively forbidden, for organic dye molecules, the interaction of electron spin and orbital motion leads to inter system crossing. Radiationless transfer can also occur by external perturbations like collisions. The rate constant k_{ST} of intersystem crossing usually occurs at a much lower rate($\sim 10^7$ s^{-1}). Since the triplet – singlet transition is spin forbidden, the lifetime of the triplet state is large. While the molecule is in the lowest level of T_1, it can also absorb radiation and optically allowed T_1 to T_2 transition may occur. This absorption tends to occur in the same wavelength region where fluorescence emission occurs and this may even quench the laser emission [3].

The rates of internal conversion and intersystem crossing processes are dependent on the energy separation between lowest vibrational levels of the states involved; the larger the separation, the slower the rate. The large energy separation between the lowest vibrational levels of S_1 and S_0 states and T_1 and S_0 states reduces the decay rate of the S_1-S_0 internal conversion and T_1-S_0 intersystem crossing which is of the order of 10^6 to $10^{12}s^{-1}$ and 10^{-2} to 10^6 s^{-1} respectively [4-5]. The decay from T_1 to S_0 state can be radiative or nonradiative and is termed as phosphorescence when it is radiative.

The process of dye fluorescence must compete with nonradiative decay of excited states by internal conversion to the ground state or by intersystem crossing to the triplet state. The long lifetime of the triplet state of the dye not only allows buildup of a species that may be chemically reactive but also provides a competitive absorber at lasing wavelengths. There is also a possibility of further excitation from the S_1 manifold to higher-lying singlet states. However, the cross section of the excited state absorption is 100 times smaller than that for ground state absorption [6].

2.1.2 Absorption and fluorescence spectral characteristics

The absorption spectra of organic dyes have a large spectral width which usually covers several tens of nanometers. In the general case of a dye molecule which consists of a large number of atoms, many normal vibrations of different frequencies are coupled to the electronic transition. The collisional and electrostatic perturbations caused by the surrounding solvent molecules further broaden the individual lines of such vibrational series. Every vibronic sublevel of electronic state has been further superimposed by rotationally excited sublevels. These are highly broadened by the frequent collisions with the solvent molecules and there is a quasi-continuum of states superimposed on every electronic level. Thus the absorption is practically continuous all over the absorption band. The same is true for the fluorescence emission corresponding to the transition from the electronically excited state of the molecule to the ground state. This results in a mirror image of the absorption band displaced towards higher wavelengths [3-4].

2.1.3 Solvent effect on fluorescence spectra

It has been shown that solvents play a decisive role in laser dye photophysics. The active medium of dye laser consists of typical organic dye concentration of 10^{-2} -10^{-5} M dissolved in a certain solvent. For this reason the dye solvents have a major role in the design of dye lasers. Lasing wavelength and energy are very sensitive to the choice of solvents. The interaction between the solvent and the fluorophore molecules affects the energy difference between the ground state and the excited states. This energy difference is attributed to the refractive index n and the dielectric constant ε of the solvent and is described by the Lippert equation

$$\bar{\nu}_a - \bar{\nu}_f \cong \frac{2}{hc}\left(\frac{\varepsilon - 1}{2\varepsilon + 1} - \frac{n^2 - 1}{2n^2 + 1}\right)\frac{(\mu^* - \mu)^2}{a^3} + const. \qquad (2.1)$$

Here h is the Planck's constant, c is the speed of light, $\mu^*-\mu$ is the change in dipole moment and a is the radius of the cavity where the fluorophore resides. The wave numbers in cm^{-1} of the absorption and emission are $\bar{\nu}_a$ and $\bar{\nu}_f$ respectively and the difference between them is the Stoke's shift [3].

Most laser dyes are polar ones and excitation into their low lying excited singlet state will be accompanied by an increase in the dipole moment. The solvent polarity have a decisive role in shifting the lasing wavelength. In most of the cases, increasing the solvent polarity will shift the gain curve towards the longer wavelength side which is known as the Stoke's shift. In high polar solvents the shift can be as high as 20-60 nm. Some solvents cannot be used in the longer wavelength side due to vibrational overtones of the solvents which will interfere with the lasing process. Solvents like water, methanol and ethanol which would appear optimal solvents for many dyes are not useful for the near-IR and IR dyes [2, 4].

2.1.4 Stoke's shift and solvent polarity function

The Stoke's shift is a property of the dielectric constant (ε) and refractive index (n) of the solvent. They have opposite effect on the Stoke's shift. An increase in n will decrease this shift, whereas an increase in ε results in an increase in the shift. These different effects are a result of Frank- Condon principle. An increase in n allows both the ground and excited states to be stabilized instantaneously by movements of electron within the solvent molecules. This electron redistribution results in decrease in energy difference between the ground and excited states. An increase in ε also results stabilization of the ground and excited states. However, the energy change of

the excited state occurs only after reorientation of the solvent dipoles. The Stoke's shift is related to the orientation polarizability term Δf which is also known as solvent polarity function which is given by

$$\Delta f = (\frac{\varepsilon - 1}{2\varepsilon + 1} - \frac{n^2 - 1}{2n^2 + 1}) \tag{2.2}$$

The first term accounts for the spectral shifts due to both reorientation of the solvent dipoles and to the redistribution of the electrons in the solvent molecules. The second term accounts only for the redistribution of the electrons. The difference of these two terms accounts for the spectral shifts due to reorientation of the solvent molecules. Thus only solvent reorientation is expected to result in substantial Stoke's shifts [3].

2.1.5 Fluorescence quantum yield

The fluorescence quantum yield is the ratio of the number of photons emitted to the number of photons absorbed by the sample.

$$\Phi = \frac{photons_{em}}{photons_{abs}} \tag{2.3}$$

The quantum yield Φ can also be described by the relative rates of the radiative and nonradiative decay pathways, which deactivate the excited state.

$$\Phi = \frac{k_r}{k_r + \sum k_{nr}} \tag{2.4}$$

where k_r is the emissive rate of the fluorophore and k_{nr} is the rate of radiationless decay. Here $\sum k_{nr}$ describes the sum of the rate constants for the various processes that compete with the emission process. These processes include photochemical and dissociative decays, where the latter includes nonradiative transitions namely

intersystem crossing and internal conversion. The rate constants k_r and k_{nr} both depopulate the excited state. Quantum yield gives the probability of the excited state being deactivated by fluorescence rather than any other nonradiative mechanism. The important competition between dye fluorescence, intersyatem crossing and internal conversion is reflected in quantum yields. Laser dyes show a high quantum yield for fluorescence emission. (Rhodamine 6G ~0.95)[5-6].

2.1.6 Fluorescence lifetime

The lifetime of the excited state is defined by the average time the molecule spends in the excited state prior to return to the ground state which is denoted by τ. The lifetime of the fluorophore in the absence of nonradiative processes is called intrinsic lifetime or natural lifetime and is given by $\tau_0 = \frac{1}{k_r}$ (2.5)

This leads to the relationship for quantum yield

$$\Phi = \frac{\tau}{\tau_0} \tag{2.6}$$

The quantum yield is the fraction of the excited fluorophores which decay by emission (k_r) relative to the total decay ($k_r + k_{nr}$) and thus by the ratio in equation 2.4. The lifetime of a fluorophore is determined by the sum of the rates which depopulate the excited state. In the absence of other quenching interactions, the lifetime is given by

$$\tau = (k_r + k_{nr})^{-1} \tag{2.7}$$

The lifetime of a fluorophore is increased or decreased by the change in the value of k_{nr}. Almost invariably, the lifetimes and quantum yields increase or decrease together [7]. The lifetime τ alone is insufficient to distinguish changes in radiative rates from changes in non radaitive rates. Measurements of fluorescence quantum yields are

needed to distinguish the two contributions. The radiative rate k_r and the nonradiative rate k_{nr} are calculated by the equations

$$k_r = \frac{\Phi}{\tau}$$

$$k_{nr} = \frac{(1-\Phi)}{\tau} \qquad (2.8)$$

Of course k_{nr} represents the sum of different processes.

2.2 Structure of Coumarin 540 (C 540)

Coumarin derivatives with an amino group in the 7-th position are very efficient laser dyes in the blue-green regions of the spectrum. Coumarin 540 is 3-(2-Benzothiazolyl)-7-diethylaminocoumarin (C 540) whose molecular structure is given in Fig.2.2 Substitution of coumarin with an amino group in the 7th position generates a merocyanine chromophore characterized by the conjugation of push pull substituents (amine electron donor and carbonyl (C=O) electron acceptor groups). This pattern of substitution gives rise to an intramolecular charge transfer (ICT) transition for which there is large oscillator strength for absorption (S_0-S_1) and a high rate of fluorescence emission. A much higher dipole moment is predicted for S_1 [2]. The details of the investigations carried out on the photophysical properties of the laser dye C 540 along with its lasing characteristics are given in the following sections.

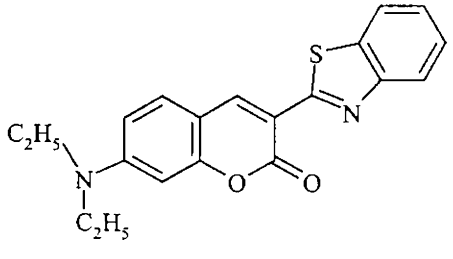

Fig 2.2 Molecular Structure of Coumarin 540 ($C_{20}H_{18}N_2O_2S$)

2.3 Experimental details

2.3.1 Absorption and fluorescence spectra

The photophysical properties of Coumarin 540 are investigated in detail in different solvent environments by selecting 10 different solvents which comprise of polar protic, dipolar aprotic and nonpolar solvents. Laser grade Coumarin 540 is obtained from Exciton. All the solvents used for the experiments are of spectroscopic grade. The absorption and fluorescence spectra are recorded using UV-VIS spectrophotometer (Jasco V-570) and Cary Eclipse spectrofluorimeter respectively. The typical form of absorption and fluorescence spectra of the dye Coumarin 540 in three different solvents is given in Fig.2.3 and Fig.2.4.

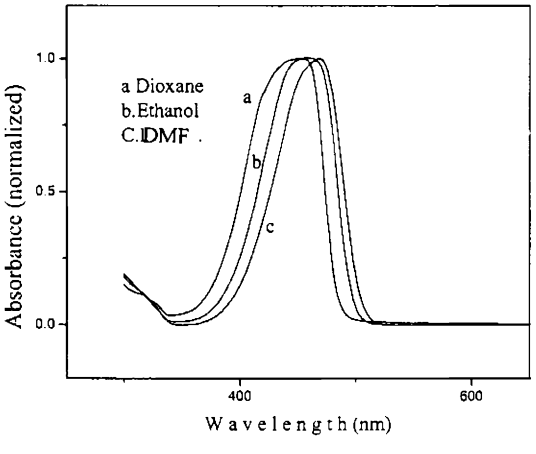

Fig.2.3 Absorption spectra of C 540 in dioxane, ethanol and dimethyl formamide

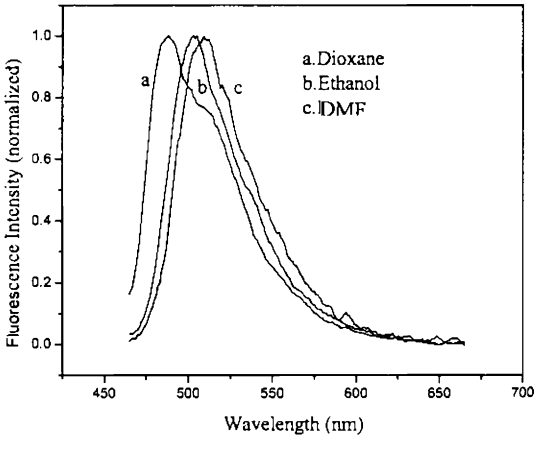

Fig.2.4 Fluorescence spectra of C 540 dioxane, ethanol and dimethyl formamide

Both the absorption spectra and fluorescence spectra exhibit wavelength shift with solvent polarity and the Stoke's shift is also different correspondingly. Since absorption is a property of the ground state and fluorescence that of the excited state with greater dipole moment, both the shifts need not be the same. For a better comparison, the solvent polarity function is calculated taking dielectric constants and refractive indices of pure solvents from literature. The absorption and emission maximum in different solvents are included in Table 2.1. Fig 2.5 shows the Stokes's shift vs Δf. Three different regions are observed in the plot. Almost a linear relation is found for dipolar aprotic solvents. For polar solvents and dipolar aprotic solvents with high polarity, there is significant red shift in the fluorescence maximum. Upon excitation, the dipole moment of the dye molecule is increased and the dipole –dipole interaction between the solvent and solute molecules will result in the reduction of excited state energy. It is reported that coumarin dye may be quite polar in nature both in the ground and excited states due to the planar intramolcular charge transfer (ICT) state [8-10]. For the non-polar solvent toluene, a deviation is observed from the linear behavior and a blue shift is observed in the peak value of absorption and fluorescence compared to the observed values in other solvents. In nonpolar solvents, the dye may not exist in the polar ICT structure. It is known that the coumarin derivatives prefer to exist in nonpolar structures in nonpolar solvents. Since the dye molecule is much less polar in nature in comparison to the polar ICT structure of the dye, a less value is expected for Stoke's shift in toluene. But the plot of Stokes' shift vs Δf shows a comparatively high value. The deviation in the Stokes's shift of the dye is attributed to a conformal change for the dye molecule at its 7-NEt_2 group in nonpolar solvents. It is inferred that C 540 exists in a non polar structure, when the 7-NEt_2 groups adopts a kind of pyramidal conformation [10-14].

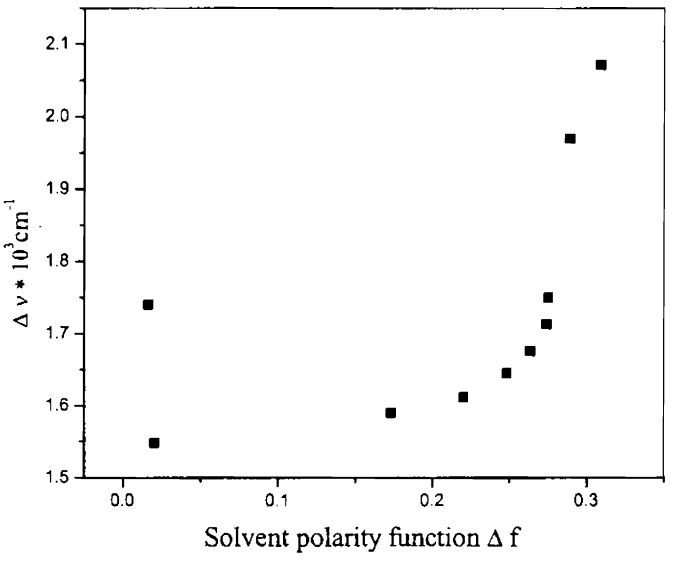

Fig.2.5 Plot of Stokes's shift ($\Delta\nu$) of C 540 against solvent polarity function Δf

2.3.2 Quantum yield measurements

The most reliable method for recording Φ is the comparative method of Williams et al. which involves the use of well characterized standard samples with known Φ values [15]. Here, the assumption made is that the samples with identical absorbance at the same wavelength can be assumed to absorb the same amount of photons. Hence a simple ratio of the integrated fluorescence intensities of the two solutions will yield the ratio of the quantum yields. Knowing the Φ of the known sample, the Φ value for test sample can be calculated. The quantum yield of the test sample is calculated from the following equation

$$\Phi_X = \Phi_{ST}\left(\frac{Grad_X}{Grad_{ST}}\right)\left(\frac{\eta_X^2}{\eta_{ST}^2}\right) \qquad (2.9)$$

where the subscripts ST and X denote the standard and test samples respectively, Φ is the fluorescence quantum yield, Grad is the gradient from the plot of the integrated fluorescence intensity vs absorbance and η is the refractive index of the solvent. Initially two standard compounds are cross calibrated using the above equation.

For the quantum yield measurements, the absorbance of the samples is determined by taking the samples in a quartz cuvette with 1 cm path length. While recording the absorption spectra care is taken to keep the absorbance of all the samples below 0.1 in order to minimize the effect of re-absorption.

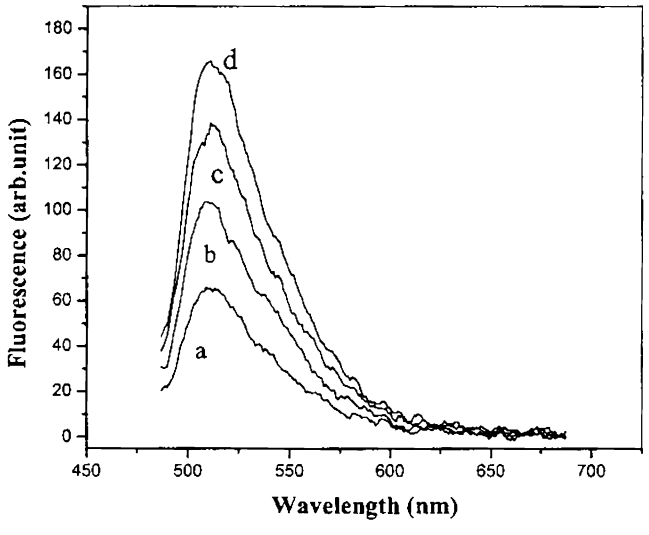

Fig.2.6 The fluorescence intensity for various absorbance of C540 (A<0.1 cm^{-1}) in DMSO used for Quantum yield calculation.

Rhodamine 6G in ethanol is taken as the reference sample for which the quantum yield is 0.95[16]. For cross calibration, Rhodamine 6G and Rhodamine B in

ethanol are taken as the standard samples. Quantum yield of each sample is calculated relative to the other and values of 0.95 ± 0.01 and 0.65 ± 0.015 are obtained which are in quite match with the literature values of 0.95 and 0.65 for Rh6G and RhB respectively [16]. For the reference sample and test samples the excitation wavelength of choice is 485 nm. For all the fluorescence measurements, the absorbance is selected as quite low (<0.1) at the excitation wavelength. The fluorescence spectra for C 540 in DMSO for different absorbance are given in Fig.2.6. Correction for the background fluorescence of the solvent is done by subtracting the emission spectrum of the solvent from the emission spectrum of the sample and the corrected emission spectrum is used for calculating the area under the curve.

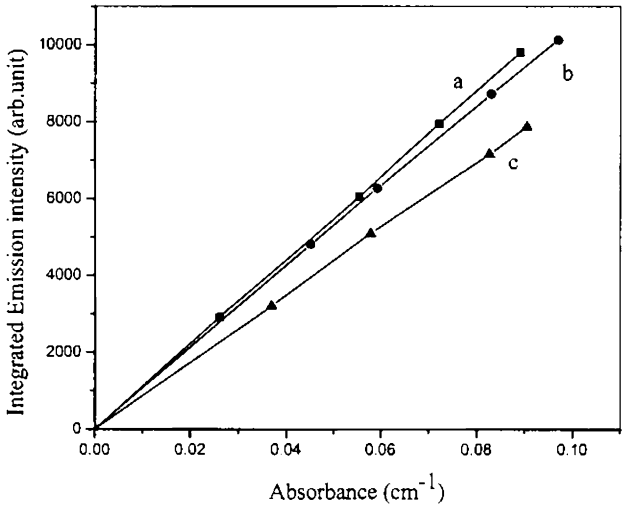

Fig.2.7 Linear plots for emission intensity of dye in two solutions
a)Ethanol b) MEK C) Reference sample Rh6G in ethanol

The quantum yield of C 540 in different solvents are calculated by plotting the emission intensity vs absorbance which is obtained as straight lines passing through

the origin (Fig.2.7). Fluorescence quantum yields estimated for the dye in different solvents are listed in Table 2.1. Though there is no well-established theory to correlate Φ and Δf, a linear relationship is found between Φ and Δf with some exceptions. The quantum yield of the dye is found to be very high in highly polar solvents which approach unity in ethanol. A clear deviation in Φ is observed for non polar solvents which are much less than the value in polar solvents.

Solvent	Polarity index	Absorption λ_{max}(nm)	Emission λ_{max}(nm)	ϕ
Toluene	2.4	440	483	0.76±0.015
Dioxane	4.8	452	486	0.8±0.02
Butyl acetate	3.9	452	487	0.85±0.015
Dichloromethane	3.4	461	498	0.98±0.02
Cyclohexanone	4.5	462	500	0.97±0.015
Dimethyl sulphoxide	6.5	469	509	0.96±0.01
Methyl ethyl ketone	4.5	458	497	0.97±0.015
Dimethyl formamide	6.4	464	505	0.94±0.02
Ethanol	5.2	456	501	0.99±0.015
Methanol	6.6	458	506	0.91±0.01

Table.2.1 Solvent effect on different decay parameters

2.3.3 Lifetime measurements

Fluorescence lifetime measurements are taken using a time-correlated-single –photon-counting spectrometer (IBH-datastation-UK) with 440 nm nano LED as an excitation source. Instrument response function for the setup is ~200 ps at FWHM with a repetition rate of 1MHz. For all the solvents studied, the fluorescence decay curves are found to be double-exponential. For data fitting, the χ^2 values are close to unity and the distribution of the weighted residuals is quite random among the data channels.

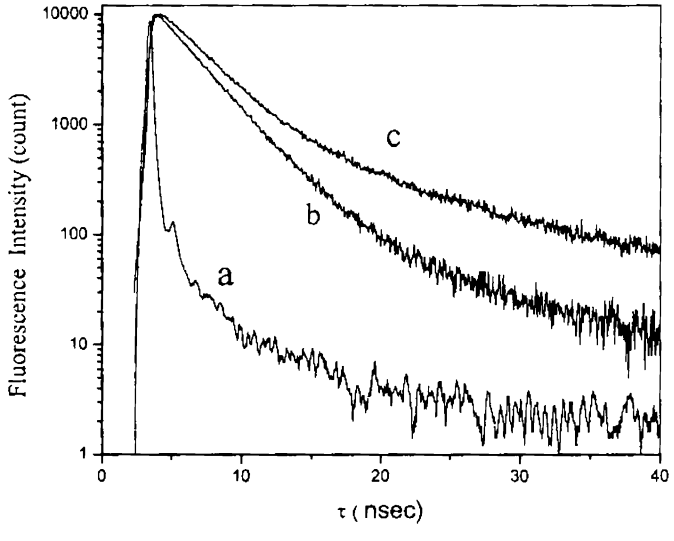

Fig.2.8 Fluorescence decay curves of dye in two solvents
a)reference b) toulene c) ethanol

The fluorescence decay values estimated for different solvents are given in Table 2.2. The lifetimes of the dye are comparatively high for solvents in which the quantum yield is high. Fig.2.8 shows the decay curves for the dye in two sample solvents.

In order to understand more about the de-excitation process, the radiative and nonradiative rate constants for the excited state of the dye are calculated using the relations

$$k_r = \Phi / \tau$$

$$k_{nr} = (1/\tau) - (\Phi/\tau) \qquad (2.10)$$

The k_r and k_{nr} values estimated for the dye in different solvents are given in Table 2.2 The radiative rates are found to be comparatively high for the dye in solvents which exhibit high quantum yield. On the other hand for solvents having less quantum yield, the nonradiative rates are found to be high. Usually the radiative rates are not much different since these rates depend on the extinction coefficient of the dye.

Solvent	ε	τ (ns)	k_r (ns^{-1})	k_{nr} (ns^{-1})
Toluene	2.4	3.06	0.248	0.078
Dioxane	2.2	3.1	0.258	0.064
Butyl acetate	5.1	3.13	0.272	0.048
Dichloromethane	9.1	3.32	0.295	0.006
Cyclohexanone	18.2	3.2	0.303	0.009
Dimethyl sulphoxide	47.2	3.11	0.308	0.013
Methyl ethyl ketone	18.5	3.3	0.294	0.009
Dimethyl formamide	38.3	3.14	0.299	0.019
Ethanol	24.3	3.41	0.290	0.0029
Methanol	33.1	3.2	0.284	0.028

Table.2.2 Solvent effect on different decay parameters

Life time changes are usually caused by changes in the nonradiative rates resulting from the additional decay routes possible in the solvent environments. The nonradiative rate is found to be high for the dye in nonpolar solvent toulene whose dielectric constant is 2.4. High nonradiative decay rates are also observed for dye in dioxane and butyl acetate whose dielectric constants are low compared to other solvents (2.2 and 5.1 respectively). A higher value of ε will result in stabilization of the ground and excited states of the dye molecule which may increase the quantum yield [3].

2.4 Photochemical effect

The effect of molecular structure of coumarin derivatives with an amino group in position 7 and the nature of the solvent on the solute/solvent interactions have attracted much attention. The formation of specific hydrogen bonds between coumarin dyes and protic solvents has been considered to explain the spectral shift and internal conversion process. The photochemical aspects of C 540 have been investigated by many researchers. The photochemical reactivity of C540 in halomethane solvents, owing to their physiochemical properties, is also studied upon radiation at 254 nm [17]. Here, we report the photochemical reactivity of C 540 in dichloromethane and chloroform under pulsed excitation at a wavelength of 475 nm.

C 540 dye undergoes a photochemical reaction in these two solvents. Absorbance of the dye solution in the two solvents is taken after irradiating the samples for different time durations which varied up to 30mts. As the time of excitation increases, a decrease in absorbance is observed for both of the samples with the generation of a new band at higher wavelengths. The intensity of the new band increases with increase in the time of irradiance as shown in Fig.2.9 A and B. For the dye in chloroform, as the time of irradiation increases to 30 mts, a reduction in

absorbance of the new band is observed. This is due to the low stabilization of the excited species by the less polar $CHCl_3$. Fig 2.9-e shows the reduction in intensity of absorption of the new band which corresponds to an excitation time of 30 mts.

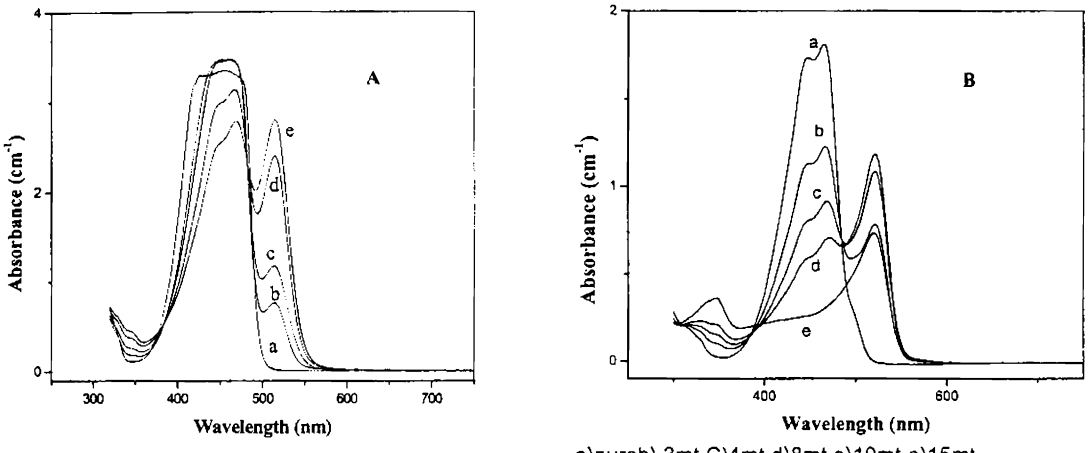

a)pureb) 3mt C)4mt d)8mt e)10mt e)15mt

Fig.2.9 Absorption spectra of C 540 after excitation for different timings.
A) in dichloromethane B) chloroform
a) pure b) 5 mt c) 10 mt d) 20mt e) 30 mt

The photoreaction observed in the chloromethanes can be explained in terms of an intermediate exciplex formation. The excited state of aromatic carbons is expected to be involved in a charge transfer interaction with chloromethane through exciplex formation. The intensity of the new band is found to be more in dichloromethane. Due to exciplex formation, the compound exhibits different emission characteristics. The chloromethanes are strong hydrogen bond donors (HBD) and form hydrogen bonds with tertiary amines. The HBD ability of CCl_4 is less compared to CH_2Cl_2. The hydrogen bond formation becomes stronger in the excited state of CH_2Cl_2 due to increasing basicity of the excited dye [17].

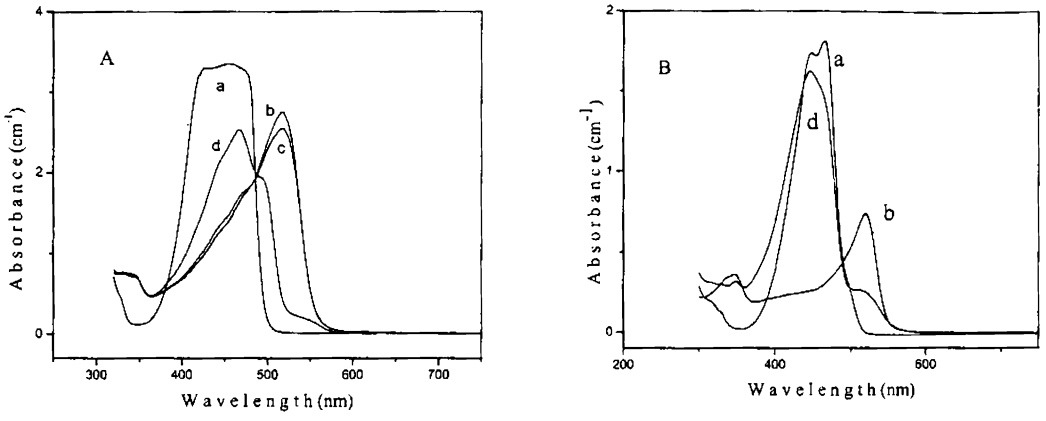

Fig.2.10 absorption spectra of C 540 A)dichloromethane B)chloroform
a) pure b) exciting for 30mt c) 30mts after excitation d) 2 days after excitation

The photochemical reactions in dichloromethane and chloroform are found to be reversible to some extent. We have taken the absorbance of the dye in the above two solvents two days after the excitation (Fig.2.10 A & B).The intensity of the new bands formed by the photochemical reaction have been observed to die out strongly. It is reported that due to the photoreactivity of C 540 in chloromethanes, a C 540 radical cation along with a chloride ion is formed as the end product [17]. This photoproduct is thermodynamically less stable. When the beam of excitation is cut off, two or more C 540 radical cations will exothermally react together to form a more stable dication or dianion. The absorbance of these more stable intermediate products in the two solvents is shown in fig.2.10 A & B. The new band with a small red shift in absorbance is found to be a stable one. The absorbance of the dye solution taken after one month does not exhibit any noticeable variation. The end product of the photochemical process exhibits a red shifted fluorescence.

2.5 Amplified spontaneous emission (ASE)

2.5.1 Introduction

Amplified spontaneous emission is a phenomenon readily observed in organic dye solution when the sample is excited by intense light pulses. The spontaneously emitted light is amplified through a single pass in the gain medium by stimulating the emission of more photons as it travels down the length. The favorable condition for strong ASE is a high gain medium combined with a long path length in the active material. This usually occurs in a gain medium with long path length either by internal multiple reflections or extended medium [18].

The shape of the medium can impose a preferred direction on the radiation it emits. As shown in Fig.2.11 the spontaneous emission along the long axis may experience a large amplification than that in the other directions producing a beam of ASE with a divergence angle depending on the length of the amplifier. This divergence is related to the length of the amplifier by the relation L/a which is also refereed to as the aspect ratio. The power emitted as fluorescence increases rapidly with gain. As the pump power increases ASE becomes the dominant mechanism. At that point, an intense emission within a solid angle Ω around the axis of the active material is observed from each end of the rod where $\Omega = a/L^2$. Here L and a are the rod length and the cross sectional area respectively. As a result of refraction at the end faces, the geometrical aperture angle of the material will increase by $n^2\Omega$. As the length of the gain medium increases, the divergence angle decreases and the output beam becomes highly directional (Fig.2.12).

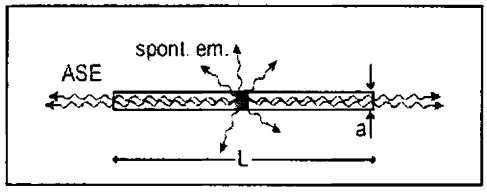

Fig.2.11 Spontaneous emission along the length is amplified to give ASE

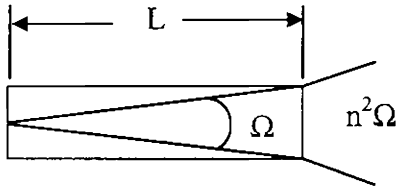

Fig.2.12 Dirtectionality of ASE with a divergence angle Ω

2.5.2 Features of ASE

In contrast to spontaneous emission, ASE possesses certain distinctive features of laser emission such as directionality, spectral narrowing, limited coherence, reduced pulsewidth, a soft threshold, intense beam and saturation of gain [19]. It is highly directional since ASE will build up in the direction of largest gain which is the direction of propagation. ASE accelerates the decay and shortens the output. The gain is the strongest at the wavelength where the cross section for stimulated emission is highest. This leads to narrowed spectral width. The ASE threshold behavior arises from the saturation .If the traveling wave becomes strong enough to extract all the stored energy (I_{SAT}), the output grows linearly with the pump power as observed in as ordinary laser. Since the ASE shows features of laser emission to some extent even in the absence of any external cavity, it is also known as a mirriorless lasing.

2.5.3 Experimental details to study ASE

The amplified spontaneous emission is studied in Coumarin 540 dissolved in methanol. The concentration chosen for the present study is $4x10^{-4}$ M. The ASE studies of the dye solution are conducted by taking the sample solution in a quartz

cuvette of 1 cm x1 cm x 3 cm dimensions. The emission spectra are recorded by exciting the sample with 476 nm radiation at which the sample has good absorption. The pump beam is taken from a Quanta Ray MOPO (MOPO 700) pumped by Q-switched Nd:YAG laser which emits pulses of 7 ns duration at 355 nm and at a repetition rate of 10 Hz. A cylindrical lens is used to focus the pump beam in the shape of a stripe on the sample. Due to the high absorption cross section of the dye solution, the pump beam is fully absorbed by the front layer of the sample and it creates a stripe like excited gain medium. A vertical slit is incorporated in the path of the beam between the cylindrical lens and the sample so as to vary the stripe length on the sample. In the present case it is adjusted to a pump beam width of 7 mm. The output is collected from the edge of the front surface of the cuvette using an optical fiber in a direction normal to the pump beam. The emission spectra are recorded with Acton monochromator attached with a CCD camera (Fig.2.13). The emitted beam from the edge of the cuvette is so strong and highly directional that we could collect it even without any focusing.

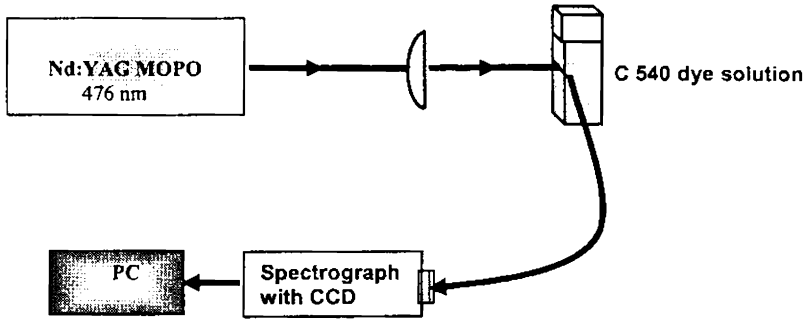

Fig.2.13 Experimental set up to study ASE from C 540dye solution

To study the nature of emission from the dye dissolved in methanol, the emission spectra are recorded for various pump intensities starting from 45 kW/cm^2 keeping the excitation length of the beam as 7 mm. For a pump intensity of 45 kW/cm^2, the fluorescence spectrum recorded is highly broad with a spectral width of 33 nm. With the increase in pump intensity, the fluorescence emission spectra become narrow and give amplified spontaneous emission (ASE). With a pump intensity of 64 kW/cm^2, ASE is observed with a spectral width of 8.3 nm. Fig 2.14 shows the spectral narrowing of the emission spectra with pump intensity. The minimum spectral width obtained from the dye in methanol is 6.2 nm for a pump intensity of 95 kW/cm^2.

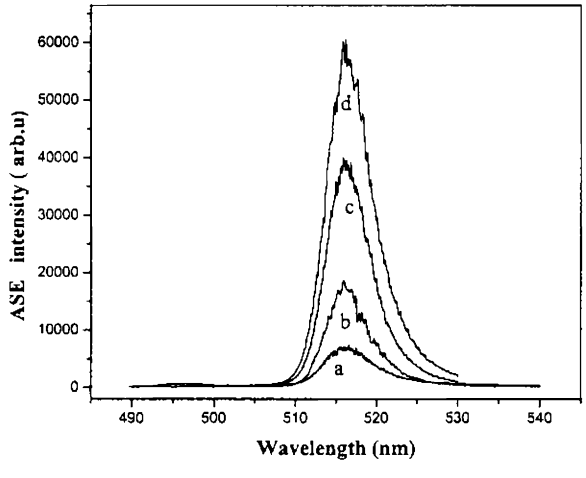

Fig.2.14 ASE intensity vs pump intensity for C 540 dye solution in methanol in kW/cm^2 a) 50 b) 64 c) 80 d) 95

2.6 Laser Emission from dye solution

When the pump intensity is increased beyond 95 kW/cm^2, a periodic modulation structure is observed in the emission spectrum. At higher pump intensities, well resolved equally spaced resonant modes are observed which could be attributed to highly directional laser emission (Fig.2.15). Occurrence of similar resonant modes was reported by Yokoyama et al. [20] in a dye medium added with dendrimers. By encapsulating the dye, the dendrimer reduced the self aggregation and molecular quenching of the dye at higher concentrations and thereby increased its gain. They had related the spacing of the modes to the penetration depth of the beam in the medium. In order to verify the validity of this explanation, in our investigations, the emission spectra are recorded for various concentrations of the dye ranging from 1×10^{-4} to 8×10^{-4} M which corresponds to different penetration depths. The same mode structure is repeated with more or less equal spacing and a red shift in the spectra. (Fig.2.16).This confirms that the mode spacing is not directly related to penetration depth.

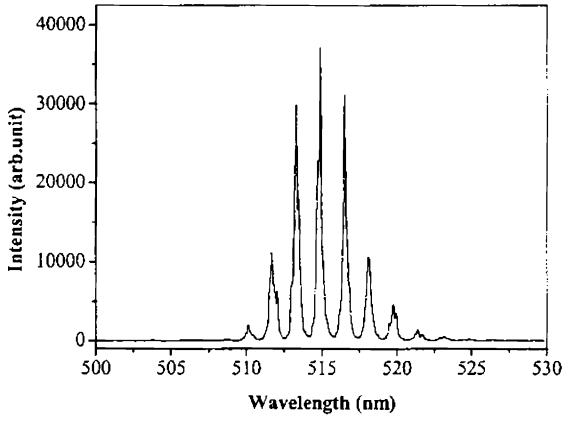

Fig.2.15 Lasing spectrum of C 540 solution in methanol
Resonant modes with spacing 1.62 nm

Further investigations are done by changing the excitation length of the pump beam. For a dye solution of concentration $4x10^{-4}$ M and pump intensity of 150 kW/cm^2, the emission spectra showed the features of ASE for an excitation length of 2 mm. The spectral width is again around 7 nm for this length but when the excitation length is further increased, the narrowed spectrum showed well resolved resonant peaks with equal spacing.

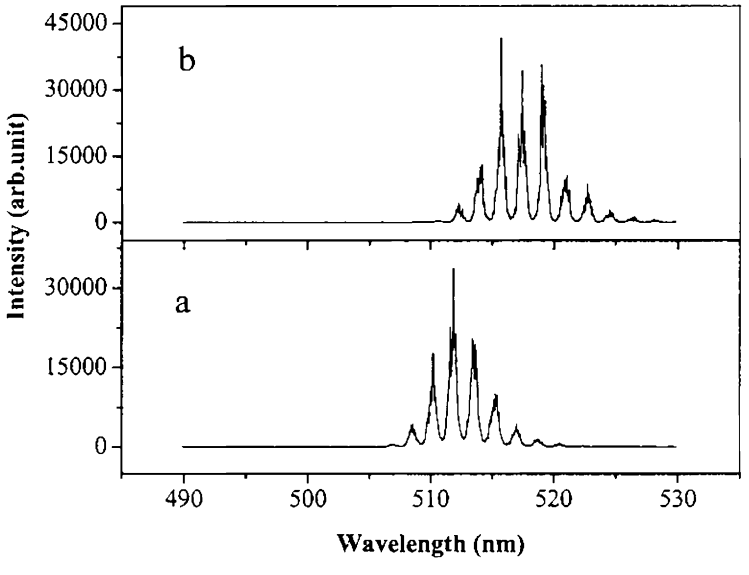

Fig.2.16 Lasing spectra in methanol for two concentrations.(a) 1x 10^{-4} M (b) 8 x 10^{-4} M

For higher excitation lengths, the modes become prominent with very high output intensity. The emission spectrum observed in the dye dissolved in methanol for an excitation length of 4 mm is exactly similar to the one observed for an excitation length of 7 mm (Fig.2.15). An increase in pump intensity resulted in the same mode

structure with the same mode spacing. However the less prominent modes increased in their strength at higher pump intensities.

The occurrence of mode structure from dye solution was also reported by Guang S et al. where the laser emission was attributed to the Fresnel reflection feedback from the two parallel optical windows of the cuvette [21]. Considering the two surfaces of the windows and the gain medium, a multi-cavity structure can be formed between the two plane parallel walls of the cuvette. (Fig.2.17). The resonant conditions for the four subcavities formed between the two windows can be written as

$$2[nL+ n' (l_1+l_2)] = K_1 \lambda$$
$$2nL = K_2 \lambda$$
$$2(nL+n'l_2) = K_3 \lambda$$
$$2(nL+n'l_1) = K_4 \lambda \qquad (2.11)$$

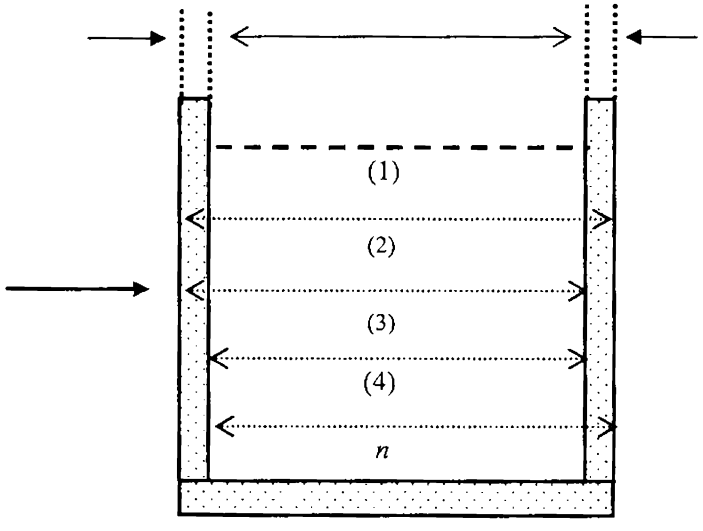

Fig.2.17.Subcavities formed between the walls of the cuvette

where L is the length of the dye medium, n' is the refractive index of quartz, l_1 and l_2 are the thickness of the two parallel windows of the cuvette, n is the refractive index of the gain medium and K_1,K_2,K_3 and K_4 are arbitrary integers [21].
The resonance condition providing the widest spectral periodicity is obtained by the subtraction of the last two equations.

$$2n' (l_2-l_1) = K \lambda \qquad (2.12)$$

where $K = (K_3-K_4)$

This equation is equivalent to the maximum transmission condition of a Fabry-Perot etalon. Thus the partial reflections from the windows of the cuvette produce the effect of a Fabry-Perot etalon and provide the optical feedback necessary for laser emission. For the lasing spectrum the wavelength spacing between the different modes is given by

$$\Delta \lambda = \lambda^2 / 2n' (l_2-l_1) \qquad (2.13)$$

where λ is the average lasing wavelength. Substituting for refractive index of quartz, n' as 1.46, the average lasing wavelength λ as 515 nm and the mode spacing $\Delta \lambda$ obtained from our studies with a cuvette of 1 cm pathlength as 1.62 nm, l_2-l_1 is estimated as 56 μm. In order to check the validity of the above conclusion, the thickness of the windows is accurately measured using a microscope with a CCD monitor and a micrometer and the l_2-l_1 value is found to be around 50-60 μm at different positions of the cuvette which is in close agreement with the observed value. To confirm this result, emission spectrum of the same dye solution in a cuvette of pathlength 0.5 cm is taken. Fig.2.18 shows the mode structure observed with a different spacing of 0.92 nm. Substituting for the peak emission as 514 nm, the thickness difference (l_2-l_1) of the parallel walls is obtained as 98 μm. The measured

value of (l_2-l_1) for this 0.5 cm cuvette is ~100 μm which confirms the existence of a Fabry-Perot optical cavity effect due to the reflections from the walls of the cuvette.

The incidence angle of the pump beam is varied in order to check whether the deviation from the cavity axis could remove the mode structure. In contradiction to the previous report, we could still observe the mode structure when the cuvette is tilted to a certain angle from the direction of incidence [20, 21]. Due to the high gain of the dye medium, even a portion of the reflection from the windows along the cavity axis is sufficient enough to produce the lasing of the cavity.

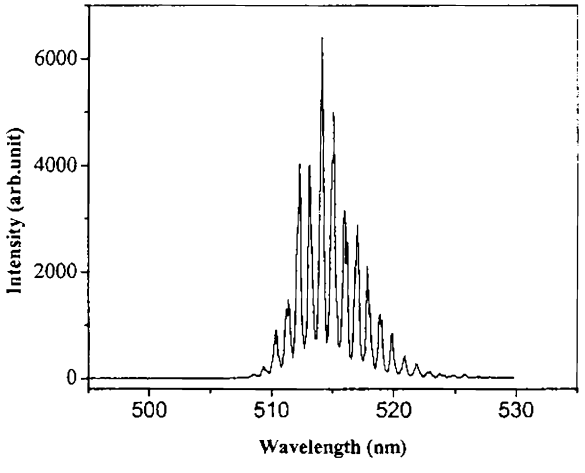

Fig.2.18 Laser emission spectrum of dye solution in a cuvette of 0.5cm. Mode spacing 0.92nm

2.6.1 Solvent effect on laser emission

In the second part of the study, the features of the mode structure are employed to investigate the effect of solvents on the laser emission of the dye. Detailed investigations are done with ten solvents whose photophysical properties are already

studied in the first part of this chapter. Both polar protic and dipolar protic solvents exhibited very high quantum yield. C 540 dye in ethanol has a quantum yield of ~ 1 and toluene which is a nonpolar solvent gives the least value of 0.76. Though a direct correlation between Φ and polarity could not be observed, generally the Φ values are found to be high with solvents of high polarity.

The emission spectra are recorded for all the solvents with a fixed dye concentration of $4x10^{-4}$M. All the experimental conditions remained the same throughout the investigations. Interesting results are observed and these show a correlation between the quantum yield of the dye in different solvents and the mode structure observed due to cavity lasing. With ethanol, which has a quantum yield of ~ 1, the emission spectum has 12 modes with a total spectral width of 7 nm (Fig.2.19). With methyl ethyl ketone (MEK) having a quantum yield of 0.97, the spectral width is 5.6 nm with number of modes equal to 9 (Fig.2.20). For butyl acetate with a quantum yield of 0.85, the number of modes is reduced to 5 (Fig.2.21). In the case of toluene with a quantum yield 0.76, no mode pattern is observed .Toluene gives only an ASE spectrum with a total spectral width of 3.4 nm (Fig.2.22). The dye medium is found to be sensitive to the polarity of the solvent in its nature of laser emission. In general, the gain of the medium increases with increase in polarity. But the laser emission is observed to be high in ethanol which is less polar compared to methanol. Table 2.3 gives a comparison of solvent polarity, refractive index, quantum yield and number of modes observed in the emission spectrum.

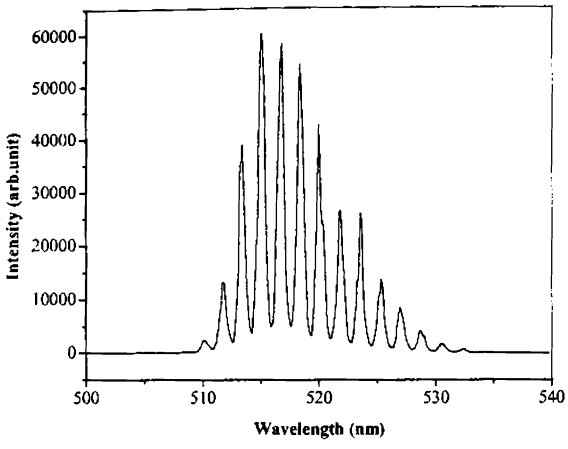

Fig.2.19 Spectrum of Laser emission from C540 dye solution in ethanol. Mode spacing 1.65nm

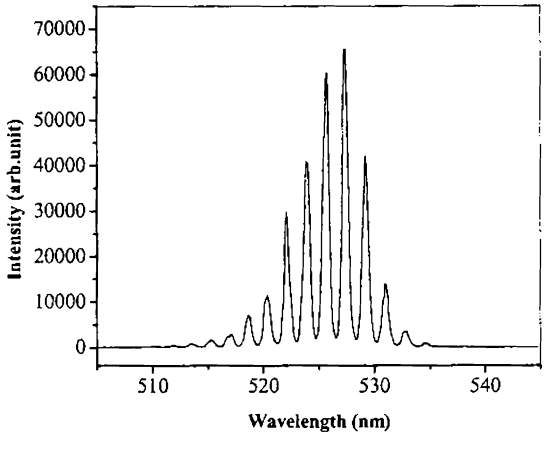

Fig.2.20 Spectrum of Laser emission from C 540 dye solution in MEK. Mode spacing 1.75 nm

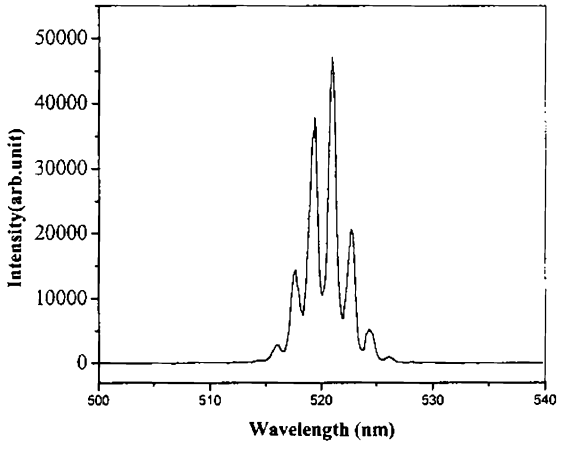

Fig.2.21 Laser emission spectrum of dye solution in butyl acetate. Mode spacing 1.69 nm

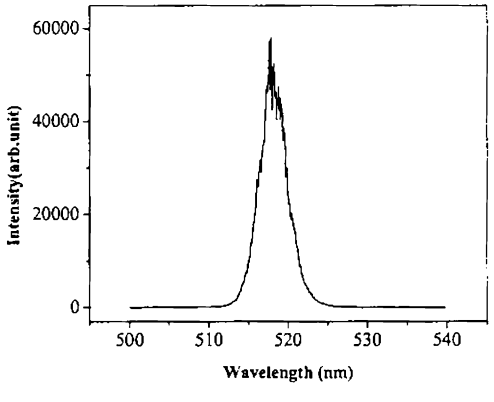

Fig.2.22 ASE spectrum of dye solution in toluene

Though Table 2.3 shows correlation between number of modes and the quantum yield of the dye in different solvents, some discrepancy is noticeable in the

case of a few high polarity solvents. In the case of DMF, the number of modes is less and for DMSO, no laser emission is observed though both of them have high quantum yields. Cyclohexanone also shows the same result which is a less polar solvent. All these solvents have a comparatively high refractive index which is close to the refractive index of quartz. The reflection coefficient of the surfaces is also an important parameter in determining the lasing threshold. For a gain medium in a resonator cavity with length L and end face reflectivities R_1 and R_2, oscillations will build up when the loop gain R_1R_2 exp(2gL) >1[18]. The reflectivity at the end face is given by

$$R = \left(\frac{n_1 - n_2}{n_1 + n_2} \right)^2 \qquad (2.14)$$

Solvent	Nature	Polarity Index	Ref.index	Q.yield	No.of modes	Rx10^{-5}
Ethanol	pp	5.2	1.36	0.99	12	125.7
Dichloromethane	dap	3.4	1.42	0.98	10	19.29
Methyl ethyl ketone	dap	4.5	1.376	0.97	9	87.7
Metahnol	pp	6.6	1.326	0.91	7	231.3
Butyl acetate	dap	3.9	1.394	0.85	5	53.4
Dimethyl formamide(DMF)	dap	6.4	1.431	0.94	4	10.06
Dioxane	dap	4.8	1.42	0.8	3	19.29
Toulene	np	2.4	1.494	0.76	-	13.24
Dimethyl sulphoxide(DMSO)	dap	6.5	1.478	0.96	-	3.75
Cyclohexanone	dap	4.5	1.45	.97	-	1.18

Table 2.3 Comparison of polarity, quantum yield, refractive index and number of modes for different solvents. pp-polar protic, dap-dipolar aprotic , np - nonpolar

The absence of lasing modes in the above solvents can be attributed to the reduced value of the reflection coefficients. For example, cyclohexanone with a refractive index of 1.45 acts as an index matching medium yielding a negligible reflection coefficient ($R= 1.181x10^{-5}$) and laser emission is not observed with such a small feedback. In the case of ethanol, where the difference in refractive indices is comparatively large giving $R = 125.7x10^{-5}$, a good lasing spectrum is obtained at a low threshold pump beam energy. It is also to be noted that dichloromethane with its rather low reflection coefficient of $19.29x10^{-5}$ exhibits a comparatively large spectral width and a good number of modes, presumably due to its high value of Φ. For a comparison, the reflectivity at the end faces for different solvent media is also included in Table 2.3. The lasing behaviour of the gain medium is explicit from the nature of the emission spectrum observed. A correlation is explicit between the gain of the lasing medium in different solvent environments and the spectral width of emission and correspondingly the mode structure exhibited by it.

As we have seen earlier, C 540 dye in dichloromethane is photochemically reactive. Exciation for a short duration will certainly reduce its quantum yield. Naturally we could expect a change in the emission spectrum and the number of modes exhibited by it. The observed result is in confirmation with the above assumption. The emission spectrum is recorded after exciting the dye in dichloromethane for a duration of 30 minutes. The sample which exhibited a broad emission spectrum with a good number of modes before photochemical reaction could give only a narrow spectrum without any mode-structure. Fig.2.23 gives a good comparison of the relation between gain and the mode structure exhibited by the samples. Here, the red shift observed in the emission spectrum denotes the change in fluorescence of the sample due to photochemical reaction.

The emission spectrum of rhodamine 6G, the best known of all laser dyes, is also recorded in methanol keeping the absorbance the same as that of C 540 dye in methanol. The emission spectrum exhibits only 2 modes with a total spectral width of 2.4 nm whereas the emission spectrum of coumarin has a total spectral width of 5 nm with 7-8 modes (Fig.2.24). Even though the quantum yield of C540 in methanol is slightly lower than that of Rh6G, the spectral width for C 540 is found to be greater than that of Rhodamine 6G which is the well known efficient laser dye.

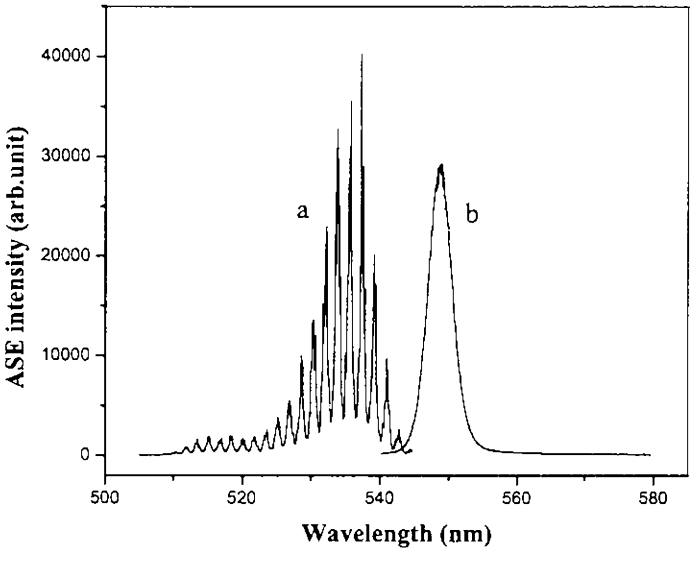

Fig.2.23 Emission from C 540 dissolved in a) dichloromethane
b) after photochemical reaction

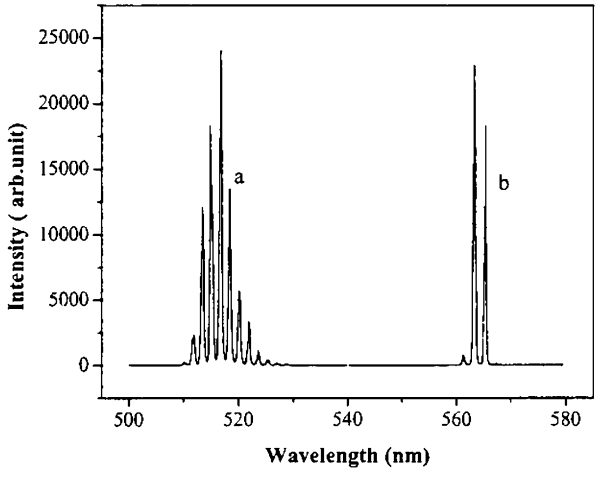

Fig.2.24 Emission spectrum in methanol (a) Coumarin 540,mode spacing 1.65 nm (b)Rhodamine 6G ,mode spacing 2.01 nm

2.6.2 Efficiency of the laser gain medium

The lasing efficiency is an important parameter concerned with any laser system. It marks the efficiency of the system in converting the input pump energy to useful output energy. It is defined as the ratio of the energy of the dye laser output to the energy of the pump radiation incident on the sample surfaces. We have determined the lasing efficiency of the gain medium in certain solvents. Since the absorption cross section is high for the dye solution, the pump energy is fully absorbed by the front layers of the sample itself. The input and output energy is measured using energy ratio-meter (Laser probe Inc.) with RjP 735 probes. Since light is emitted in both directions, the measured energy is multiplied by two to get the total emission. For the dye in methanol medium the efficiecy observed is 32% for a pump energy of 800 μJ. This value takes into account of all losses due to reflection, scattering, diffraction etc.

2.7. Frequency up-conversion emission

Recently, efforts are going on to design frequency up-converted laser devices which can produce a shorter- wavelength output in the visible or UV region. This can be achieved by pumping the gain medium with a longer-wavelength input using mainly IR sources. Frequency up-conversion is based on two photon absorption process. Here the excitation of the gain medium occurs by the simultaneous absorption of two photons of longer- wavelength.

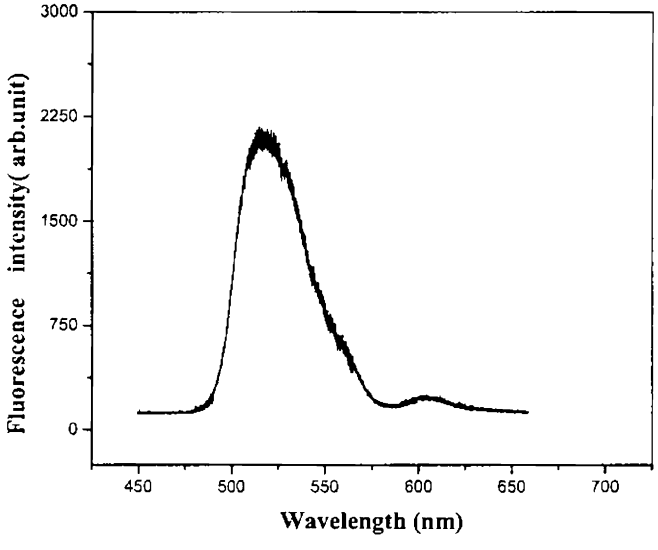

Fig.2.25 Frequency up-converted emission from C 540 dye solution in methanol exciting by 790 nm radiation.

Two photon induced emission studies are carried out in C 540 dye solution in methanol. The gain medium is excited with a radiation of 790 nm from a mode-locked Ti: Sapphire femtosec laser (Spectra Physics) with pulses of 80 fs duration and average input power of 2.3 W. Emission spectrum recorded shows the peak at 515 nm with a FWHM of 44 nm.

2.8. Conclusions

The fundamental photophysical properties of C 540 are investigated in detail in different solvent environments. The quantum yield and lifetime measurements are done to compare the solvent effect in radiative and nonradiative decay mechanisms of the dye. Coumarin 540 dye exhibited significant quantum yield in certain solvents. Hence the ASE and lasing characteristics are investigated in different solvent media. Laser emission is observed from dye solution taken in a quartz cuvette. The subcavities formed between the windows of the cuvette produced the effect of a Fabry-Perot optical cavity resulting in well resolved equally spaced resonant modes. The mode spacing is related to the difference in thickness of the parallel walls of the cuvette.

The features of the mode structure in the emission spectra are employed to study the effects of solvents on laser emission of the dye. The number of modes exhibited by the emission spectra of the dye solutions is correlated to the quantum yield in the respective solvents and to their refractive indices. The observation of mode structure is a clear evidence of laser emission form C 540 dye solution.

References

1. F.J.Duarte, L.W.Hillman, *Dye laser Principles*, Academic press,New york (1999)
2. F.P.Schafer, *Dye lasers,* Springer-Verlag,Berlin (I989)
3. J.R Lakowicz, *Principles of Fluorescence Spectroscopy*, Plenum press, New York,1983 (Chapter 9)
4 A.J.Pesce, C.G.Rosen, T.L. Pasby, *Fluorescence spectroscopy*, Marcel Dekker Inc, New york (1971)
5. J.B.Birks, *Phtophysics of aromatic molecules*, Wiley Interscience, London(1970)
6. M.Kempe, G.A.Berger, A.Z.Genack, *Stimulated emission from amplifying media,*
7 J.R.Lakowicz, *Radiative Decay engineering*: *Biophysical and Biomedical applications*, Analytical biochemistry **298** (2001) 1-24
8 G.Jones II, W.R.Jackson,C.Choi, *Solvent effects on emission yield and lifetime for coumarin laser dyes*, J.Phys.Chem.**89** (1985) 294-300
9 A.K.Satpati,M. Kumbhakar,D.K.Maity, H.Pal, *Photophysical investigations of the solvent polarity effect on the properties of Coumarin -6 dye* Chem.Phys.Lett. **407** (2005)114-118
10 A.Barik, S.Nath,H. Pal, *Effect of solvent polarity on the photophysical properties of coumarin-1 dye.* J.Chem.Phys. **119** (2003) 10202-10208
11 S.Nad, H.Pal, *Unusual photophysical properties of Coumarin -151* J.Phys.Chem.A **105(** 2001)1097-1106
12 M.A Haidekker, T.P Brady,D.Lichlyter E.A Theodorakis, *Effects of solvent polarity and solvent viscosity on the fluorescent properties of molecular rotors and related probes.*Bioorganic chemistry **33** (2005) 415-425

13 U.S Raikar,C.G.Renuka,.F.Nadaf, B.G.Mulimani, *Solvent effects on the absorption and fluorescence spectra ofCoumarin6 and 7 molecules.* Spectrochimica Acta A **65** (2006) 673-677

14. H.Pal, S.Nad, M.Kumbhakar, *Photophysical properties of Coumarin-120, unusual behavior in non polar solvents*, J.Che.Phys.**119** (2003)443-452

15. A.T.R Williams , S.A Winfield ,J.N Miller, Analyst **108** (1983) 1067

16. D. Madgde,R. Wong,P. G.Seybold, *Fluorescence quantum yield and their relation to lifetimes of Rhodamine 6G and Fluorescein in nine solvents* Photochem.Photobiol.**75** (2002)327-334

17 A.H.Hemeay, T.A.Fayed, H.a.El-Daly, *Kinetic studies of the oxidation of Coumarin -540 laser dye*, Monatshefte fur Chemie **131**(2000)749-759

18. W.Koechner, *Solid–State laser engineering*,Springer-verlag,Vol.**1**,New York (1992)

19. O.Svelto ,D.C.Hanna, *Principles of Lasers,*4th ed.Plenum Press, New York (1998)

20. S. Yokoyama, A. Otomo, *S. Mashiko, Laser emission from high –gain media* of dye doped dendrimers, Appl.Phys.Lett. **80** (2002) 7-9

21. S.Gaung He, R.Signorini, P.N.Prasad, *Two-photon pumped frequency–upconverted blue lasing in coumarin dye solution,* App. Opt. **37**(1998) 5720-25

Chapter 3

Light Amplification in Dye Doped Solid State Polymer Matrices

"The important thing is not to stop questioning. Curiosity has its own reason for existing".
Einstein

Abstract

Light amplification and laser emission from C 540 dye doped polymer matrices are reported in this chapter. PMMA, polystyrene and polyvinyl chloride are the polymer matrices used as host media. ASE and laser emission are compared in samples prepared both by the bulk polymerization and free cast evaporation methods. Light amplification and optical gain are much higher in free standing films prepared by the free cast method and laser emission is exhibited even by a short length of the excited gain media. The well polished surfaces of the free standing films of dye doped polystyrene produce a Fabry-Perot optical cavity effect enabling laser emission from a very short length of 1.25 mm. The light amplification and optical gain studies in different dye doped polymer matrices are carried out by varying the pump intensity and excitation length of the gain medium.

3.1 Introduction

The dye lasers with its versatility and wide range of tunability from near UV to near IR have proved to be powerful sources of coherent radiation. They have made enormous impact in different fields of basic sciences, technology, communication,

industry and medical sciences. Though the early investigations were done in liquid dye lasers and proved to be superior to many other laser sources with their unique level of performance, the need to replace them with their solid counterpart was very evident. The need for large volume of gain media, the complex and bulky laser designs, the handling problems and the toxicity of organic solvents used, made them less attractive. With the technical and economical advantages of solid state dye lasers over classical liquid dye lasers, their development attracted much interest. Investigations were done from the early days of developments of liquid dye lasers, to incorporate the organic dyes into solid host materials to achieve laser gain media of high optical quality and photostability and to overcome the problems posed by liquid dye lasers [1-4].

3.2 Solid State Dye Lasers

The first solid state lasers were reported in the late 1960s by Soffer and Mcfarland [5] and Peterson and Snavely [6]. They demonstrated stimulated emission from polymeric matrices doped with organic dyes. The development of solid state dye lasers has paved the way for an intense research in incorporating dye molecules into solid matrices. The main research had been devoted to material hosts which disperse well with the dye molecules and for which laser conversion efficiency and operational photostability were high. But the main draw backs of solid state dye lasers like the low laser damage resistance, low photobleaching threshold of dyes and relatively low laser efficiency delayed the commercial development of these materials for tunable lasers. Synthesis of new high performance laser dyes and effective incorporation of them into solid matrices resulted in a new thrust in the field of dye lasers in 1980s. With enormous investigations carried out in this line, solid state dye lasers were developed with different classes of solid host materials in order to meet the wide range of applications offered by liquid dye lasers [7-9].

Higher laser damage resistance and better thermal stability are exhibited by inorganic glasses of silica gel compared to polymer matrices. Incorporation of dyes into inorganic materials by the sol-gel process yielded relatively photostable materials with acceptable laser efficiency [9]. The dye doped sol gel derived solid matrices are also chemically stable under high power repetitive laser excitation. But the high porosity of glasses remained undesirable for lasers and other applications. Later the methods of sol-gel process offered new channels for the improvement of inorganic glasses as host materials. The sol-gel process leads to hybrid organic/inorganic materials which are known as organically modified silicates or ORMOSILS [10]. Compared to inorganic glasses, ormosils are characterized by better mechanical and optical properties due to the relatively high flexibility and low porosity. Several organotrialkoxysilane compounds have been tried as ormosil precursors to improve the lasing performance. Inorganic silica-zirconia glasses and silica –zirconia ormosils are also demonstrated as effective solid state host materials for dye lasers [11].

Among the different classes of materials experimented, both inorganic and organic, as stable and efficient solid host materials for the development of practical tunable solid-state dye lasers, the polymers are found to be most promising with their obvious merits. They possess high optical quality, better chemical compatibility with organic dyes, control over medium polarity and viscosity in a way similar to conventional solvents. The inexpensive processing techniques facilitated the miniaturization and design of integrated optical systems. They also provide desirable flexibility in the development of improved host materials for dye lasers [12-14].

3.3 Dye doped polymer matrices

The basic requirements imposed on any solid host material for dye lasers are good optical transparency at pump and lasing wavelengths, good solubility of the dye in the

material, good thermal stability and mechanical strength and resistance to pump radiation [15]. The polymeric matrices have many advantages compared to other host materials. Polymers used are in general polyacrylics, polyurethanes, polycarbonates etc. In polyacrylic class, the widely used polymeric host is polymethyl methacrylate (PMMA) due to its excellent optical transparency in the visible wavelengths and its relative high laser damage resistance. But polymers are poor thermal conductors and have large time of heat dissipation and their lifetime is limited. Another disadvantage is the insolubility of the common dyes in PMMA. Modifying the PMMA by the incorporation of low molecular weight additives such as ethyl alcohol, ethylene glycol, polyether are found to be an effective way of increasing the solubility to certain extent. The laser damage of polymeric matrices are found to be energy dependent and this in turn depends on the viscoelastic properties of the polymer matrix. Doping of low molecular weight additives could also improve the viscoelastic properties which can enhance the laser damage resistance. Modified polymers have already been developed with resistance to laser radiation as high as that of inorganic glasses [15-16].

Another method adopted to improve the plasticity of the polymer matrix internally is co-polymerization in which a co-monomer is added. When the heterogeneous mixture is polymerized, it provides enhanced crosslinking and compatibility of dye with macromolecules. MMA and HEMA (2-hydroxyethyl methacrylate) are found to be such a pair of monomers with improved laser operation. Costela et al. has done detailed investigations on a large number of combinations [16]. Recently the same group have demonstrated significant enhancement in the laser action of rhodamine 6G doped solid state dye lasers prepared from the hybrid matrices of organic polymers and inorganic sol-gel glasses. They have simultaneously polymerized poly (2-hydroxyethyl methacrylate) (HEMA) and poly (2-hydroxypropyl

methacrylate) (HPMA) along with different weight percentage of tetraethoxysilane (TEOS) or tetramethoxysilane (TMOS)[17].

Polystyrene is another class of polymer widely used to develop solid state dye doped optical devices. The polymer is characterized by its rigidity, sparkling clarity and ease of processing. They exhibit compatibility with many laser dyes and good solubility in many organic solvents. Good optical quality dye doped films are prepared by many groups with better thermal stability than PMMA films [18-19]. They can also be easily processed at low cost.

Polyvinyl group of polymers are important with their thermal and mechanical stability, flexibility and compatibility with organic compounds. Polyvinyl chloride (PVC) is perhaps the widely used materials in the vinyl group which can also be tested as solid state host media for organic dyes.

3.4 Optical gain studies in dye doped polymer matrices

3.4.1 Amplified Spontaneous Emission

As described in the previous chapter, ASE is a common phenomenon observed in high gain laser media. It is not purely a spontaneous emission but spontaneously emitted photons are amplified via stimulated emission while they pass through the excited region of the gain medium [20]. It does not require a population inversion but a sufficient number of excited states along the optical path length. Gain occurs when the amplified spontaneous emission of photons exceeds loss due to reabsorption and scattering. In materials with high gain, ASE intensity can be high similar to that of multiple pass gain build up in a cavity with mirrors. A signature of ASE is the gain narrowing of the fluorescence spectrum. As the pump energy increases the spectrum changes from a normal fluorescence to pure ASE [21-22].

The measurement of optical gain in terms of the ASE intensity exhibited by extended length of the gain medium is an efficient way of analyzing the potential of the medium as a laser material. A single pass gain measurement proposed by Shaklee et al. is the widely used method to determine the gain of a medium [23]. According to this method, gain medium is excited with a cylindrical lens to form a stripe like structure. ASE gain is the ratio of light intensity emitted to incident intensity per unit length of the pumped gain material.

3.4.2 Gain coefficient

Shaklee et al. had introduced a simple theory for the measurement of optical gain in which a one-dimensional approximation is described. According to this theory the rate of change of fluorescence intensity with the length of the pumped region is;

$$\frac{dI}{dx} = AP_0 + gI \tag{3.1}$$

where I - the fluorescence intensity propagating along the x axis

$g = g' - \alpha$, is the net optical gain where g' is the gain due to stimulated emission and α account for all the optical losses

AP_0 – the spontaneous emission proportional to pump intensity

The solution of this equation with respect to pump length is;

$$I = \frac{AP_0}{g(\lambda)}[\exp(g(\lambda)l) - 1] \tag{3.2}$$

where P_0 – pump intensity

A – a constant related to spontaneous emission cross section

l – length of the pumped stripe

The relation shows the exponential growth of the output emission intensity from the dye doped films with the excitation length of the gain medium. For positive values of $g(\lambda)$ the output intensity will exponentially grow and correspondingly a spectral narrowing will be observed since the amplification occurs to a greater extent in certain wavelengths. Thus gain coefficient is wavelength dependent .Shaklee et al. measured the single pass gain of dye medium by comparing the intensities of ASE for two excited stripes of length l and $l/2$ for a constant wavelength [23]. The gain equation for a length of $l/2$ can be written

$$I(\lambda, l/2) = \frac{P_0 A(\lambda)}{g(\lambda)}[\exp(g(\lambda) l/2)) - 1] \tag{3.3}$$

From equations (3.1) and (3.2), the net gain can be obtained as,

$$g = \frac{2}{l} \ln\left[\frac{I(l)}{I(l/2)} - 1\right] \tag{3.4}$$

Equation (3.4) applies only for pump powers up to the onset of saturation. The gain coefficient can also be calculated by fitting the function for emission intensity of ASE with the experimental data.

Most of the optical gain studies are done in dye doped disk like samples of several mm thickness [24-25]. Currently lots of investigations are going on in dye doped thin films fabricated on some substrates [26-28]. In these methods, by the sample geometry, the dye doped films act as asymmetric waveguides. In the present investigation, we demonstrate the ASE and lasing behavior in free standing dye doped films of micrometer thickness which act as symmetric waveguides. The ASE and

optical gain in these films are compared with that of bulk samples of thickness ~ 1cm. The lasing efficiency of these samples is also found to be extremely high.

3.5 Experimental details

3.5.1 Fabrication of dye doped polymer matrices

Two methods are available for the fabrication of dye doped polymer matrices. One of the methods uses the uniform spreading of the polymer and the dye in an organic solvent over the appropriate optical surfaces and is known as the free cast method [20]. Good optical quality polymer films are obtained by the subsequent removal of the solvent by evaporation. Second method is the bulk radical polymerization of the initial monomer/ fluorophore composition.

3.6 Dye doped PMMA matrices

Bulk samples: Preparation

Freshly purified monomer MMA is used to prepare the samples. The dye is dissolved in ethanol at a concentration of 0.5mM .The mixture of dye solution and purified MMA taken in 1:4 (v/v) ratio is placed in an ultrasonic bath for the complete dissolution of the dye and filtered with a 0.6 μm pore size paper (Whatman Div.). 0.03 gm/*l* of 2,2'-azobisisobutyronitrile(AIBN) is added as the free radical initiator. It acts as the thermal polymerization initiator. The resulting solution is again filtered and taken in cylindrical tubes and the molds are sealed. Polymerization reaction is performed in dark at 50° C over a period of two days and then at 45° C for two days. The temperature is gradually decreased to room temperature. Then the samples are unmolded .This procedure is followed to reduce the build up of stresses in the polymer samples due to thermal shock.

The dye doped samples formed are cylindrical rods of 1 cm diameter and 2 cm length with a cut parallel to the axis of the cylinder defining a lateral flat surface. This surface as well as the end surfaces are hand polished to the required optical quality. The absorption spectra recorded using UV-VIS spectrophotometer (JascoV-570) of the dye doped bulk sample are given in Fig.3.1

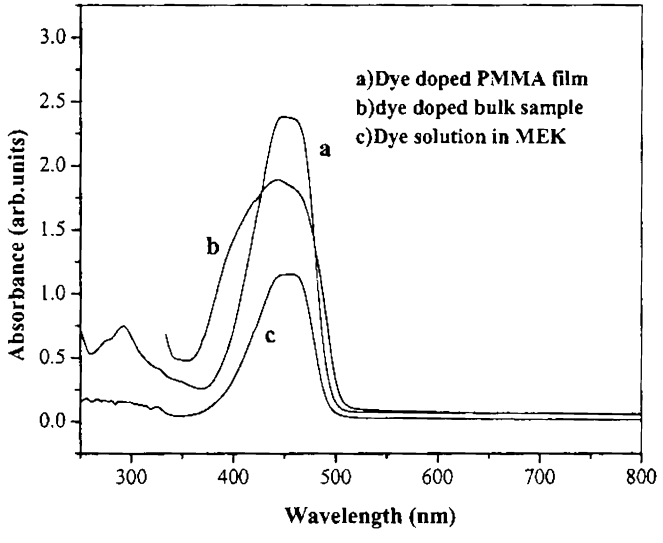

Fig.3.1 Absorption spectra of different C 540 samples

3.6.1 Gain studies

The experimental set up(Fig.2.13) described in the pervious chapter for ASE measurements is used for the gain and ASE studies of bulk and thin film samples. The light amplification in dye doped polymer rods is investigated for various pump intensities and different excitation lengths of the gain medium. The pump beam is focused on the polished cut surface of the dye doped disk sample of 1.5 cm length by a cylindrical lens to form a stripe-like structure of dimensions 0.5 mm x 9 mm. An

adjustable slit is incorporated in the path of the beam between the cylindrical lens and the sample so as to vary the stripe length on the sample. In order to ensure that the intensity of the stripe is uniform along its length, only the central portion of the beam is used for the measurements. Light emitted from the edge of the disk is focused by a 10 cm focal length lens and collected by an optical fiber and recorded using an Acton monochromator with a CCD camera. The emission spectra are recorded for different pump intensities keeping a constant excitation length of 6 mm. Fig.3.2 shows the features of ASE exhibited by the thick dye doped samples for various pump intensities.

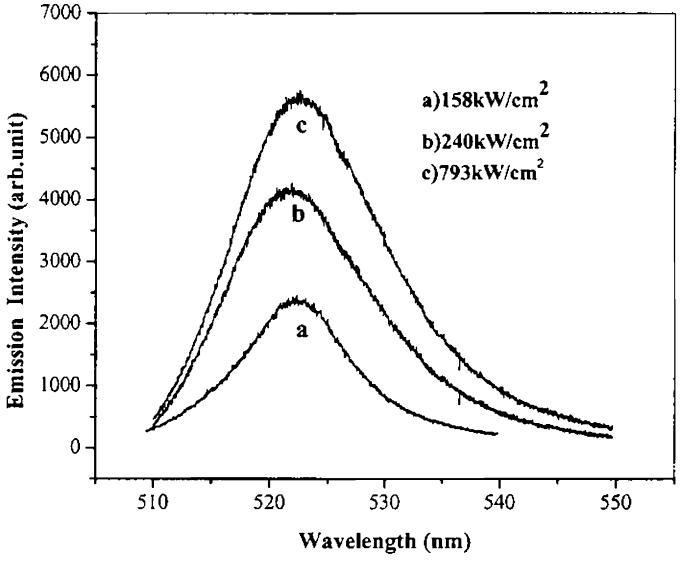

Fig.3.2 Fluorescence emission from bulk PMMA sample for three different pump intensities

Even though the output intensity increases with pump power, emission spectra do not exhibit any significant spectral narrowing. The minimum spectral width observed with a pump intensity of 793 kW/cm^2 is 15 nm. Compared to the

fluorescence spectral width of 33 nm, reduction in spectral width is observed due to ASE. But the increase in output emission is observed to be not in step with the increase in pump intensity.

3.7 Solid State Thin Films:Preparation

Solid state thin films are prepared by incorporating Coumarin 540 dye in polymethyl methacrylate (PMMA). Commercially available PMMA of 10% by weight is dissolved in methyl ethyl ketone (MEK). The weight percentage is chosen to get optimum viscosity for the formation of good quality films. The dye is dissolved in this solution at a concentration of $5x10^{-4}$ M. The films for the present studies are formed on micro glass slides by free cast evaporation method. Utmost care is taken by stirring for a long time to get films of uniform thickness and of good optical quality. When the solvent is fully evaporated, good optical quality films could be peeled off from the glass slides. Films of thickness in the range 80 to 200 micrometers are fabricated for the studies. The thickness of the films is measured by a micrometer with a least count of 0.001mm (Mitutoya No.193-111 with a digit display).

3.7.1 Gain studies

Amplified spontaneous emission (ASE)

The absorption spectra of the thin film and the dye solution prepared in methyl ethyl ketone are given in Fig.3.1. The gain studies are repeated in dye doped thin films. Since an unusal narrowing of the emission spectrum is observed, dependence of the emission intensity and spectral linewidth of the emission, on pump intensity and the excitation length of the pump beam is studied in detail.

The spectra are recorded by varying the excitation length of the medium up to 6 mm at a constant pump intensity. Fig.3.3 shows the emission spectra corresponding to

three different pump intensities. They narrowed very gradually with the excitation length at lower pump intensities. For a pump intensity of 47 KW/cm^2 no significant spectral narrowing is observed with an excitation length of 6 mm but for a pump intensity of 158 kW/cm^2, the FWHM of the emission spectrum is 7 nm for an excitation length of 2.4 mm. At higher pump intensities, the spectral narrowing occurred more rapidly with a high gain. While increasing the pump intensity to 825 kW/cm^2, the FWHM is reduced to 3.5 nm at an excitation length of 1.5 mm. As is evident from Fig.3.3C, at higher pump intensities, the gain increased so that ASE becomes prominent with a reduced spectral width.

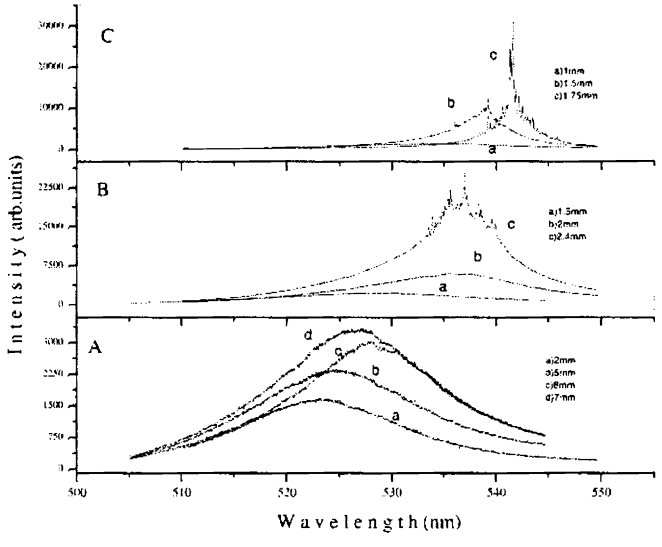

Fig.3.3 ASE from dye doped films for different excitation lengths of the pump beam at three different pump intensities A) 32 kW/cm^2 B)158 kW/cm^2 C) 793 kW/cm^2.

At lower pump intensities, the characteristic fluorescence maximum with peak at around 530 nm is observed. But they are red shifted at higher pump intensities since the self absorption from the blue side of the spectrum is more prominent at these intensities. With increase in pump intensity, a gradual increase in red shift is seen and it is as high as 15 nm for a pump intensity of 793 kW/cm^2 (Fig.3.3).Fig.3.4 shows the output intensity at the peak of the emission spectrum as a function of excitation length of the gain medium for different pump intensities. We have considered the emission intensity up to an excitation length of 2mm. The gain coefficient of the dye doped films is calculated by fitting the function for emission intensity of ASE with the experimental data. At low pump intensity, the gain coefficient is small (11cm^{-1}) but at higher intensities, a gain coefficient of 29 cm^{-1} is observed which is comparatively large in the case of dye doped films[19].

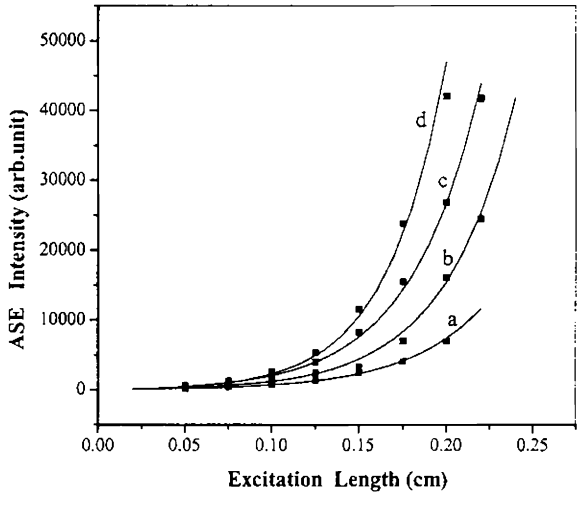

Fig.3.4 Dependence of emission intensity of ASE on excitation length of pump beam for different pump intensities.
a)51kW/cm^2 b)158kW/cm^2 c)240 kW/cm^2 d)793 kW/cm^2

To understand the nature of ASE in detail, the dependence of emission intensity on incident pump intensity is studied (Fig.3.5). As is evident from the plot, corresponding to the change of slope, a threshold pump intensity of around 51 KW/cm^2 is observed for the occurrence of ASE.

On a detailed study of the emission spectrum of the dye doped thin film, it is found that the emission spectrum exhibits all the features of ASE namely, the property of directionality, narrow bandwidth and presence of soft threshold behaviour [29-30]. Directionality of the output beam is so obvious that no focusing is required to collect the beam. The minimum spectral width observed for ASE is 3.5 nm at a pump intensity of 825 KW/cm^2. A threshold pump intensity of around 51 KW/cm^2 is also observed for the occurrence of ASE

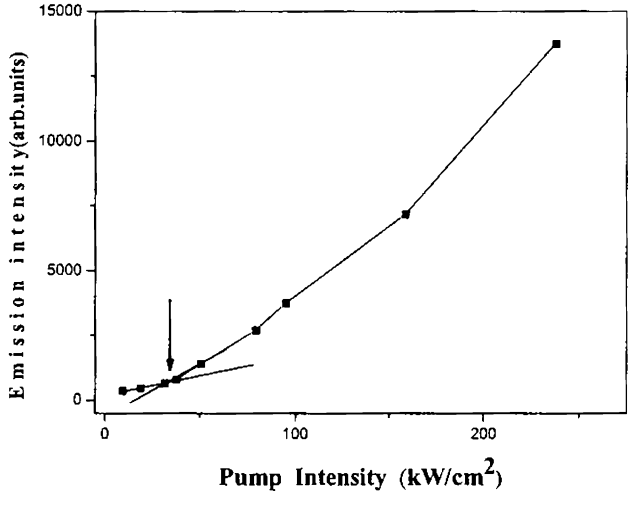

Fig.3.5 Variation of emission intensity with pump intensity for an excitation length of 2mm.

3.7.2 Laser Emission

In most of the earlier reports of ASE exhibited by dye doped polymer films, gain saturation is observed at longer excitation lengths of the gain medium [21-23, 28]. Once gain saturation occurs, light is not amplified further as the length of the stripe is increased. When gain saturates, line narrowing ceases and the FWHM of the emission is found to be a constant which is usually less than 10 nm. In contrast to this, in the present study, when the stripe length is increased beyond 2-3 mm, a sudden spectral narrowing is observed in the emission spectrum at all pump intensities above the threshold for ASE (Fig.3.6). The FWHM of the spectral lines is found to be less than 1 nm. Such a spectral narrowing can be attributed to laser emission. The spectral narrowing is very prominent at higher pump intensities. The FWHM is reduced to a value of 0.3 nm for a pump intensity of 240 kW/cm^2.

The output intensity is also found to increase with pump intensity, but not in an exponential manner. For different pump intensities, the excitation length of the medium needed for laser emission is found to be different. For a pump intensity of 51 kW/cm^2 , an excitation length of 3 mm gives rise to laser emission but it is reduced to 1.75 mm for a pump intensity of 825 kW/cm^2. Fig.3.7 denotes the variation of excitation length with the threshold pump intensity which produces laser emission.

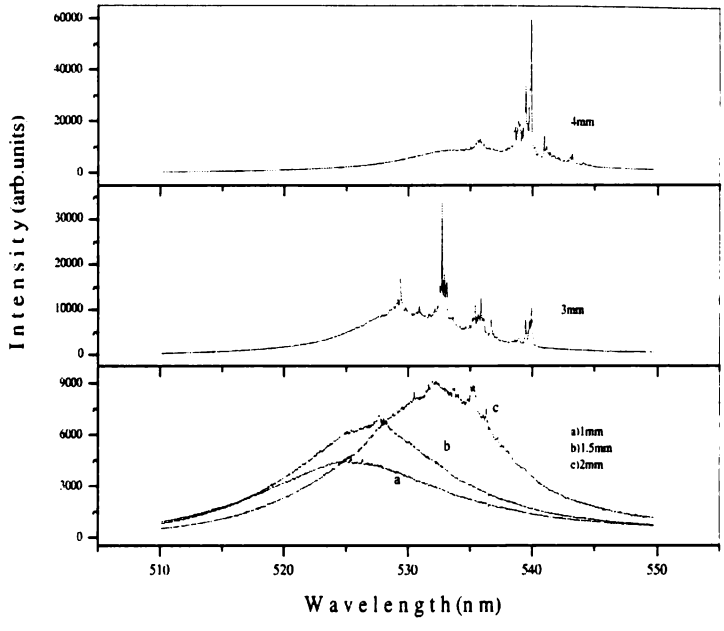

Fig.3.6 ASE and laser emission spectra from a dye doped film with the increase in excitation length. Pump intensity is 79 kW/cm^2.

Laser emission requires an external feedback. In the present case no feedback is provided with external mirrors. But the free standing film with air medium on both sides can be considered as an optical cavity. The lateral faces of the film are of good optical quality and they behave like external mirrors partially reflecting the beam, though the reflectivities are very small compared to conventional mirrors. These reflecting surfaces produce the effect of a Fabry –Perot optical cavity whose length is the thickness of the film.

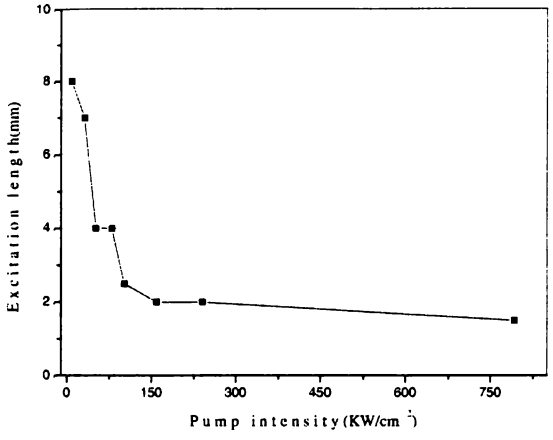

Fig.3.7 Plot of excitation length vs. threshold pump intensity for laser emission

The excited active medium can be considered as a number of serially connected Fabry –Perot optical cavities [31-32].The axis of the optical cavity is normal to the direction of propagation of light through the film. The multiple pass between the film surfaces increases the gain. When the gain of the active medium compensates the losses in the medium, laser emission occurs. According to laser theory, the gain per pass in the active medium is $\exp \sigma (N_2-(g_2/g_1) N_1)l$ where σ is the stimulated emission cross section and l is the length of the active medium [29].

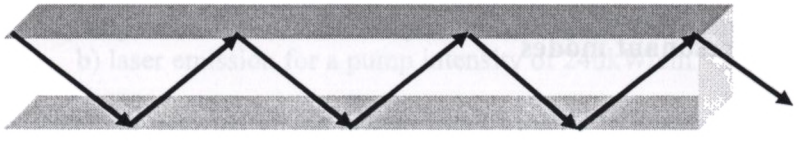

Fig.3.8 Light propagation in the dye doped thin film represented by serially connected F-P etalons

Due to the sample geometry and mode of excitation, there can be a guiding effect in the gain medium even though the film thickness is around 100-200 micrometers. Fig.3.8 shows the light propagation through the excited region of the medium with the guiding effect. The excited portion of the thin film behaves like a planar waveguide. The axial modes of the F-P cavity can be considered as the transverse modes of the waveguide [31]. When the excitation length of the gain medium and the pump intensity are sufficiently increased, laser emission is observed. Thus the guiding effect in the direction of the excited stripe and the feedback from the lateral faces of the thin film induce the high gain necessary for the laser emission. Since the active medium is highly optically dense, even a small length of 1.75 mm of the medium could produce laser emission with a pump intensity of 825 kW/cm^2.

Once laser emission is observed for a particular pump intensity and excitation length, further increase in excitation length does not show any significant change in the spectral width. Fig.3.9 clearly gives a comparison of reduction in FWHM for ASE and laser emission. The values of the excitation stripe length needed for spectral narrowing, wavelength of peak emission, the magnitude of the line narrowing and the red shift observed for different excitation lengths are sensitive to certain physical and chemical characteristics of the sample. These variations may be attributed to the differences in microscopic structure of the polymer thin films which occur during the fabrication process.

3.7.3 Laser resonant modes

The existence of a Fabry-Perot optical cavity between the lateral faces of the free standing film is confirmed by the occurrence of well-resolved discrete peaks in the emission spectrum of dye doped film of known thickness (90 μm). A number of

equally spaced resonant modes are observed (Fig.3.10).These modes can be considered as the axial modes of the Fabry – Perot cavity formed between the flat film surfaces [31-32]. The spacing of the modes is found to be around 1.1nm. In a Fabry-Perot cavity, the spacing between the modes is given by $\Delta\lambda = \lambda^2/2nL$ where n is the refractive index of the medium and L is the optical path length of the resonator cavity. By substituting n as 1.49, the refractive index of the undoped PMMA, λ, the peak emission wavelength observed in the spectrum, and L, the thickness of the polymer film as 90 μm in the above equation, the spacing is calculated to be 1.02 nm which is in agreement with the observed value of ~ 1.1nm. To confirm this observation, dye doped film with a different thickness is studied. With a film thickness of 190 μm, the spacing observed is ~ 0.5nm against the theoretical value of 0.55nm.

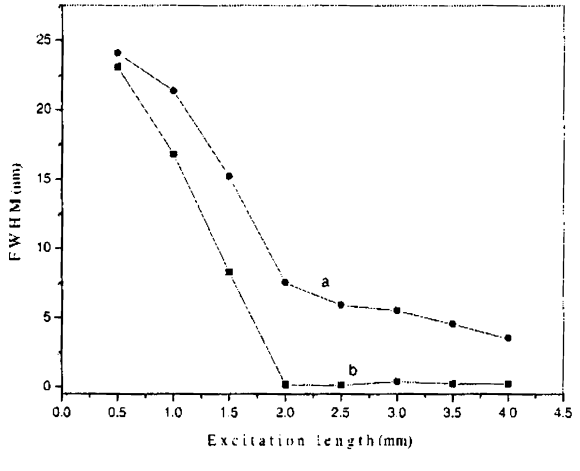

Fig.3.9 Dependence of linewidth on excitation length of pump beam for a) ASE for pump intensity of 79kW/cm^2 b) laser emission for a pump intensity of 240kW/cm^2

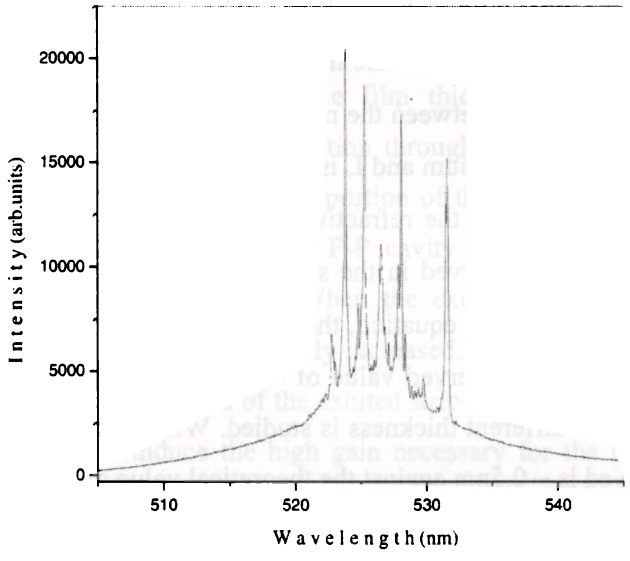

Fig.3.10 Resonant modes with a spacing of 1.1 nm
from a 90 micrometer thick dye doped film.
Pump intensity 51 kW/cm^2. Excitation length is 4mm.

3.8 Dye Doped Polystyrene Matrices

Polystyrene is a commonly used polymer in optical applications due to its transparency and better thermal stability [19]. We have fabricated dye doped polystyrene thin films in the free cast evaporation method. Toluene is the solvent of choice which has good solubility for polystyrene. To get good optical quality films we have dissolved 4% by weight of commercially available polystyrene in toluene and the dye is dissolved at a concentration of 5 x10^{-4} M. After stirring for a long time, the resulting viscous fluid is evenly distributed on micro glass slides. Thin films are

peeled off from the glass slides when the solvent is fully evaporated. The films formed are of thickness in the range 100-180 microns. Keeping all the experimental conditions same as in the previous case, the gain studies are conducted in dye doped polystyrene films.

In the first part of the experiment, keeping the excitation length constant the intensity of the pump beam is increased in steps and the emission spectra are recorded. Amplification of the light emission and spectral narrowing are observed when the pump intensity is gradually increased. Fig.3.11 shows the emission spectra obtained from a length of 1.5 mm of the excited dye doped sample. The FWHM of the emission spectrum is observed to be 3 nm for a pump intensity of 507 kW/cm^2.

In order to calculate the gain coefficient of the sample, the experiment is repeated by recording the emission spectra for different lengths of the gain media keeping the pump intensity constant. We have varied the excitation length up to 1.75 mm. This is repeated for different pump intensities and a graph is plotted between excitation length of the gain medium and the corresponding emission intensity. The gain coefficient is obtained by fitting the experimental data to the gain equation as in the previous case. Fig.3.12 shows the typical length dependence of the ASE intensity at the gain maxima.

Though the quantum yield of C 540 is less in toluene compared to MEK, the gain is found to be higher than that of dye doped PMMA samples. For a pump intensity of 635 kW/cm^2, the net gain obtained is 31 cm^{-1}. This may be due to a better solubility of dye in polystyrene than that in PMMA. Also, other optical losses such as self absorption and reflection may be reduced in dye doped polystyrene matrices.

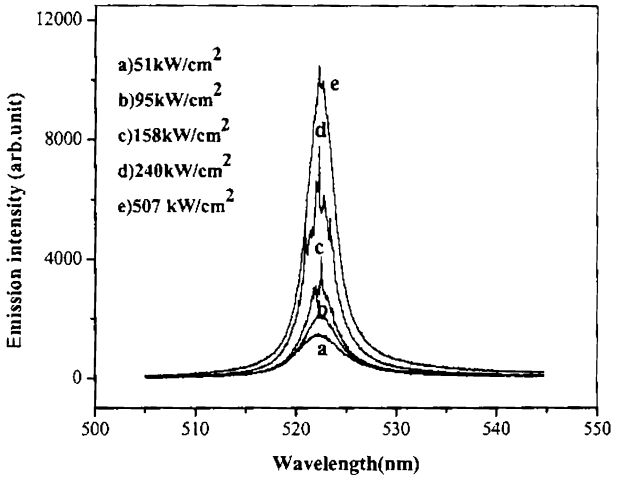

Fig. 3.11 Variation of emission spectrum with pump intensity for an excitation length of 1.5mm

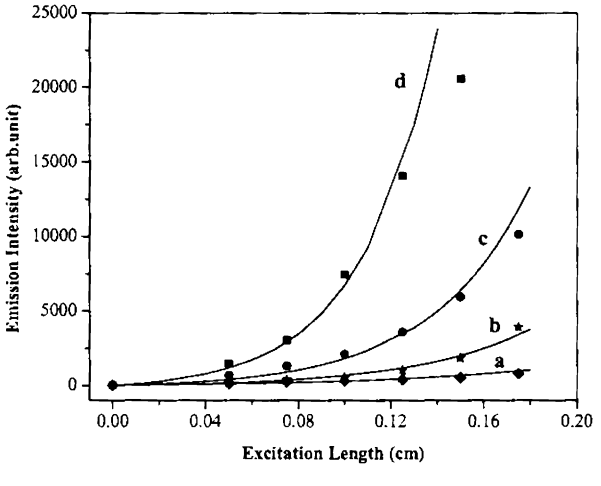

Fig.3.12 Dependence of intensity of ASE on excitation length of pump beam for different pump intensities. a)51kW/cm^2.b)158kW/cm^2 c)240 kW/cm^2 d)635 kW/cm^2

To investigate the lasing behavior of these samples, we have recorded the emission spectra for various excitation lengths and intensities. When the excited length of the gain medium is increased beyond 1.5 mm, good line narrowing is observed. Fig.3.13 shows the shift from ASE to laser emission when the excitation length is increased keeping the pump intensity a constant. As seen in the case of gain coefficient, the laser emission also occurs at reduced length of the excited medium compared to dye doped PMMA samples. When the pump intensity is further increased, the laser emission occurs at a still reduced length. The laser emission which occurs at a short excitation length of 1.5 mm (Fig.3.14) for a pump intensity of 635 kW/cm^2 is observed even at 1.25 mm, for a pump intensity of 793 kW/cm^2 (Fig.3.15)

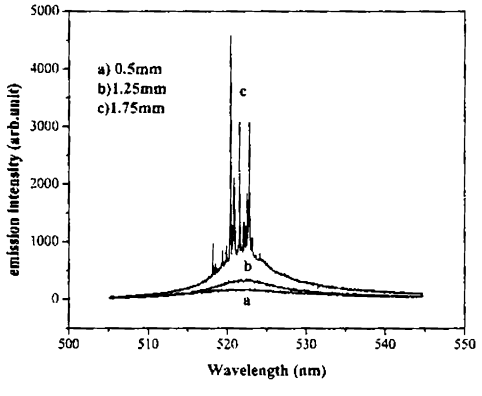

Fig.3.13. Emission spectra with excitation length.Pump intensity 507 kW/cm^2

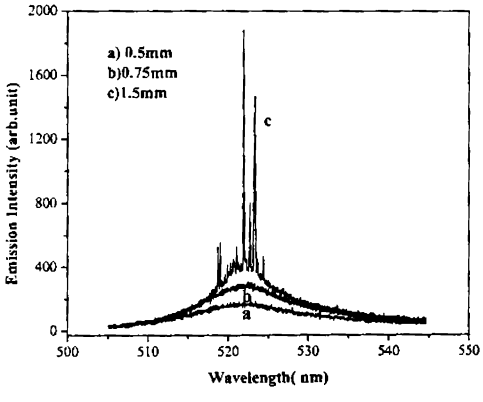

Fig.3.14. Emission spectra with excitation length.Pump intensity 635 kW/cm^2

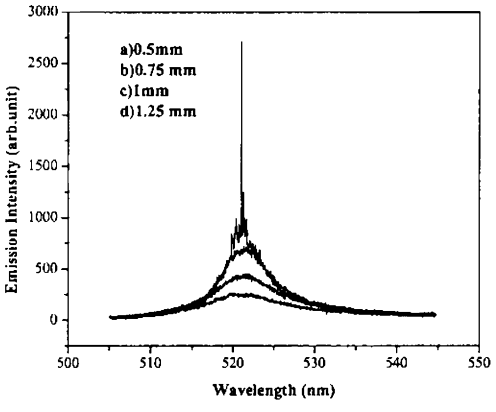

Fig.3.15. Emission spectra with excitation length. Pump intensity 793 kW/cm^2

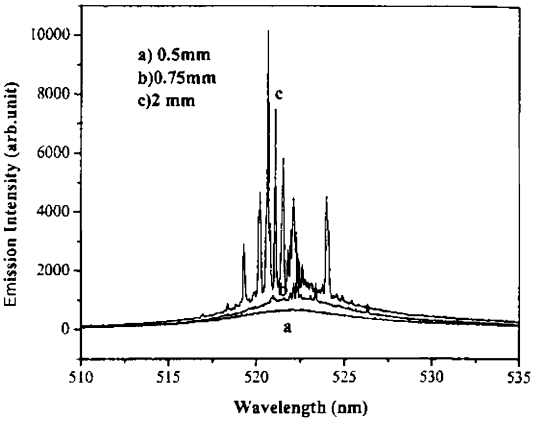

Fig.3.16. Emission spectra with excitation length. Pump intensity 635 kW/cm^2

At greater pump intensities, the laser emission becomes more prominent with increased total spectral width of the emission spectrum. Correspondingly the mode structure becomes more resolved with a good number of modes. The increase in excitation length also generates high gain at a smaller value of the pump intensity which is sufficient enough to start laser oscillations. Fig.3.16 shows the laser emission and mode structure at an excitation length of 2 mm for pump intensity of 635 kW/cm^2. These results substantiate the assumptions made in the case of dye doped PMMA films. The multiple reflections from the parallel surfaces of the thin film and the waveguiding effect result in laser emission from a short length and at a less pump intensity. The dye doped polystyrene films exhibit better optical gain and a lower threshold for laser emission compared to dye doped PMMA films.

Though dye doped polystyrene matrices show better results regarding gain and laser emission, the formation of homogenous, good quality film is critical. The weight percentage of polystyrene in the dye solution, the evaporation rate and the selection of solvents are to be tailored more to achieve better films with better optical quality. Due to the inhomogeneities observed in the film, pump energy is lost due to scattering. The lack of good optical quality of the thin films is reflected in the mode structure observed in the emission spectra (Fig.3.16).

In the search for good optical quality films with polystyrene, cyclohexanone is proved to be a good solvent medium. Thin films are well formed on glass substrate with thickness around 50-60 micrometers. The quantum yield of the dye is also found to be high in cyclohexanone (0.98). Gain studies are conducted to test the potential of the film as a gain medium. But the results are not so promising. Though the dye doped samples exhibit ASE and laser emission, higher pump intensities and longer excitation lengthes are needed to obtain significant gain. A comparison of the performance of the dye doped polystyrene films in the two solvent media is given in Fig.3.17. For a pump intensity of 635 kW/cm^2 the polystyrene samples in toluene medium exhibited a broad emission spectrum at an excitation length of 2 mm while a similar spectrum is obtained at a higher excitation length of 4 mm in cyclohexanone medium. One possible reason for the requirement of higher values of pump intensity and excitation length is the reduced thickness of the films formed in cyclohexanone medium.Here, the amount of the pump intensity absorbed by the gain medium is comparatively less. As the gain observed in this media are very small, a detailed study is not carried out in these samples. The experimental results with these two dye doped films present the possibility of tuning the laser emission by the choice of proper solvents. The separation between the peak emission wavelength is observed to be 18 nm (Fig.3.17).

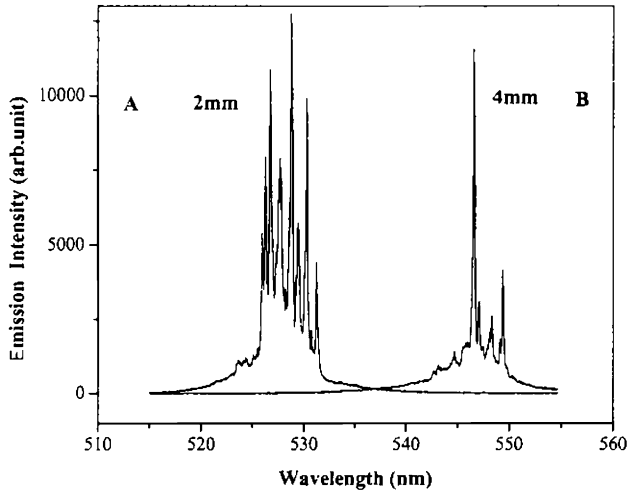

Fig.3.17.Emission spectra from dye doped polystyrene films for two solvent media A) Toluene B) cyclohexanone. Pump intensity 635 kW/cm^2

3.9 Dye doped Polyvinyl chloride films

The third class of polymer material investigated as a solid state matrix for the dye is polyvinyl chloride (PVC) which also is a transparent material with good solubility for the dye. Cyclohexanone is found to be a good solvent for the medium. 4% by weight of PVC is dissolved in cyclohexanone to get a viscous medium. Dye is added to the solution and good films are formed on micro glass sides as described earlier. Good optical quality dye doped films are obtained from PVC. In contrast to the other dye doped films, we could not peel off the films from the substrate. Hence the laser gain studies are performed in the film along with the substrate. With this arrangement the film acts as an asymmetric waveguide with air and glass on both sides of the film. In

the previous cases, the existence of a Fabry-Perot like optical cavity is assumed between the film surfaces, and the laser emission along with the high gain is well explained with the optical feedback provided by them. In the present case, such a cavity effect could not be achieved which in turn will reduce the gain of the medium. Fig.3.18 shows the emission spectra obtained for various excitation lengths of the gain medium at a constant pump intensity of 503 kW/cm^2. These results establish the assumption of a Fabry-Perot like cavity effect in free standing films which significantly enhances the ASE and optical gain. At sufficiently high pump intensities and longer excitation lengths, laser emission is also observed from dye doped thin polymer films due to the high gain obtained from this feedback effect.

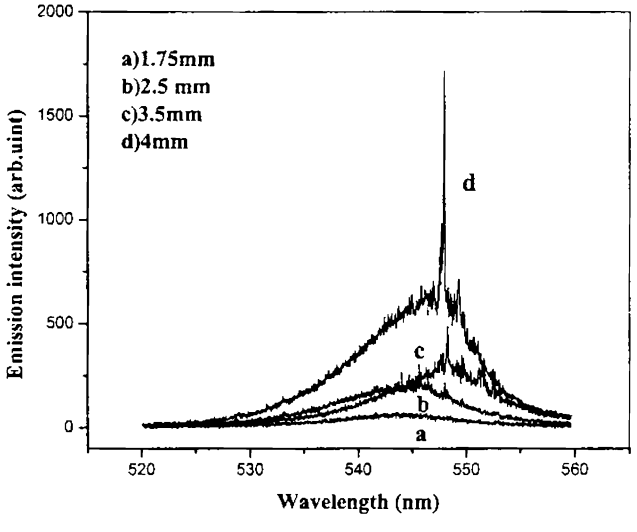

Fig.3.18 ASE spectra from dye doped PVC film (solvent cyclohexanone).Pump intensity 503 kW/cm^2

4.6 Conclusions

Different polymer matrices are experimented as solid state host material for C 540 dye. Dye doped matrices are fabricated both by bulk polymerization and free cast evaporation methods. PMMA, polystyrene and PVC polymers are used to form dye doped films of micrometer thickness by the free cast evaporation method. The performance of the materials as laser gain medium is investigated by analyzing the light amplification and optical gain in these samples. The dye doped free standing polymer films exhibit significant light amplification with increased optical gain compared to bulk samples. The prominent increase in light amplification is attributed to the feedback from Fabry-Perot like optical cavity formed between the lateral surfaces of the film. The mode structure exhibited by the emission spectra of dye doped thin films confirms the existence of an optical cavity. These results establish the occurrence of laser emission in dye doped polymer films of micrometer thickness and could be of considerable application in the design of active optical IC chips.

References

1. A.Costela,I.Garcia-Moreno J.M.Figuera,F.Amat-Guerri ,R Satre, *Polymeric matrices for lasing dyes: recent developments*, Laser Chem.**18** (1998) 63-84
2. F.J.Duarte, A.Costela, G.Moreno,R.Satre, T.J.Ehrlich ,T.S.Taylor, *Dispersive solid state dye laser oscillations*, Opt.and Quant.Elect.**29** (1997)461-472
3. D.Lo, J.E.Parris,J.L.Lawless, *Multi-megawatt superradiant emission from coumarin doped sol-gel derived silica*, App.Phy.B.**55** (1992) 365
4. O.G.Peterson B.B.Snavely , *Stimulated emission from flash lamp excited organic dyes in polymethyl methacrylate* Appl.Phy.Lett.**12** (1968) 238-240
5. H.Soffer, B.B.McFarland, *Continuously tunable, narrow-band organic dye lasers*, App.Phy.Lett.**10** (1967) 266-267
6. B.B.Snavely, O.G.Peterson, R.F.Reithel, *Blue laser emission from a flashlamp –excited organic dye solution*, App.Phy.Lett. **11**(1967)275-276
7. M.A Diaz-Garcia, S Fernandez , M G Kuzyk, *Dye doped polymers for blue organic diode lasers*, Appl.Phys.Lett. **80**(2002) 4486-4488.
8. F J Duarte , R O James, *Tunable solid-state lasers incorporating dye-doped,polymer nanoparticle gain media*, Opt. Lett. **28** (2003) 2088-91
9. D.A.Gromov, K.M. Dyumaev, A.A.Manenkov, A.P.Maslyukov, G.A.Matyushin, V.S.Nechitailo, A.M.Prokhorov, *Efficient plastic-host dye lasers* ,J.Opt.Sco.Am.B.**2** (1985) 1028
10. Y.Sorek,R.Reisfeld,I.Finkelstein, S.Ruschin, *Light amplification in a dye doped glass planar waveguide*,Appl.Phys.Lett. **66** (1995) 1169-1171
11. E,Yariv, S.Schultheiss, T.Saraidarov, R.Reisfeld, *Efficiency and photost-ability of dye-doped solid-state lasers in different hosts,*Opt.Materials, **16** (2001) 29-38,

12. K. M. Dyumaev, A. A. Manenkov, A. P. Maslyukov, G. A. Matyushin, V. S. Nechitailo, A. M. Prokhorov, *Dyes in modified polymers: problems of photostability and conversion efficiency at high* intensities, Opt.Soc.Am.B.**9**(1992)143

13. A.Ishchenko, *Molecular engineering of dye doped polymers for optoelectronics*, Polymers for Advanced Technologies **13** (2002)744-752.

14. Jiu Yan Li,F.Laquai , A.Ziegler ,G. Wegner, *Amplified spontaneous emission in optically pumped neat films of novel polyfluorene derivatives*, Proc. 8th polymers for Advanced Technologies Int. Symp.(2005)1-3

15. A.Costela,I.Garcia-Moreno J.M.Figuera,F.Amat-Guerri ,R Satre, *Polymeric matrices for lasing dyes: recent developments*, Laser Chem.**18** (1998) 63-84

16. R.Satre, A.Costela, *Polymeric solid-state dye lasers*, Adv.Materials, **7** (1995) 198-202

17. A.Costela,I.Garcia-orena,C.Gomez,O.Garcia,L.Garrido,R.Sastre, *Highly efficient and stable doped hybrid organic –inorganic materials for solid-state dye lasers,* Che.Phys.Lett. **387** (2004)496-501

18. Maria A Diaz- Garcia,*Dye-doped polymers for blue organic diode lasers*, Appl. Phys.Lett. **80** (2002) 4486-4488

19. Wu Lu , B. Zhong , D.Ma , *Amplified spontaneous emission and gain from optically pumped films of dye -doped polymers*, Applied optics, **43** (2004)5074-5078.

20. M.D McGehee, R,Gupta, S.Veenstra , E K Miller , M.A.Diaz-Garcia ,A.J. Heeger ,*Amplified spontaneous emission from photopumped films of a conjugated polymer*, Phy.Rev.B , 58 (1998) 7035-9

21. A V Deshpande E.B. Namdas ,*Lasing action of Rhodamine B in polyacrylic acid films*.Appl.Phys.B:Lasers & Opt. **64** (1997) 419-22

22. Kretsch K P, Belton C, Lipson S, Blau W J , Henari F Z, Rost H, Pfeiffer S,

Teuschel A, Tillmann H and Horhold H ,*Amplified spontaneous emission and optical gain spectra from stilbenold and phenylene vinylene derivative model compound*s, J.Appl.Phys.**86** (1999)6155-8.

23. K.L.Shaklee, R .F. Leheny, *Direct determination of optical gain in semiconductor crystals*, Appl.Phy.lett, **18**(1971)475-477
24. F.J.Duarte, L.S.Liao,K.M.Vaeth,A.M.Miller, *Widely tunable laser emission using the coumarine 545 tetramethyl dye as the gain medium*, J.Opt.A: Pure.Appl.Opt. **8** (2006) 172-174
25. A.Maslyukov, S.Sokolov, M.kaivola, K.Nyholm, S.Popov, *Solid state dye laser with modified poly(methyl methacrylate)-doped active elements* App. Opt.**34** (1995)1516-1519
26. H.J Brouwer, V.V.Krasnikov , A.Hilberer, G. Hadziioannou, *Stimulated emission from neat polymer films* Adv. Materials **8** (1997)61-75
27. S. Yap, W.Siew, T.Tou, S.Ng, *Red-green-blue laser emissions from dye-doped poly*[vinyl alcohol films] ,Applied optics,**41** (2002)1725-1728,
28. Otomo A, Yokoyama S, Nakahama T and Mashiko S *Supernarrowing mirrorless emission in dendrimer –doped polymer waveguides.* Appl.Phy.Lett.77 (2000)3881-3883
29. W. Koechner , *Solid state laser engineering*, Springer-Verlag (1972)
30. O.Svelto, D.C.Hanna, *Principles of lasers* 4th ed.Plenum press,New York(1998)
31. K.Geetha,M. Rajesh , V.P.N.Nampoori , C.P.G.Vallabhan,P. Radhakrishnan ,*Laser emission from transversely pumped dye doped free standing polymer films*, J.Opt.A:Pure Appl.Opt.**8** (2006) 189-193

32 R.J.Nedumpara, K.Geetha, V.J.Dann, V.P.N.Nampoori , C.P.G.Vallabhan ,P. Radhakrishnan ,*Light amplification in dye doped polymer films*, J.Opt.A:Pure Appl.Opt.**9** (2007)7-14

UNIVERSITY LIBRARY

Chapter 4

Photostability of Dye Doped Polymer Matrices -A Photoacoustic Study

"Our greatest weakness lies in giving up. The most certain way to succeed is always to try just one more time." Thomas Edison

Abstract

Laser induced photoacoustic studies on the photostability of laser dye C 540, doped in different polymer matrices prepared by both the bulk polymerization and free cast evaporation techniques are presented in this chapter. The dependence of photostability of the dye on various experimental conditions such as nature of solvents, incident optical power, dye concentration, wavelength and modulation frequency of incident radiation is investigated in detail. Photostability of the dye doped polymer matrices fabricated by the two techniques are compared. The possible photodegradation mechanisms are also discussed.

4.1 Introduction

Organic dyes impregnated into different solid matrices have found wide applications in modern photonic technology. They are significant materials in different areas such as active laser media, passive Q-switches, optical data storage, photonic displays and optical wave guide. The availability of a variety of organic dyes and possible host

materials and the technical easiness with which low cost systems can be fabricated, make dye doped materials quite attractive.

For all applications of the dye doped solid state matrices, a through knowledge of the photophysics of the dyes and its photostability is essential for its efficient performance. Dye doped solid state matrices as a laser gain media are very popular and widely studied area of application. In order to overcome the many drawbacks raised by liquid dye lasers, the dye doped solid state matrices are found to be quite attractive. The combined use of photostable laser dyes and improved polymeric materials have made solid state dye lasers a practical alternative to liquid dye lasers.

Though the polymer matrices are superior to many other solid state host materials, the finite lifetime for stable operation of the dye incorporated into the polymer host and the low quantum efficiency still remain as limitations to the commercial exploitation of these types of active laser gain media. The low quantum efficiency is due to the photodestruction of the dye molecules. The photostability of the dye doped polymer matrix depends on the inter-molecular and intra-molecular interactions of the dye molecule with surrounding chemically active materials such as the polymer macromolecules, unreacted monomers, absorbed atmospheric oxygen molecules and another dye molecule. The photodeactivation is enhanced by the mobility and concentration of the dye molecules [1]. Intense research is going on to improve the photostability and lifetime of dye doped devices. In general, the photodeactivation of the dye from the excited state is due to photchemical reaction, formation of dimers that absorb the incident light without any emission and thermal destruction that cause photodegardation of the dye [1-2].

Another possible reason for the degradation of the dye molecule is the thermal destruction of the dye due to the poor thermal conductivity of the polymer host. The excited dye molecule heats up the host through non radiative thermal relaxation. The

accumulated heat in the polymer host due to the large time of heat dissipation increases the mobility of the dye and facilitates the photodeactivation reaction with the surrounding chemically active molecules [1, 3].

Many possible mechanisms are experimented to reduce the photodegradation of the dye. One important parameter to reduce the photodegradation is to optimize the rigidity of the host material. Dissipation of the excess energy of photoexcitation can be favoured by a phononic coupling of the dye molecule to the host media. This can be achieved by optimizing copolymer mixtures as matrix materials or by covalently linking the dye molecule to the polymeric chains to provide additional channels for the dissipation of the excess heat energy [4].

4.2 Photodegradation measurements

The photodegradation of organic dyes is essentially a photoinduced reaction. A dye molecule excited to a higher energy state shall return to the ground state unless it gets involved in a photochemical reaction and loses its identity. An excited molecule can dissipate its excitation energy in a number of ways. Among the different paths of decay, the most important channels are radiative relaxation such as fluorescence and phosphorescence, nonradiative relaxation as thermal radiation and excited state chemical reaction.

In the radiative or nonradiative relaxation process, the energy released is determined by the energy absorbrd by the number of dye molecules present in the ground state and those in the excited state. Any type of photodegradation will change the number density of the dye molecules in the ground state .This in turn will reduce the amount of optical absorption or the amount of energy released radiatively or nonradiatively. By measuring any of these three quantities we can have a quantitative measurement of the photodegradation occurring in the sample. Two methods are

generally employed to evaluate the photostability of the medium. In the optical method, the quantity measured is the optical absorption, transmission or the energy released radiatively. In the second method, which is the photothermal technique, the nonradaitive part of deexcitation is measured [5]. The photothermal methods are found to be highly sensitive for the thermal characterization of a sample. The fundamental principle of a photothermal method is the photo-induced change in the thermal state of a sample. Measurement of the temperature, pressure or density changes that occur due to optical absorption form the basis of the photothermal method. Sample heating is a direct consequence of the optical absorption and hence the photothermal signal is directly dependent on the quantity of the light absorbed. Scattering and reflection losses do not produce photothermal signals. Hence photothermal methods more accurately measure optical absorption in samples.

In a photochemical process, some intermediate species are created which are usually associated with nonradiative energy transfer that generates thermal effects. Thus photothermal methods are more effective for detecting the excited state processes. Photoacoustic technique is one of the efficient techniques that comes under photothermal methods.

4.3 Photoacoustic method

Photoacoustic effect is a phenomenon which has become quite popular as well as effective in recent years for the thermal and optical characterization of various classes of materials. It is basically the generation of sound waves from the material when it is irradiated with intensity modulated light beam. Absorption of the intensity modulated light and the periodic heating of the sample through nonradiative de-excitation is transferred to the surrounding gas layer generating pressure fluctuations. The acoustic signals thus generated are detected by a microphone attached to the cell. The resulting

PA signal is a measure of the absorption coefficient of the sample[6]. Both the amplitude and phase of the signal contain valuable information regarding the material characteristics.

4.4 Rosencwaig-Gersho Theory

The standard theory on photoacoustic effect was introduced in 1976 by Rosencwaig and Gersho which is referred to as R-G theory [7]. The formulation of R-G model is based on the light absorption and thermal wave propagation in a simple configuration shown in Fig.4.1. This theory is essentially a one dimensional analysis of the heat flow in the experimental configuration. Generally the thermal oscillations due to the absorption of modulated light at a point beneath the surface of a sample contributes to the photoacoustic signal and it is governed by the thermal diffusion length μ_i defined as $\mu_i = \left(\frac{2\alpha_i}{\omega}\right)^{1/2}$ where $\omega = 2\pi f$ and f is the frequency of light. A simple cylindrical cell of length L and diameter D is considered for the formulation of the PA theory. The other specifications of the cell are;

l - thickness of the sample; l_b- thickness of the backing material

l_g- length of gas column ; ρ_i - density of material

k_i - thermal conductivity; c_i – specific heat of material

$\alpha_i = \frac{k_i}{\rho_i c_i}$ - thermal diffusivity

$a_i = \left(\frac{\omega}{2\alpha_i}\right)^{1/2}$ - thermal diffusion coefficient

$$\mu_i = \frac{1}{a_i}$$ - thermal diffusion length of the material

where i denotes sample s, gas g and backing material b.

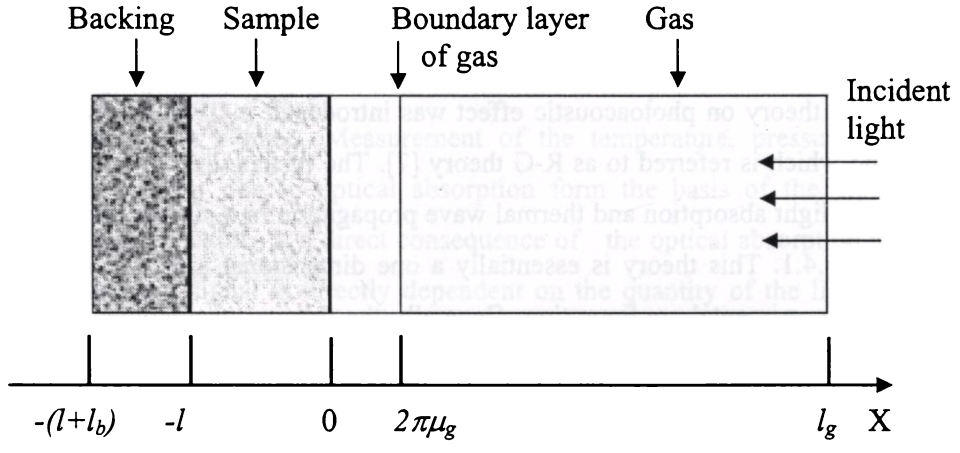

Fig.4.1 Schematic representation of photoacoustic experimental configuration

When a monochromatic light of wavelength λ is incident on a solid with intensity

$$I = \frac{1}{2} I_0 (1 + \cos \omega t) \tag{4.1}$$

where I_0 is the incident monochromatic light flux (W/cm^2), the heat density produced at any point x due to light absorbed at that point in the solid is given by

$$\frac{1}{2} I_0 \beta \exp(\beta x)(1 + \cos \omega t) \tag{4.2}$$

where β is the absorption coefficient of the sample. Since the solid extends from x = 0 to x = -l, x takes negative values .The light is incident at x =0. The air column extends from x = 0 to x = $\mathbf{l_g}$ and the backing material from x = -l to x = -$(l+l_b)$ The thermal diffusion equation in the solid taking into account the distributed heat source can be written as

$$\frac{\partial^2\theta}{\partial x^2} = \frac{1}{\alpha_s}\frac{\partial\theta}{\partial t} - A\exp(\beta x)(1+\exp j\omega t) \quad \text{for } -l \le x \le 0 \tag{4.3}$$

$$\text{with } A = \frac{\beta I_0 \eta}{2k_s} \tag{4.4}$$

where θ is the temperature and η is the efficiency with which the absorbed light at wavelength λ is converted to heat by nonradaitive deexcitation process. η=1 is a reasonable assumption for most solids at room temperature.

For the backing and the gas, the heat diffusion equations are

$$\frac{\partial^2\theta}{\partial x^2} = \frac{1}{\alpha_b}\frac{\partial\theta}{\partial t} \quad ; \qquad -l - l_b \le x \le -l \tag{4.5}$$

$$\frac{\partial^2\theta}{\partial x^2} = \frac{1}{\alpha_g}\frac{\partial\theta}{\partial t}; \qquad 0 \le x \le l_g \tag{4.6}$$

The real part of the complex valued solution θ(x,t) is of physical interest and represents the temperature in the cell relative to the ambient temperature as a function of position and time. After applying proper boundary conditions for temperature and heat flow continuity and by neglecting the convective heat flow, the periodic temperature fluctuations at he sample-gas interface can be obtained as

$$\theta_0 = \frac{\beta I_0}{2k(\beta^2-\sigma^2)}\left[\frac{(r-1)(b+1)e^{\sigma l} - (r+1)(b-1)e^{-\sigma l} + 2(b-r)e^{\beta l}}{(g+1)(b+1)e^{\sigma l} - (g-1)(b-1)e^{-\sigma l}}\right] \tag{4.7}$$

where

$$b = \frac{k_b a_b}{ka}\ ;\ g = \frac{k_g a_g}{ka};\ r = \frac{(1-i)\beta}{2a};\ \sigma = (1+i)a\ ; \tag{4.8}$$

The periodic thermal waves damp completely as it travels the thermal diffusion length $2\pi\mu_g$. Thus the gas column within this distance expands and contracts periodically so that it acts as an acoustic piston for the remaining gas in the PA cell. Assuming that, the rest of the gas responds adiabatically to the action of acoustic piston, the adiabatic gas law can be used to derive an expression for the pressure variation Q as

$$Q = \frac{\gamma P_0 \theta_0}{\sqrt{2} T_0 l_g a_g} \tag{4.9}$$

where γ,P_0 , T_0 are the ratio of heat capacities of air, ambient pressure and temperature respectively. Equation 4.9 can be used to evaluate the magnitude and phase of the acoustic pressure wave in the cell due to photoacoustic effect. This expression takes simple forms in special cases.

4.5 Photostability investigations using PA technique

Though the actual mechanism responsible for photostability is not fully known it is essentially a photo induced modification of the dye molecule by which the absorption and emission characteristics may change. The photobleaching has shown a linear dependence on the incident intensity of radiation. By measuring either the emission or absorption, one can estimate the amount of photodestruction taking place in the sample. In the present investigation, the nonradiative part of the deexcitation in the sample is measured using PA technique.

According to the special cases denoted by R-G theory, the dye doped samples are optically transparent and thermally thick, as the thermal diffusion length in polymer sample is only a few microns in the frequency range of investigations[3]. Then, the complex amplitude of the PA signal produced is given by

$$Q = \frac{-i\beta\mu^2\gamma P_0 I_0}{4\sqrt{2}T_0 l_g a_g k} \tag{4.10}$$

Here β is the optical absorption coefficient of the sample, μ is the thermal diffusion length in the solid material, I_o is the incident light intensity, l_g is the length of gas column inside the cavity, a_g is the thermal diffusion length in the gas and k is the thermal conductivity of the sample. If the β value changes in any case, the PA signal amplitude will also vary accordingly. Any kind of photochemical or thermal reaction will result in a change in the number density or concentration of the original molecule. This in turn will result in a change in the absorption properties of the sample. Doping of an organic dye in a solid matrix does not change the thermal properties of the host material [8]. Similarly the thermal properties of the polymer matrix are unaffected by the photochemical or photothermal changes in the dye molecule [3,9]. Thus, when a dye doped sample is investigated by PA technique, any change in the PA amplitude is essentially a measure of the rate of photodegradation of the dye.

The aggregation of the dye molecules at high concentrations may decrease the optical gain or reduce the photostability through some photochemical reactions resulting from the dimer of the dye molecules.

4.6 Experimental Details

The continuous wave (cw) laser induced photoacoustic technique is employed to investigate the photo induced degradation of the C 540 dye doped polymer matrices. The photostability investigations are carried out in samples fabricated by both the bulk polymerization and free cast evaporation techniques. The photostability is studied under different environments such as different solvents, varying optical powers, modulating frequencies, concentrations of the dye and pump wavelengths. Detailed investigations are done in samples prepared by the bulk polymerization method to get

the general behaviour of the dye molecule. Investigations are restricted to pump power variations in respect of samples prepared by free cast method. The experimental set up used for the PA study is as shown in Fig.4.2. The source of light used is an Argon Ion laser (Liconix 5400) and its different emission lines. The laser beam is intensity modulated by using a mechanical chopper(Ithaco HMS 230). The modulated beam at specific power levels is allowed to fall on the sample which is kept in a non –resonant PA cell. A highly sensitive electret microphone (Knowles BT 1834) is used to detect PA signal collected in the reflection mode. The PA signal is processed using a digital lock in amplifier (SR850 DSP). The thickness of the bulk samples used for the study is of the order of 0.5mm.

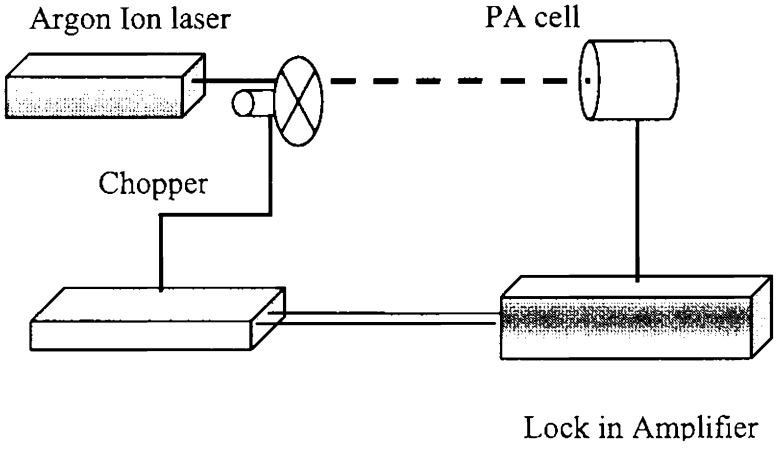

Fig.4.2.Schematic diagram of the photoacoustic set up for the photostability studies

4.6.1 PA studies in bulk samples

The nature of the PA signal variation with time has been studied under different environments. The photostability of the coumarin 540 doped PMMA with different solvents is shown in Fig 4.3. The dye has good solubility in all the three solvents. But the polymer matrix with ethanol as the solvent shows better stability though the difference is not very prominent. The photo destruction of the dye molecule is initiated by chemically active radicals of the basic polymer matrix. These radicals interact effectively with dye molecule at excited states and stimulate their destruction. The incorporation of a low molecular weight additive is found to suppress the generation of these radical chains [8]. In this case ethanol may be more effective in suppressing the generation of the radicals. The polymerization process also gives high quality samples with ethanol. Thus ethanol is selected as the solvent for all further investigations.

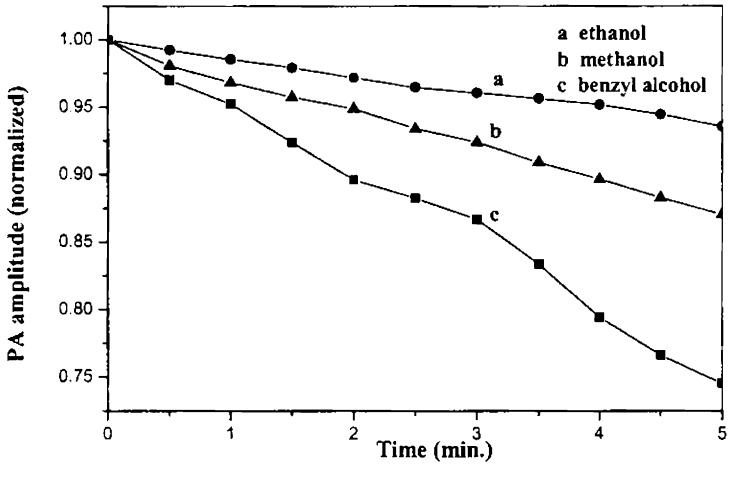

Fig.4.3 PA signal amplitude versus time plot of C 540 doped PMMA for different solvents.

The effect of laser power on the stability of the dye doped polymer matrix is investigated for different optical powers varying from 10 mW to 50 mW. The PA signal variation with different powers is as shown in Fig .4.4. It is clear from the plot that bleaching rate increases with increasing input power. The fact that logarithmic plot of laser power versus bleaching rate (Fig.4.5) gives a slope approximately equal to one shows that, photobleaching is a linear process attributed to one photon absorption. This is in agreement with the earlier reported studies by different authors [8-9]. This indicates that photobleaching in Coumarin 540 doped PMMA takes place when the system is in the first excited singlet state or triplet state and multi photon absorption may not have any significant role in the photodegration of the dye.

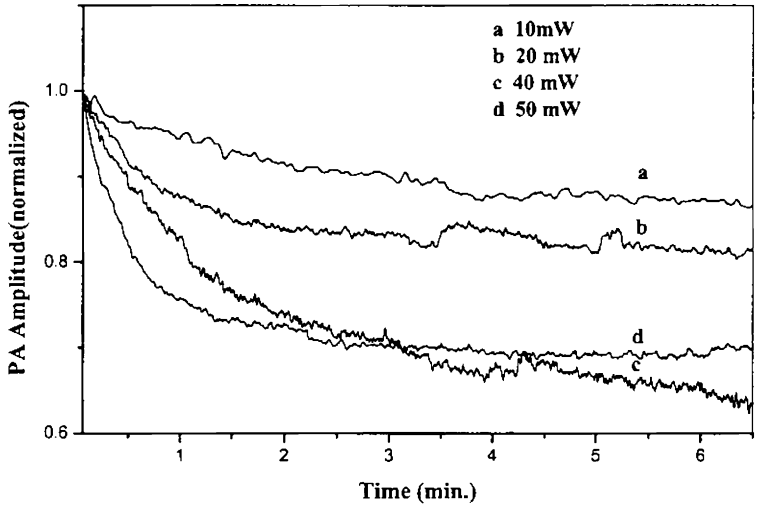

Fig.4.4 PA signal amplitude versus time plot for different optical powers. Chopping frequency 30 Hz

The absorption spectrum of the sample recorded using a spectrophotometer before and after bleaching is shown in Fig.4.6. This shows that photodestruction of the dye molecule takes place during irradiation of the sample and the resultant product

does not absorb any radiation at 476 nm where a strong absorption exists for the original dye molecule. The decrease in the PA signal is due to the photodegradation of the sample .The observed PA signal after the bleaching of the sample is attributed to the solid PMMA matrix. The photo bleaching causes a colour change and the irradiated region becomes transparent. For higher input powers the bleaching takes place at a faster rate.

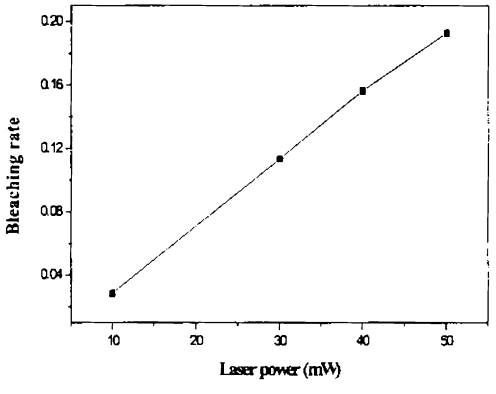

Fig.4.5 Variation of rate of bleaching with incident laser power.

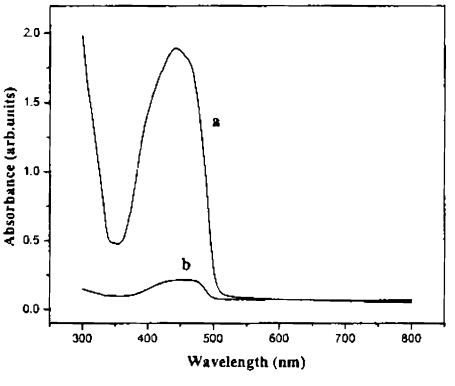

Fig.4.6 Optical absorption spectrum of C 540 doped PMMA samples a) before and b)after bleaching.

The variation of photodestruction is studied for concentrations varying from 5 x 10^{-3} M to 1 x 10^{-6} M and is shown in Fig. 4.7. We have used laser radiations of 30 mW power at a chopping frequency of 30 Hz. In the lower concentration range it is observed that photodestruction increases with decreasing concentrations of the dye, (Fig.4.7 b,c)which is due to the reduced number density of the dye molecules [6]. But for very small concentrations (Fig.4.7 d,e) the PA signal showes no considerable variation with time. At these concentrations, the activation time is very small so that the observed variation is insignificant (12).

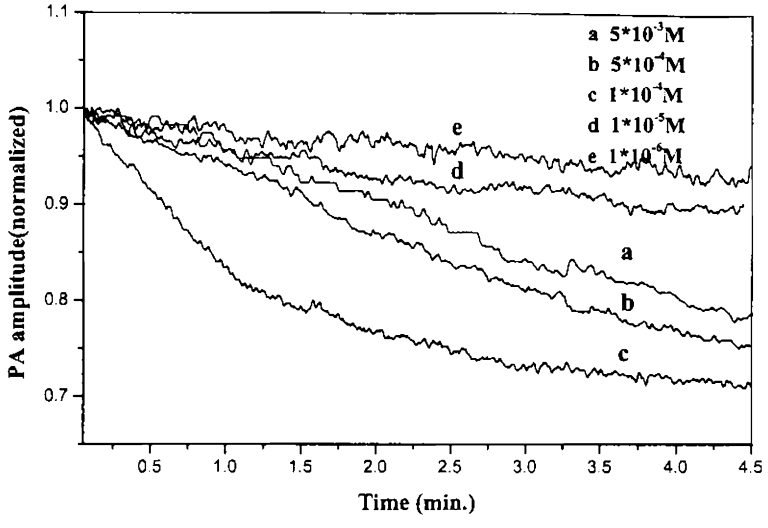

Fig.4.7 PA signal amplitude versus time plot
for different concentration of the dye

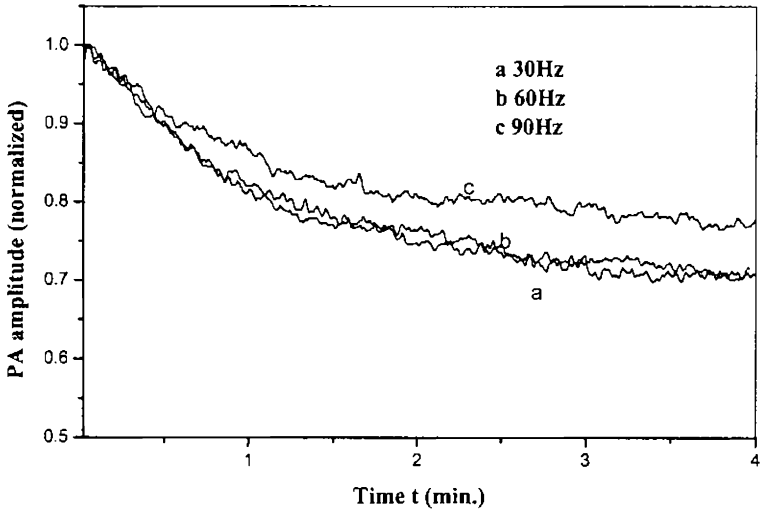

Fig.4.8 PA signal amplitude versus time plot for different modulation frequencies.

The influence of the modulating frequency on photostability has also been studied (Fig.4.8). Though incident intensity is reduced with increased chopping rate this has very small effect on photodestruction. This implies that the stability of the dye doped polymer matrix depends on the total energy per unit time incident on the sample which is the same for all chopping frequencies. This is not the case with all dyes. A decrease in bleaching rate is observed with increased chopping rate in certain cases indicating the role of exposure time in the bleaching process. [10]

The Coumarin 540 has two absorption bands, one in the UV region and the other in the visible region [11]. The dependence of photodestruction on different wavelengths available from the Argon Ion laser shows that significant photobleaching is observed mainly for 476 nm (Fig.4.9). Photobleaching is insensitive to radiation at wavelength 514 nm which is in agreement with the absorption spectrum of the sample.

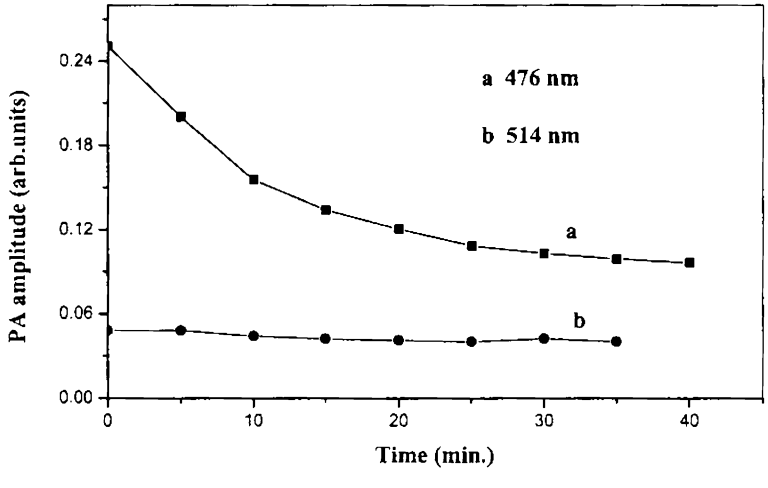

Fig.4.9 PA signal amplitude versus time plot for different wavelengths.

The main photodegradation mechanism can be a photochemical or photothermal process or both, but the specific contribution of each process is unknown [13]. The commonly accepted reasons for the degradation of dye molecules are thermo destruction due to the poor thermal dissipation in the polymer host, photo deactivation from the excited states which results in the transformation of the dye molecule into components that no longer absorb light in its absorption band and thirdly the formation of dimers that absorb radiation without any fluorescence [1].

Assuming that the degradation rate of the dye obeys an exponential relation, the PA signal amplitude can be written as $Q(t) = Q_0 \exp(-t/\tau)$ at constant exposure to incident optical power[13]. The degradation rate can be obtained from the slope of the curve plotted between time and log Q. The decay rates at various concentrations of the dye are tabulated in Table 4.1. From the table it is obvious that the photobleaching is a concentration dependent process .Two distinct mechanisms are found to be prominent in the bleaching process. Except in the case of 5×10^{-3} M concentration, the first process is found to be faster than the second.

Concentration Of the dye	$\frac{1}{\tau 1}$ **(ms^{-1})**	$\frac{1}{\tau 2}$ **(ms^{-1})**
5×10^{-3} M	0.22	0.66
5×10^{-4} M	0.52	0.42
1×10^{-4} M	1.35	0.46
1×10^{-5} M	0.63	0.18
1×10^{-6} M	0.31	0.14

Table 4.1 Decay rates of the dye at various concentrations.

4.6.2 PA studies in dye doped polymer film samples

C 540 dye, doped in polymer matrices such as PMMA, polystyrene and poly vinyl chloride are prepared to form films of thickness in the range 20-200 microns. The effect of laser power on the photodegradation rate of these films is carried out under different optical pump powers. All the experimental conditions are the same as that of bulk samples.

Good optical quality films are formed by doping C 540 with commercially available PMMA with a weight percentage of 10 using MEK as the solvent. We have used films of thickness 150-200 microns for the photostability studies. The variation of signal amplitude as a function of time for various pump powers is as shown in Fig.4.10 For a small pump power there is a gradual decrease in PA signal amplitude while at greater pump powers the signal variation occurs at a faster rate. Very quick saturation of PA signal is observed at a pump power of 80mW due to complete photodegaradation of the dye.

For the dye doped polystyrene films, the photodegradation of the films with power is as shown in Fig.4.11. The PA studies are performed for the same pump powers as earlier. As in the previous case for lower pump powers, the photobleaching rate is slow which increases with increase in pump power. But saturation of PA signal is not observed within the range of measurements carried out. The thickness of the samples studied is within the range of 130-180 microns which is almost the same as in the case of PMMA films .The polystyrene matrix is found to be more stable than PMMA matrices.

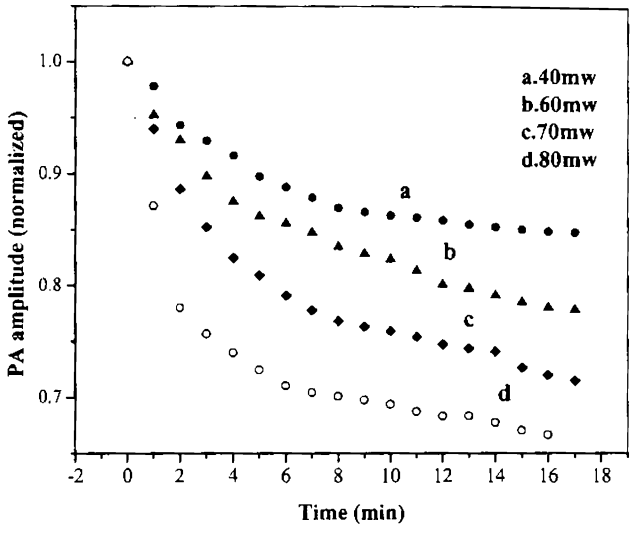

Fig.4.10 Variation PA signal with pump power
for C 540 doped PMMA films

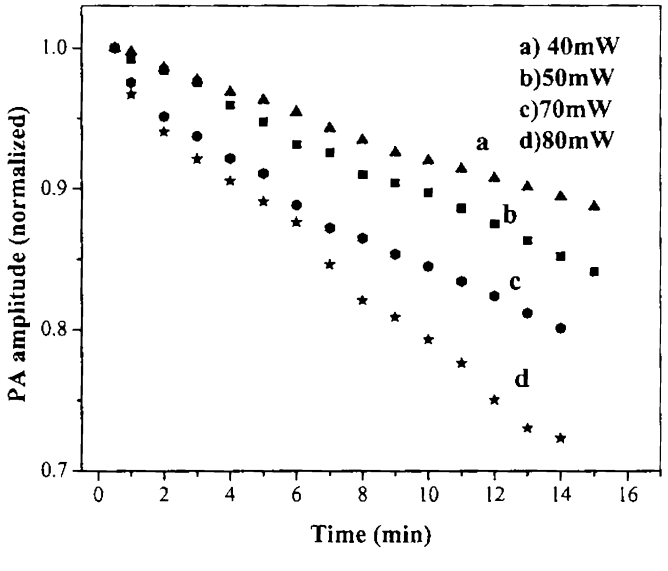

Fig.4.11 Variation PA signal with pump power
For C 540 doped polystyrene films

The difference in photostability of the two matrices could not be related to the nature of thermal dissipation since PMMA is a better thermal conductor than polystyrene [14]. Since the same concentration of the dye is used for the formation of both types of dye doped polymer films, the role of dimer formation need not be significant in photodegradation. The excited state photodeactivation of the dye is different in different polymer matrices and solvent environments. Hence the photo chemical reaction of the dye in its excited state with PMMA molecules may be more significant than with polystyrene molecules which lead to the photodestruction of the dye at a faster rate.

Fig.4.12 shows the results of photoacoustic studies carried out in dye doped PVC polymer films. Compared to dye doped PMMA and polystyrene films, degradation rate is found to be much higher in PVC films. One possible reason is the lower thickness of the selected PVC polymer films. The investigations are carried out in films of thickness in the range 20-60 microns which are considerably less than PMMA films. The excited state photochemical reaction of the dye with the PVC molecule may be more destructive. Though good quality dye doped films are formed with PVC, its performance as a solid host for laser gain media is not promising.

A comparison of the performance of dye doped bulk PMMA sample fabricated by free radical polymerization method is made with the dye doped PMMA thin film prepared by free cast evaporation method at a pump power of 50 mW (Fig.4.13). The dye doped PMMA film is found to be more stable than the bulk samples. The faster degradation of dye molecule in bulk samples may due to intermolecular interaction between the dye molecule and the free radical of the polymer formed during the polymerization process.

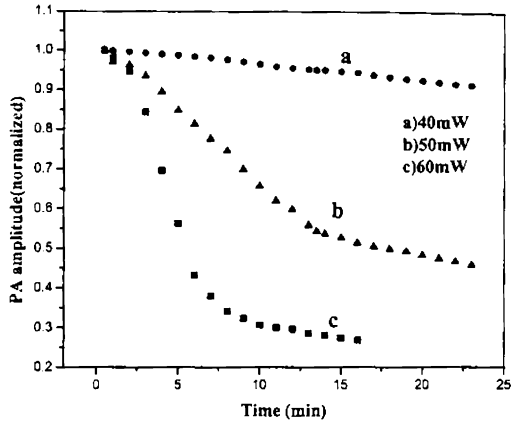

Fig.4.12 Variation of PA signal with pump power for C 540 doped PVC films

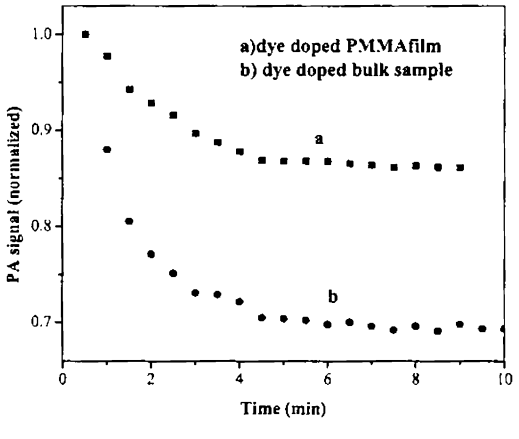

Fig.4.13 Comparison of PA signal amplitude for dye doped PMMA polymer film and thick sample

4.7 Conclusion

The photostability of C 540 dye doped polymer matrices fabricated by bulk polymerization and free cast evaporation techniques is investigated successfully employing the photoacoustic technique. The investigations are carried out under different experimental conditions such as pump power, concentration of the dye, modulation frequency and excitation wavelength. The photodestruction of the dye is found to be a linear process. Photostability of the dye in different polymer matrices are compared. Dye doped polystyrene matrix exhibits better stability than PMMA and PVC matrices. A comparison of photostability is also carried out among samples of bulk polymerization and free cast evaporation techniques in which the latter gives better photostability.

References

1. S.Singh, V.R. Kanetkar, G.Sridhar, V.Muthuswamy, K.Raja, *Solid state polymeric dye lasers*, Jou.of luminescence, **101** (2003) 285-291
2. Sastre R and Costela A ,*Polymeric solid-state dye lasers*. Adv.Mater. **7** (1995)198-202.
3. N.A.Georgre, B.Aneeshkumar, P.Radhakrishnan,C.P.G.Vallabhan, *Photoacoustic investigations on the photostability of Rhodamine 6G doped PMMA,* Appl.Phys.**32**(1999) 1745
4 Costela A,Garcia-Morena I and Figuera J.M,*Polymeric matrices for lasing dyes:recent develppments*, Laser Chem.**18** (1998)63-84.
5. E.L.Arbeloa, T.L.Arbeloa , .L.Arbeloa Costela,A Moreno I.G, J.M.Figuera, F.A.Guerri, R.Sastre, *Relations between photophysical and lasing properties of rhodamines in solid polymeric matrices,* App.Phy.B:Las.Opt.**64** (1997) 651
6. J.A.Sell, *Photothermal investigations of solids and fluids,* Academic Press,Bosto (1989)
7. A.Rosencwaig,A.Gersho, *Theory of the photoacoustic effect with solids* J.Appl.Phys.**47** (1976)64-69
8. K.M.Dyumaev,A.A.Manenkov,A.P.Maslyukov,G.A.Matyushin,V.S.Nechitailo ,A.M.Prokhorov, *Dyes in modified polymers: problems of photostability and conversion efficiency at high intensities* ,Opt.Soc.Am.B.**9**(1992) 143-151,
9. I.P.Kaminov,L.W.Stulz,E.A.Chandross,C.A.Pryde, *Photobleaching of organic dyes in solid matrices*, App.Opt.,**11** (1972)1563
10. A.Philip, P.Radhakrishnan, V.P.N.Nampoori, C.P.G.Vallabhan ,*Photoacoustic study on photobleaching of cresyl violet in polyvinyl alcohol by laser light*, Int.J.Opt.Elec. **8**(1993)501
11. E.P.Schafer (Ed.) *Dye lasers*, Springer, Berlin (1977)

12. R.J.Nedumpara, Binoy Paul, Santhi.A, P.Radhakrishnan, V.P.N.Nampoori, *Photoacoustic investigations on the photostability of dye doped PMMA* Spectrochemica Acta Part A ,**60** (2004) 435-441

13. R.Duchowicz, L.B.Scaffardi, A.Costela, I.G.Moreno, R.Sastre, A.U.Acua, *Photothermal characterization and stability analysis of polymeric dye lasers*, App.Opt. **39** (2000)4959

14. C.A.Harper(ed) *Handbook of Plastics and Elastomers,* McGraw-Hill book,New York (1975)

Chapter 5

ASE and Energy Transfer Studies in Dye Mixtures

"If I have made any valuable discoveries, it has been owing more to patient attention than to any other talent." Issac Newton

Abstract

The energy transfer mechanism in C 540-Rhodamine 6G and C 540-Rhodamine B donor-acceptor (d-a) pairs are investigated. The good spectral overlap and the proximity of d-a pair molecules which is around 60 Å denote the possibility of resonance energy transfer between the d-a pairs. Energy transfer is studied in four solvent environments. C 540-Rh 6G and C 540 - RhB d-a pairs behave in quite different manner in different solvent environments.

5.1 Introduction

The concept of energy transfer in which electronically excited molecules transfer their energy to neighbouring molecules is widely used as an effective tool for the measurement of nanometer scale distances and for the investigations of molecular interactions. It is referred to as a spectroscopic ruler due to its sensitivity over distances of few nanometers [1]. The different mechanisms by which an electronically excited molecule decay to the ground state loosing its excitation energy provide lot of information about the structure and dynamics of macromolecules, the interactions of

macromolecules with each other, the environmental effects, conformation changes and proximity between molecules. Detection techniques based on energy transfer are very attractive due to their high sensitivity and find wide applications in different fields such as photochemistry, analytical biochemistry, environmental analysis and diagnostics [1-5]. The energy transfer between donor and acceptor pairs is also found to be very effective in controlling and tuning light emission in laser gain media [6-10].

5.2 Different Energy Transfer Mechanisms in a d-a Pair

An electronically excited molecule which is short lived will decay to the ground state dissipating its excess energy of excitation in three different ways:

1) Radiationless transitions from one electronic state to another
2) Radaitive transitions between electronic states
3) Electronic energy transfer between different molecules.

Thus energy transfer process is an intermolecular deactivation of the excited state. It is the transfer of the electronic excitation energy of a molecule or group (donor), to another molecule or group of a different species (acceptor). Similar transfer of energy to the molecules of same species is described as energy migration [11]. The energy transfer is a complex process which includes different mechanisms for the transfer of energy from donor molecule to acceptor molecule. Energy transfer may occur by a radiative process, involving the emission of a photon by the donor molecule and its subsequent absorption by the acceptor molecule. It may also occur by a nonradiative process, due to the interaction between the donor and the acceptor molecules during the excitation lifetime of the donor, prior to the emission of a photon. Nonradiative transfer can be due to electron exchange interaction or coulombic (dipole-dipole) interaction between D* and A where D* represents the excited state of donor. The former one may take place over distances ~ 6-15 Å, which is comparatively closer to the molecular diameter while the latter takes place over

intermolecular distances (30-70 Å) which are large compared to the molecular diameter[11-12]. These mechanisms of energy transfer which are termed as radiative transfer, short-range transfer and long-range transfer are briefly described below.

5.2.1 Radiative transfer

In radiative transfer of electronic energy, the photons emitted by the excited state of the donor, travel through the medium and are absorbed by the acceptor. It is a two step process. There is no direct interaction between the donor and acceptor. Radiative energy transfer occurs for that part of the spectrum where there is an overlap between the emission spectrum of the donor and absorption spectrum of the acceptor. The donor emission lifetime is invariant in radiative energy transfer. The generalized mechanisms of radaitive energy transfer can be described as follows.

Donor emission: $D^* \rightarrow D + h\nu_A$

Acceptor absorption: $A + h\nu_A \rightarrow A^*$

5.2.2 Radiationless transfer due to electron exchange interaction

The electron- exchange interaction occurs at a short range ($\leq$ 15 Å). Energy from the donor D* is transferred to acceptor A if the intermolecular separation between the two species approaches the collision diameter. It is not necessary for the two molecules to collide since transfer can occur at distances slightly greater than the collisional diameter [13]. Its magnitude is proportional to the overlap integral. This exchange interaction is usually dominant at close approach of D* and A and if the virtual transitions between the donor and acceptor molecules are spin forbidden so that the coulombic interaction is negligible. One necessary condition for the transfer of energy by the short-range process is that the multiplicities of the states involved in the transfer must be in accordance with the Wigner spin conservation rule [13]. It is a

diffusion controlled process and dependent on the solvent viscosity and temperature. The electron exchange energy transfer can be described as follows.

$D^* + A \rightarrow D + A^*$

5.2.3 Radiationless transfer due to Coulombic interaction.

This energy transfer occurs as a result of the dipole-dipole coupling between the donor and acceptor and does not involve the emission and reabsorption of photons. Transfer of energy can occur even when the donor and acceptor molecules are separated by distances much greater than the donor-acceptor collision diameter. The basic requirement for the energy transfer to occur is compatibility and proximity [1]. A compatible acceptor is a molecule whose absorption spectrum overlaps the emission spectrum of the donor molecule. The degree to which they overlap is decided by the spectral overlap integral *J*. Proximity means that a compatible acceptor molecule is close enough to the donor for the energy to excite it. Also, the donor and acceptor dipole orientations must be approximately parallel. Spectral overlap indicates that the energy differences between the vibrational levels of ground and first excited state of the donor correspond to the energy differences between the vibrational levels of ground and first excited state of acceptor. The schematic representation of nonradiative energy transfer is given in Fig.5.1. Thus when two fluorophores, a donor and an acceptor are very close together (less than100 Å) and the donor emission is of the same energy as that of the acceptor excitation, a quantum of energy is transferred to the acceptor raising the electrons of the acceptor to higher energy state as the donor returns to the ground state. This is also known as resonance energy transfer. The acceptor can be fluorescent or non fluorescent. If it is fluorescent, the transferred energy is emitted as the fluorescence characteristics of the acceptor. If it is not fluorescent, the energy is transferred to the solvent. The process can be represented as

$D^* + A \rightarrow D + A^*$

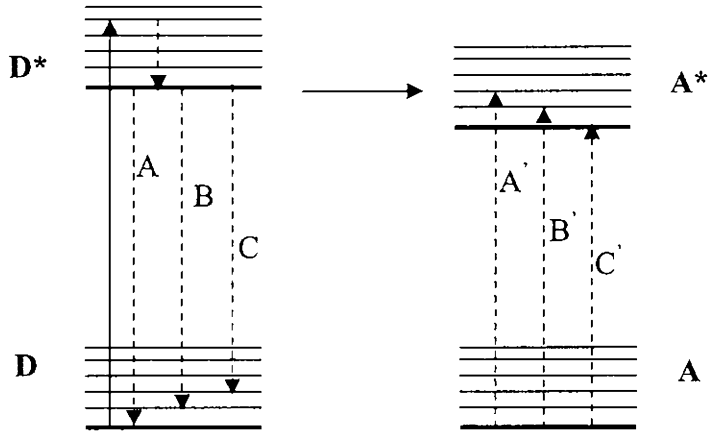

Fig.5.1. Resonance energy transfer from an excited donor D* to ground state acceptor A.A and A', B and B',C and C' are coupled and transitions A,B,C induce transitions A',B',C'

5.3 Importance of fluorescence resonance energy transfer

Fluorescence energy transfer is a distant-dependent excited state interaction. Due to its extreme sensitivity and distance –dependence, energy transfer mechanism is widely used as a means of detecting molecular interactions and conformational changes in the nanometer scale distances, both *in vitro* and *in vivo*[13]. Recent advances in the technique have led to qualitative and quantitative improvements including increased spatial resolution, distance range and sensitivity [2]. The importance of energy transfer process is that it contains molecular information which is different from that revealed by solvent

relaxation, excited state reactions and fluorescence quenching or fluorescence polarization [3].

The energy transfer mechanism is also proved to have significant application in the area of characterizing laser materials to control light emission. It has been shown that by using highly efficient acceptor materials, it is possible to improve the quantum efficiency of the system in comparison to that of the pure host system [6-7]. In the context of solid state lasers, efficient energy transfer between numerous donor – acceptor dye pairs have been reported to improve the laser performance and to broaden the spectral range of laser operation [6-8]. In donor–acceptor pairs, the emission region is shifted away from the absorption and hence self absorption is considerably reduced. Also, owing to the negligible concentration of the acceptor (1%-10%), concentration quenching is also reduced. Both these factors can reduce the threshold of amplified spontaneous emission (ASE) [6, 9]. Energy transfer dynamics is also made use of to improve the optical properties of polymer blends used as emissive layers in organic light emitting diodes [10].

5.4 Theory of resonance energy transfer

The quantitative theory for the singlet –singlet energy transfer has been developed by T.Forster assuming that the transfer occurs as a result of dipole-dipole coupling of donor and acceptor and does not involve the emission and reabsorption of photons. [14]. According to this theory the rate of energy transfer from a specific donor to the acceptor is given by

$$k_{ET} = \frac{1}{\tau_d}\left(\frac{R_0}{r}\right)^6 \qquad (5.1)$$

where τ_d is the lifetime of the donor in the absence of acceptor, r is the distance between the donor and acceptor, and R_0 is a characteristic distance called the Forster

distance, at which the efficiency of transfer is 50%. He also demonstrated that the efficiency of the energy transfer process (E) can be expressed in terms of the characteristic distance R_0 by the relation

$$E = \frac{R_0^6}{(R_0^6 + r^6)} \tag{5.2}$$

From equation 5.2 it is clear that when $R_0 = r$ the efficiency of transfer E= ½. At an intermolecular distance R_0, the energy transfer competes equally well with all other decay routes. There exist equal probabilities for transfer and intramolecular deactivation of the excited state by radiative and nonradiative processes. Thus at Forster radius, the efficiency of energy transfer is 50 %. The relation for R_0 is given as

$$R_0^6 = \frac{9000 \ln 10 k^2 \Phi_D}{128\pi^5 N n^4} \int \frac{F_D(\bar{\nu})\varepsilon_A(\bar{\nu})d\bar{\nu}}{\bar{\nu}^4} \tag{5.3}$$

where Φ_D is the quantum yield of the donor in the absence of acceptor, n is the refractive index of the medium, N is Avogadro's number, $F_D(\bar{\nu})$ is the corrected fluorescence intensity of the donor in the wave number range $\bar{\nu}$ to $\bar{\nu} + d\bar{\nu}$ with the total intensity normalized to unity and $\varepsilon_A(\bar{\nu})$ is the extinction coefficient of the acceptor at $\bar{\nu}$. k is a factor describing the relative orientation in space of the transition dipoles of the donor and acceptor and is taken as 2/3 for isotropic media[9]. This relation shows that R_0 is independent of the donor oscillator strength or lifetime. But it depends on a number of factors including the fluorescent quantum yield of donor in the absence of acceptor, the refractive index of the solution, the dipole angular orientation of each molecule and the spectral overlap integral of the donor and

acceptor. According to Forster theory the energy transfer rate constant K_{ET} is also expressed as

$$k_{ET} = \frac{9000 \ln 10 k^2 \Phi_D}{128 \pi^5 N r^6 \tau_D} \int \frac{F_D(\bar{\nu}) \varepsilon_A(\bar{\nu}) d\bar{\nu}}{\bar{\nu}^4} \tag{5.4}$$

where r is the distance between the donor and acceptor and τ_D is the lifetime of the donor in the absence of acceptor. All energy transfer mechanisms are characterized by a reduction in the emission intensity of the donor and an enhancement in the emission intensity of the acceptor if it is a fluorescent molecule. They also predict a decrease in lifetime of the electronically excited state of the donor. In the presence of an acceptor molecule to which energy can be transferred, a new mode of deactivation is added which depopulates the excited state. Thus a reduced lifetime is one of the characteristics of resonance energy transfer. The average lifetime of the donor has to decrease with increase in transfer efficiency [14-16]. In the relation for the resonance energy transfer rate (Eq.5.1) the lifetime of the donor in the presence of energy transfer is modified as

$$\tau = (k_r + k_{nr} + k_{ET})^{-1} \tag{5.5}$$

The conventional way of determining energy transfer efficiency is to compare the donor emission intensity of the donor-acceptor sample in the presence and absence of acceptor which can be expressed as [16]

$$E = 1 - \frac{F}{F_0} \tag{5.6}$$

where F and F_0 represent the fluorescence intensities of donor in the presence and absence of acceptor respectively. Since the efficiency of energy transfer depends on

the extent of overlap between the emission and absorption spectra of donor and acceptor, the energy transfer can be extremely rapid when there is large overlap. It can exceed the rate at which the donor and acceptor species can diffuse through the medium [15].

Since the conditions for radiative and radiationless energy transfer are similar, in some cases it may be difficult to distinguish between the two processes. Radiative transfer is considered as a trivial process due to the simplicity of the physical process involved in it. But it cannot be neglected in studies of energy transfer.

There exist still some other intermolecular processes by which electronically excited states can be deactivated. These can either be a collisional deactivation or a complex formation [12]. In the former process, on collision with other molecules the excited state energy is given up as heat to the surroundings. The rate of such a collision process is equal to the rate at which the molecules diffuse through the solvent medium. The constant for such a diffusion controlled bimolecular process is given as

$$k_{diff} = \frac{8RT}{2\eta} x10^3 \text{ dm}^3 \text{ mol}^{-1}\text{s}^{-1} \qquad (5.7)$$

where R is the gas constant ,T is the temperature (°K) and η solvent viscosity. For organic solvents at room temperature the value of k_{diff} ranges from $1x10^{10}$ to $4x10^{10}$ dm^3 $mol^{-1}s^{-1}$. In the latter case a complex formation in the excited state is involved. A donor molecule in its excited state can form short-lived exciplexes with acceptors in the ground state. In solution there is a possibility of exciplex formation [16]. These exciplexes may or may not emit their own characteristic emission which is likely to be different from that of the original molecule. In short, energy transfer can take place from the excited state of a donor to the ground state of an acceptor in quite different ways such as by collisional interaction, radiative transfer, electron-exchange, dipole-dipole coulombic interactions and exciplex formation.

Here, we report the energy transfer investigations carried out in laser dye mixtures of C 540 as donor and Rhodamine 6G and Rhodamine B as acceptors in different solvent environments by measuring the amplified spontaneous emission from these systems.

5.5 Experimental Details

The energy transfer and ASE studies are done in four solvent environments under pulsed optical excitation. C 540, Rhodamine 6G and Rhodamine B laser dyes (Exciton) are used as supplied. All the reagents used in the present study, viz, methanol, ethanol, dimethyl formamide (DMF) methyl ethyl ketone (MEK) are of spectroscopic grade. The absorption spectra are recorded using UV-VIS spectrophotometer (JascoV-570). For all the energy transfer experiments, stock solutions of concentration 4 x 10^{-4} M of both donor and acceptors are prepared. A fixed amount of donor is taken for all experiments and different amounts of acceptor are added to vary its concentration. The quantum yield of the donor C 540 is determined as explained in chapter 2.

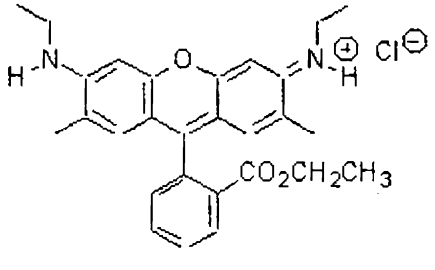

Rhodamine 6G

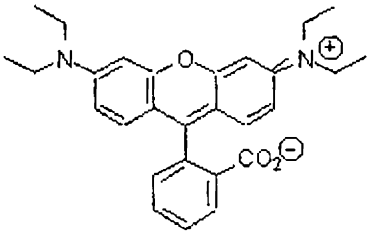

Rhodamine B

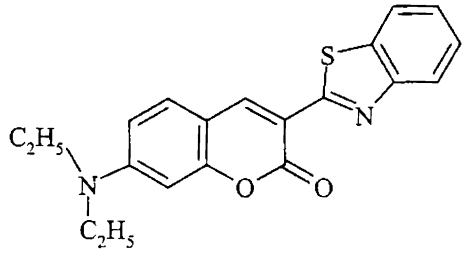

Coumarin 540

The energy transfer mechanism and ASE from laser dye mixtures are studied by taking the sample in a quartz cuvette of dimensions 1 cm x 1 cm x 3 cm. The sample is excited by 476 nm radiation from a Quanta Ray MOPO (MOPO 700) pumped by Q-switched Nd:YAG laser at 355 nm that emits pulses of 7 ns duration at a repetition rate of 10 Hz. Light emitted from the front layer of the sample is collected in a transverse direction using an optical fiber without any focusing. The emission spectra are recorded with an Acton monochromator (Spectrapro) attached with a CCD camera.

5.6 Results and discussions

As noted earlier, spectral overlap between the fluorescence spectrum of donor and absorption spectrum of acceptor is the prerequisite for any energy transfer experiment. Fig.5.2 shows the emission spectrum of the donor C 540 and absorption spectra of Rh6G and RhB as acceptors. There is a good spectral overlap between the donor and acceptor which makes the energy transfer possible. The degree of spectral overlap between the donor emission and the acceptor absorption is given by the overlap integral

$$J_{DA}(\bar{\nu}) = \int \frac{F_D(\bar{\nu})\varepsilon_A(\bar{\nu})}{\bar{\nu}^4} d\bar{\nu} \qquad (5.8)$$

5.6.1 ASE in C 540 – Rhodamine 6G d-a pair.

A successive quenching of ASE intensity of the donor C 540 is observed with the increase in the concentration of Rh6G for the d-a pairs in all the four solvents viz. ethanol, methanol, DMF and MEK, with a transfer of emission intensity to the acceptor side. But the rate of energy transfer is quite different in different solvents. For the d-a pair in methanol, even for 1.2% by volume of Rh6G, the emission intensity of the donor is reduced to half its maximum recorded value. For a concentration by volume of Rh6G of nearly 5%, the fluorescence intensity of the donor is almost quenched and the acceptor intensity is increased to a maximum.

Fig.5.4 shows the ASE of the d-a pair in methanol. The concentration of the acceptor for which the emission intensity of the donor decreases to half its maximum recorded value is estimated to be 5 $x10^{-6}$ M. A blue shift of 4.5 nm in the donor side and a red shift of 4 nm in the acceptor side are observed in the emission spectra. Since the conditions for radiative and nonradiative energy transfer are quite similar, both types of energy transfer occur simultaneously. The blue shift of the donor ASE spectra observed with increasing acceptor concentration can be attributed to the radiative transfer phenomenon. The increased number of acceptor molecules quenches the longer wavelength portion of the donor ASE spectrum more effectively than the shorter wavelength of the spectrum by reabsorption. The red shift observed in the acceptor emission spectra is due to the reabsorption of the fluorescence emission by the acceptor molecules themselves and is the usual concentration dependent red shift observed in dye solutions [18].

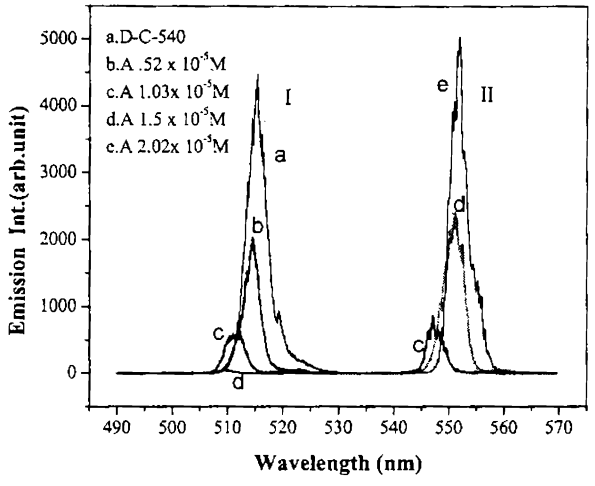

Fig.5.4 The emission spectra of C540 –Rh6G d-a pair for different concentrations of Rh6G in methanol. Spectra I corresponds to donor ASE and spectra II corresponds to acceptor

C 540 and Rh6G in ethanol and DMF give somewhat similar results for the ASE spectra with that of d-a pair in methanol. However the concentration of the acceptor needed to quench the emission intensity of the donor to half its maximum value is increased. The acceptor concentrations for the above pairs are estimated to be $1.5x\ 10^{-5}$ M and $2x10^{-5}$ M respectively. Figure 5.5 shows the emission spectra for the d-a pair C-540 and Rh-6G in DMF.

For the d-a pair in methyl ethyl ketone (MEK), certain differences are observed in the emission spectra of the donor. In the absence of acceptor, the ASE peak of C-540 occurs at 527 nm with a very small peak observed around 510 nm. With the addition of 2% by volume of acceptor, the major peak at 527 nm is highly quenched and no significant reduction is observed for the peak at around 510 nm. By further increasing the acceptor concentration, donor ASE is completely quenched and the acceptor ASE intensity gradually increases.

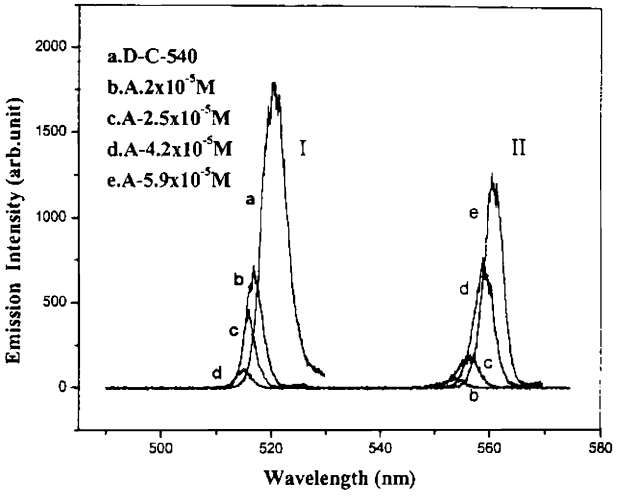

Fig.5.5. The emission spectra of C540 – Rh6G d-a pair for different concentrations of Rh6G in DMF. Spectra I for donor and II for acceptor

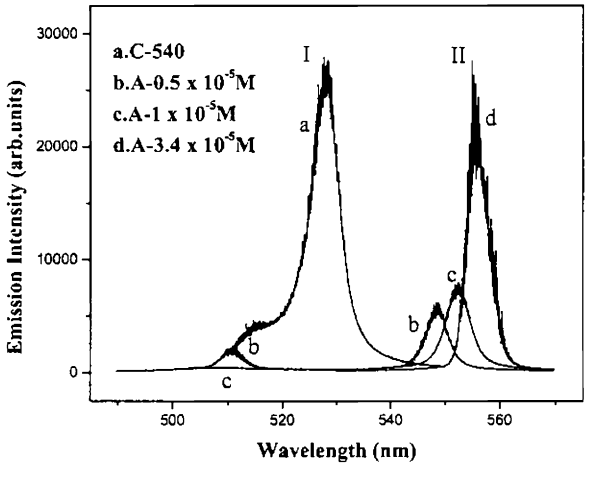

Fig.5.6. Emission spectra of C 540- Rh 6G pair for different concentration of Rh6G in MEK
Spectra I for donor and II for acceptor

The sudden quenching of the prominent peak in the donor emission spectrum may be due to strong coupling between the corresponding vibrational levels of the donor and acceptor. Fig.5.6 shows the emission spectra of C540 –Rh6G pair for various concentrations of the acceptor in MEK.

5.6.2 C 540-Rhodamine B as d-a pair

The ASE investigations are repeated with the d–a pairs of C 540 and RhB in the same solvents. We have observed very striking results using these pairs. With d-a pairs in methanol and ethanol, somewhat similar results are observed as in the case of C540 –Rh6G pairs. But in these two solvents, the acceptor concentrations needed for quenching the emission intensity of the donor to half its maximum value are considerably high (10%-20%).But the emission intensity of the acceptor is also significantly high for these two pairs. The emission spectra for d-a pair in ethanol is given in Fig.5.7. The blue and red shifts observed in the emission spectra of the d-a pairs in methanol and ethanol are included in Table.5.2.

The d-a pair in DMF and MEK behave quite differently from the above, pointing out a different mechanism responsible for the decay process. For the d-a pair in DMF, even after the complete quenching of donor emission intensity due to acceptor, no emission is observed in the acceptor side. The concentration of the acceptor for the complete quenching of donor ASE is around 8.4×10^{-5} M which is 25% by volume of the donor. The blue shift observed is even less than 2 nm which suggests that the role of radiative transfer and quenching is less compared to other d-a pairs. The RhB molecule is acting as a dark quencher for the donor without giving any fluorescence. This can be of great importance in biological studies due to

the absence of any background fluorescence from the acceptor molecule [19].The ASE spectrum of d-a pair DMF is given in Fig.5.8

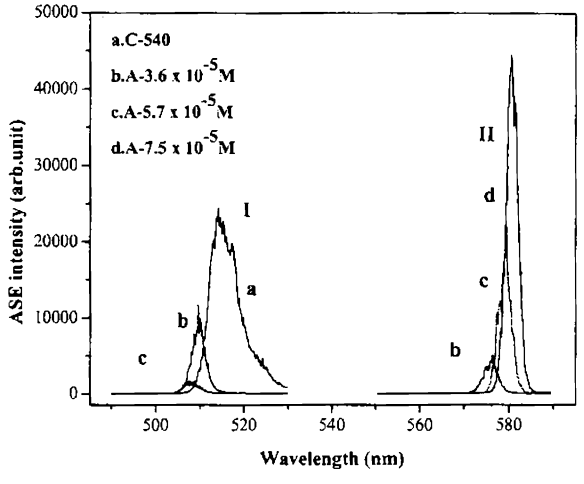

Fig.5.7. Emission spectra of C540- RhB pair in ethanol
I-spectra of donor. II.Spectra of acceptor.

Similar to C 540 - RhB in DMF, for the d-a pair of C 540 - RhB in MEK, almost complete quenching of the donor ASE is observed with no emission in the acceptor side. As in the case of C540-Rh6G d-a pair in MEK, the main peak at 526 nm is gradually quenched with the increase of acceptor concentration. At higher concentration of the acceptor, the peak is shifted to 507 nm and then completely quenched by further increase of acceptor concentration. A concentration of 1.14×10^{-4} M (~ 40% by volume) of the acceptor completely quenches the donor ASE. No appreciable blue shift is observed in these two peaks. Similar to C-540 –RhB pair in DMF, RhB in MEK can also be considered as a dark quencher.

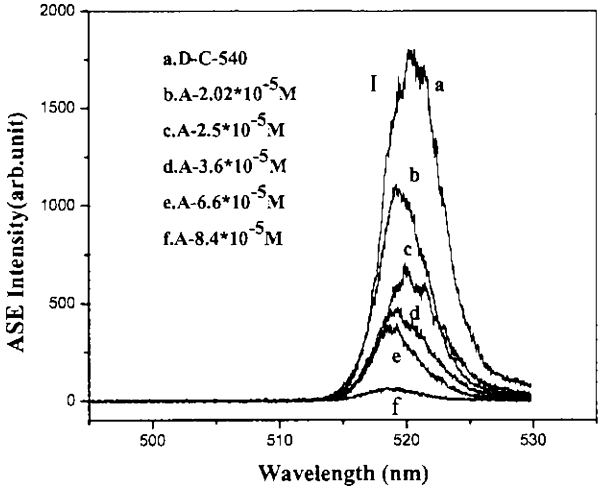

Fig.5.8. Emission spectra of C540- Rh B pair in DMF. I-spectra of donor

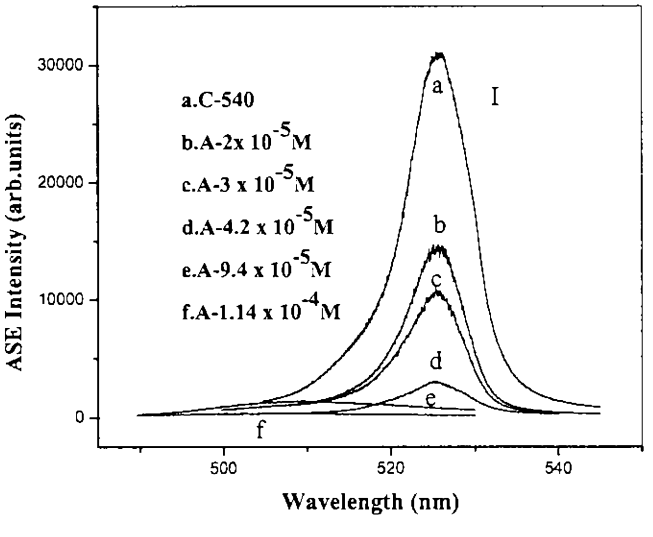

Figure 8. Emission spectra of C540- RhB pair in MEK.I-spectra of donor.

Acceptor	Solvent	Blue shift for donor (nm)	Red shift for acceptor (nm)
Rh-6G	Ethanol	7	2
Rh-B		8	7
Rh-6G	Methanol	4.5	4
Rh-B		5	11
Rh-6G	DMF	5.5	5
Rh-B		2	-
Rh-6G	MEK	15	9
Rh-B		0.4	-

Table 5.2 The blue shift for the donor spectra and red shift for the acceptor aspectra.

In order to check the role of background fluorescence in the emission spectrum of the acceptor in the C540- Rh6G and C 540- RhB d-a pairs due to the direct absorption of the excitation pump beam, the spectra are recorded for different concentrations of the acceptor alone. The results obtained for Rh6G in MEK are included in Fig.5.9 for comparison with the emission spectra of the C 540 – Rh6G d-a pair in the same solvent. The spectrum shown in Fig.5.9e is recorded for a concentration which is more than double the acceptor concentration in the d-a pair. The observed background fluoresnce is not significant. It is evident from this figure that the contribution of fluorescence emission from the direct absorption of energy by the acceptor is very small and hence the enhancement in ASE of the acceptor can only be attributed to different energy transfer mechanisms.

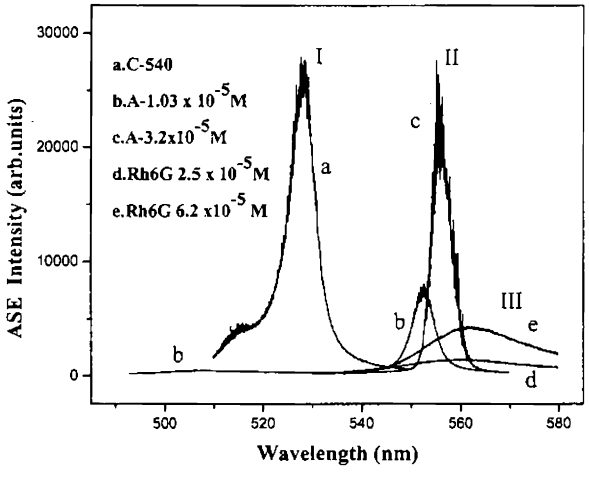

Fig.5.9 Emission spectra of C540- Rh6G pair in MEK
I-spectra of donor. II.Spectra of acceptor.
III spectra for Rh6G alone in MEK

The different experimental results exhibited by all d-a pairs of C 540- Rh6G in different solvents, establish that efficient energy transfer is taking place between the donor and the acceptor. The simple mechanism of radiative transfer, where the emitted photon of the donor is simply absorbed by the acceptor could not be the sole mechanism behind the quenching of the ASE intensity of the donor. Even 5 % by volume of Rh-6G in methanol and 10% by volume in ethanol resulted in the complete transfer of ASE intensity to the acceptor side. It is reported that generally very small concentration of the acceptor (1%-10%) can produce efficient energy transfer in dye mixtures due to resonance energy transfer [6-7].If radiative transfer is the prominent process one would expect more or less the same level of concentration for C 540 and Rh-6G since both of them have high absorption cross section and quantum yield. These observations of energy transfer can be explained by a dipole –dipole interaction

that exists between the molecules of the d-a pairs which causes non-radiative energy transfer between the molecules.

In order to check the role of resonance energy transfer, we have to consider the Forster distance R_0 for the d-a pair of C 540 - Rh6G in all the four solvents. It is the average distance between the donor and acceptor molecules at which the probability of intermolecular energy transfer is just equal to the sum of the probabilities of all deexcitation processes of the excited state of the donor. Taking the experimental values of overlap integral J and the quantum yield of the donor in different solvents, the value of R_0 is calculated for the d-a pairs of C 540 - Rh 6G. The R_0 values obtained for all the d-a pairs, which varied within the range 6.4nm -6.7 nm are very much within the limit proposed for the efficient resonance energy transfer between donor and acceptor molecules due to dipole-dipole long range interaction. The values of R_0 are given in Table 5.3. Since the performance of C 540 - RhB d-a pair in methanol and ethanol are very much similar to C 540-Rh6G d-a pairs, the R_0 values are determined. The values obtained are 6.48 nm and 6.16 nm respectively. The calculated values of R_0 for different d-a pairs, which fall within the range 5.9 nm to 6.7 nm indicate the possibility of a dipole-dipole long range interaction being responsible for the energy transfer between these donor-acceptor pairs.

The energy transfer process is found to be more complex in C 540- RhB pairs in DMF and MEK. In both of these solvent environments, the donor fluorescence is completely quenched without giving any fluorescence emission in the acceptor side. In general, collisional deactivation, nonfluorescent ground state complexes or excited state complexes (exciplexes) may lead to fluorescence quenching of the donor without any transfer of energy to the acceptor side. Another possibility of the fluorescence quenching of RhB is that it acts as a dark quencher where the energy transferred to the acceptor molecule is not reemitted as fluorescence but converted as heat.

The normal collisional deactivation could not be considered as the possible mechanism of quenching in the above d-a pairs. Collisional quenching is a function of solvent viscosity as given by equation 5.7. The differences in viscosities are very less for ethanol and DMF (1.2 and 0.92 respectively), but the d-a pair in ethanol exhibit good energy transfer. No new peaks are observed in the absorption spectrum of C 540 –RhB d-a pair in DMF which rule out the possibility of complex formation in the ground states of the donor-acceptor pairs resulting in a static quenching (Fig.5.9). The formation of exciplexes between the excited state of the donor and the ground state of the acceptor molecules can quench the fluorescence emission. The short range electron-exchange interaction may be considered as occurring through short-lived exciplex intermediates [11]. Also,the emission spectra of the d-a pairs show no new bands which may originate from exciplexes. This denotes the absence of any fluorescent exciplexes. Formation of nonfluorescent excited state complexes may be a quenching mechanism failing to give any characteristic emission.

In order to analyze the mechanism behind the quenching of acceptor fluorescence in C 540 - RhB pairs in DMF and MEK, we have recorded the emission spectrum of RhB alone in DMF by exciting the sample at a wavelength where C 540 has no significant absorption but has only emission. It is clear from the absorption spectrum of C 540 that it has negligible absorption beyond 520 nm (Fig.5.10a). The sample is excited at 540 nm where RhB has good absorption. In the present case we have kept the absorbance of RhB less than 0.1 in order to avoid the possibility of any quenching due to concentration. C 540 dissolved in DMF is then added to this sample at different concentrations and the emission spectra are recorded. The concentrations of C 540 are chosen in such way that the condition matches with previous energy transfer studies conducted in C 540-RhB d-a pair. It is interesting to observe that the increase in concentration of C 540 in the mixture resulted in a decrease in the fluorescence emission of RhB. The emission spectra of Rh B in the presence of

different concentrations of C 540 are given in Fig.5.11.These investigations are carried out using a Cary Eclipse spectrofluorimeter(Varian).

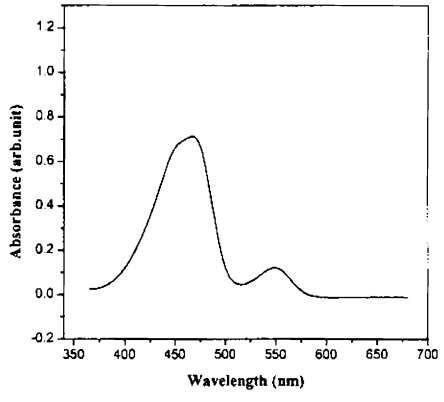

Fig 5.10 Absorption spectrum of C 540-RhB mixture in DMF.

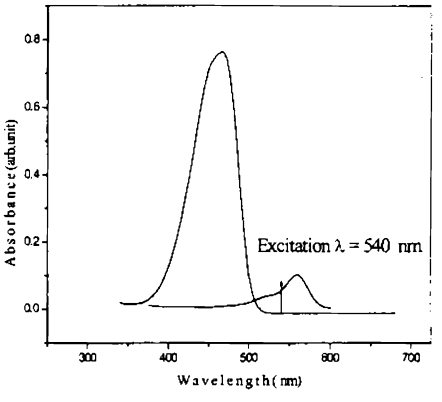

Fig.5.10Absorption spectra of C 540 and rhodamine B in DMF

The above studies lead us to assume that some quenching mechanism is active in RhB in DMF solvent in the presence of C 540. For further understanding of the quenching mechanism, we have considered the Stern-Volmer relation for quenching. The quenching rate constant is determined from the relation [16]

$$\frac{F_0}{F} = k_{sv}[A] \tag{5.9}$$

where F_0 and F represent the fluorescence intensities of the donor in the absence and presence of acceptor and A is the concentration of the acceptor. The quenching constant k_{SV} is the slope of the Stern-Volmer plot drawn between the concentrations of the acceptor and the emission intensity of the donor. In the present case, we analyze

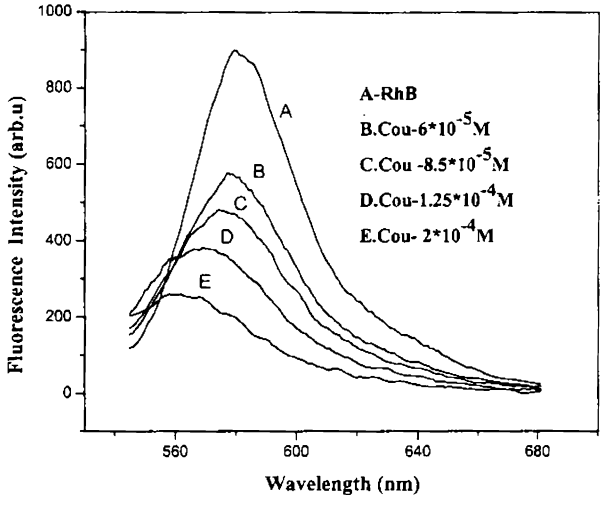

Fig.5.11 Quenching of fluorescence emission of RhB in DMF in the presence of C 540 at different concentrations.

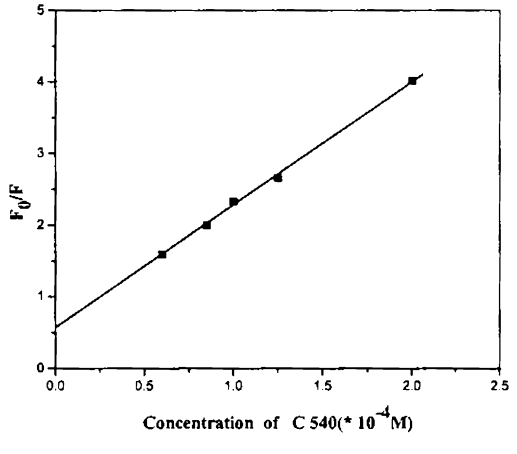

Fig.5.12 Stern-Volmer plot for the emission intensity of RhB in DMF for various concentrations of C 540.

the quenching of RhB in the presence of C 540. The Stern- Volmer plot drawn for the emission intensity of RhB vs concentration of C 540 gives a linear plot (Fig.5.12)which suggests that a fluorescence quenching mechanism is active for acceptor Rh B in the presence of donor C 540. More detailed investigations are necessary to specify the exact mechanism behind this quenching process.

The energy transfer rate k_{ET} can be determined for the d-a pairs using the relation given in equation 5.9. The Stern –Volmer plots between the ASE intensity of the donor C 540 and the various concentrations of the acceptor in different solvent environments provide the value of the quenching rate constant k_{SV}. The energy transfer rate can be obtained from these plots according to the relation [17]

$$k_{ET} = k_{SV}/\tau_D \qquad (5.10)$$

where τ_D is the fluorescence lifetime of the donor in the absence of the acceptor.

In the present study, the experimental data show that the Stern-Volmer linear relation of the ratio of fluorescence intensity and acceptor concentration is not followed under pulsed laser excitation. Instead, the plot of F_0/F vs concentration of the acceptor displays almost an exponential growth . Fig.5.13 shows the F_0/F vs acceptor concentration plots for different d-a pairs. The deviation from the linear nature of the Stern-Volmer plot suggests the possibility of more than one mechanism responsible for the decay of the donor from its electronically excited state.

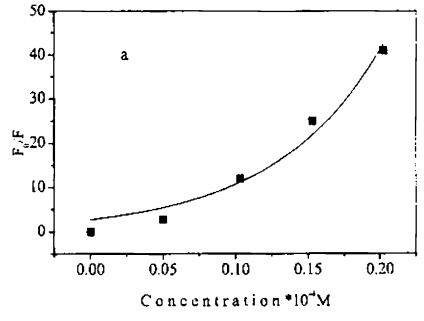

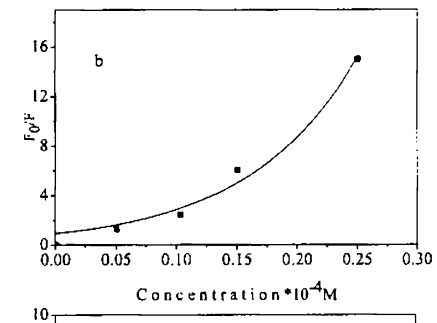

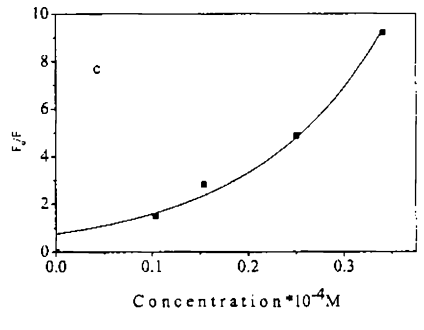

C 540-Rh6G

Fig.5.13 A. Plot of fluorescence quenching of the donor vs concentration of the acceptor for C-540-Rh6G d-a pairs a) in methanol b) in ethanol c)in DMF

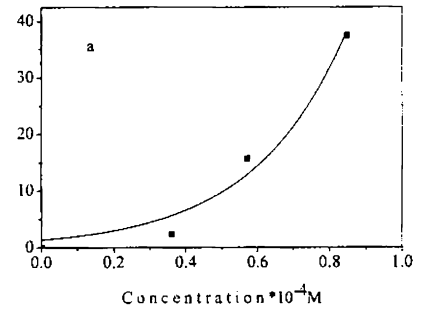

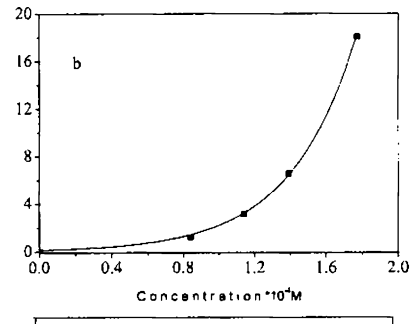

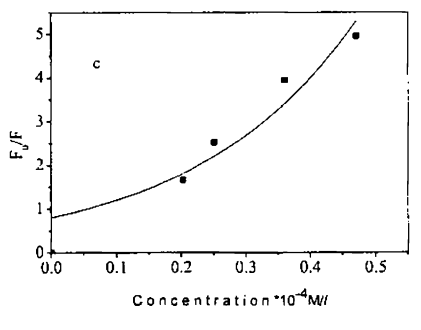

C 540-RhB

Fig.5.13 B. Plot of fluorescence quenching of the donor vs concentration of the acceptor for C-540-Rh B d-a pairs a) in methanol b) in ethanol c)in DMF

The complete transfer of ASE intensity from the donor side to the acceptor side, the good overlap integral , the range of critical distance from 5.9 nm to 6.7nm and the increased energy transfer rates emphasize the role of dipole-dipole long range coulombic interaction for the energy transfer in the dye mixtures of C540 - Rh6G and C540-RhB.

For a better comparison of the energy transfer between different donor-acceptor pairs, the transfer efficiency

$$E = 1 - \frac{F}{F_0} \qquad (5.11)$$

for a particular concentration of the acceptor is calculated and is given in Table 5.3. F and F_0 are the ASE intensities of the donor in the presence and absence of acceptor [16].

Acceptor	**Solvent**	**R_0 (nm)**	**E (con.1.5x10^{-5} M) %**
Rh-6G	Ethanol	6.64	83
Rh-B		6.48	46
Rh-6G	Methanol	6.43	95
Rh-B		6.16	33
Rh-6G	DMF	6.41	65
Rh-B		6.27	40
Rh-6G	MEK	6.57	93
Rh-B		5.92	48

Table.5.3 The critical transfer radius for different pairs and the energy transfer efficiency for a constant concentration of the acceptor in different solvents.

The energy transfer efficiency values give a comparison of the effect of solvents on the mechanism of energy transfer between different donor acceptor pairs. Compared to the C 540 –Rh6G d-a pair, the efficiency is considerably less for C540-RhB pair. This is supported by the comparatively lower overlap integral (Table 5.1) for C 540-RhB d-a pair in all solvents. Since RhB is having an extended emission, more energy may be decayed before being transferred to the acceptor molecules which again reduces the efficiency.

5.7 Conclusions

Amplified spontaneous emission and excitation energy transfer for the dye mixtures C-540 as donor and Rh-6G and Rh-B as acceptors in different solvent environments are studied. The ASE from the donor and acceptors is studied under pulsed optical excitation. Efficient energy transfer from the donor to the acceptor is observed in different d-a pairs. The high energy transfer rate, the good spectral overlap between the emission spectra of donor and absorption spectra of acceptor and the calculated Forster distance which varies in the range of 5.9 nm to 6.7 nm suggest a significant role for the resonance energy transfer between the donor and accepter molecules in dye mixtures. The energy transfer mechanism between the donor and acceptor molecules is found to be profoundly influenced by the solvent media of the d-a pair. When Rh B is selected as the acceptor in different solvent media, there is transfer of ASE intensity of the donor to the acceptor as well as quenching of the ASE intensity of the donor by the acceptor. Since the background fluorescence is absent in the latter case, this can be of great importantance in biological studies.

References

1. J.N.Miller, *Fluorescence energy transfer methods in bioanalysis,*Analyst, **130** (2005) 265-270
2. P.R.Selvin, *Nature structural biology* **7** (2000) 730-734
3. J.R.Lakowicz, *Radiative Decay engineering: Biophysical and Biomedical applications*, Analytial biochemistry **298** (2001) 1-24
4. N.U.Kemnitzer, A.Zilles, J.Arden-Jacob, K.H.Drexhage, M.Gross M.Hamers, *Fluorescenct dyes –Detection methods for the future,* BIOforum International **5** (2002)242-243
5. D.Seth, D.Chakrabarty, A.Chakrabarth, N.Sarkar, *Study of energy transfer from7-amino coumarin donors to rhodamine 6G acceptor in non-aqueous reverse micelles* J.Che.Phys.Lett.**401**(2005)546-552
6. A.K.Sheridan,A.R.Buckley,A.M.Fox,A.Bacher,D.D.C.Bardley, *Efficient energy transfer in organic thin films –implications for organic lasers,* J.Appl.Phys.**92** (2002) 6367-6371
7. T. H.Nhung, M. Canva, F.Chaput, H.Goudket, G.Roger, A.Brun ,D.D. Manh, N.D.Hung, J.P.Boilot ,*Dye energy transfer in xerogel matrices and application to solid-state dye lasers,* Opt.Commun.**232** (2004) 343-351
8. D.Su, Yu Yang, G.Qian, Z.Wang, M.Wang, *Influence of energy transfer on fluorescence and lasing properties of various dyes co-doped in ORMOSILS*, Che.Phy.Lett, **397** (2004) 397-401
9. R.Ghazy,S.A.Zim.M.Shaheen,F.El-Mekawey, *Energy transfer and excited state lifetime of some anthracene laser dyes*, Optics & Laser Tech.**36**(2004)463-469

10. A.R.Buckley, M.D.Rahn, J.Hill. J.C.Gonzalez, A.M.Fox D.D.C.Bradley,*Energy transfer dynamics in polyfluorene-based polymer blends*,Chem.Phys.Lett.**339**(2001) 331-336

11. J.B.Birks, *Photophysics of Aromatic molecules, Wiley-Interscience London* (1969)

12. A.J.Pesce, C.G.Rosen, T.L. Pasby, *Fluorescence spectroscopy*, Marcel Dekker Inc, New york (1971)

13. L.Stryer, R.P.Haugland, Proc.Natl.Acad.Sci.,USA, **58** (1967) 719-726

14. T.Forster, *Intermolecular energy migration and fluorescence* ,Ann.Phys,**2** (1948) 55-75

15. C.H.J.Wells, *Introduction to molecular photochemistry*, Chaman and Hall ,London (1972)

16. J.R Lakowicz,*Principles of Fluorescence Spectroscopy*,Plenum press,New York(1983)

17. R.Ghazy, S.A.Zim. M.Shaheen, F.El-Mekawey, *Experimental investigations on energy-transfer Characteristics and performance of some laser dye mixtures,* Optics & Laser Tech.**34**(2002)99-105

18. K.A.Kozyra,J.R.Heldt,H.A.Diehl,J.Heldt, *Electronic energy transfer efficiency ofmixed solutions of the donor-acceptors pairs: coumarin derivative-acridine orange*,J.Photoche.Photobiol.A **152**(2002)199-205

19 M. A.Behlke,L.Huang,L. Bogh,S. Rose,E. J.Devor,Integrated DNA technologies (2005)

Chapter 6

Nonlinear characteristics of Coumarin 540

"I start where, the last man left out." Thomas Edison.

Abstract

Open aperture Z scan studies carried out to investigate the nonlinear properties of C 540 dye solution and dye doped polymer matrices are presented in this chapter. Nonlinear absorption studies are performed at a two photon resonance wavelength of 590 nm and at a near resonance wavelength of 650 nm where the absorption is comparatively less. Along with the dye solution in toluene, thin films of C 540 dye doped in PMMA, polystyrene and PVC are the samples used for the investigations. The optical limiting behaviour of the dye doped films is also discussed

6.1 Introduction

Nonlinear optics is an important branch of science which took birth with the advent of highly intense laser systems. It is concerned with the study of the phenomena that result from highly intense light induced modifications in the optical properties of the materials. The field of nonlinear optics (NLO) explores the coherent coupling of two or more electromagnetic fields in a nonlinear medium [1-3]. The discovery of the important nonlinear effect, the second harmonic generation (SHG) introduced a new branch of experimental investigation in the area of laser-matter interaction. Later on many interesting nonlinear optical effects are discovered which have significant

applications in the field of telecommunication, optical storage, optical switching, optical power limiting etc[4-8].

The nonlinear effects are broadly classified into two categories. One is concerned with frequency conversion and the other with optical modulation. Sum and difference frequency generation comes under the frequency conversion process and Kerr effect, self phase modulation etc. are examples of optical modulation processes. New frequency generations are due to the oscillations of induced nonlinear polarization at appropriate frequencies. In optical modulation process, light modulates the properties of the medium such as the refractive index [9-10].

Study of nonlinear effects leads us to a new understanding of fundamental light-matter interaction. Implementation of the various NLO effects in the appropriate areas of technologies like optical communication, optical switching, optical data storage demands a detailed knowledge of the NLO processes and their dynamics. Nonlinear optics is observed with lasers which have high degree of spectral purity, coherence and directionality with which atoms and molecules can be irradiated with an electric field that is comparable to interatomic field. These fields are of the order of 10^{10} Vm^{-1} corresponding to an incident light of ~100$GWcm^{-2}$. In practice it is possible to observe many nonlinear optical effects at much lower intensities due to enhancement of the nonlinear effect. If the induced diploes in the medium oscillate coherently, the field that they radiate can add together constructively to produce a much larger intensity. This condition is called phase matching and is often used to enhance nonlinear effects. If the frequency of the light lies near the internal resonance frequency of the oscillating diploes, there is resonance enhancement of the nonlinearity. Multiphoton process is an example of such resonance enhancement [11].

The property of optical nonlinearity can be well understood by considering the dependence of dipole moment per unit volume or polarization P(t) of the material

on the strength E(t) of the applied electric field. In the case of linear optics the induced polarization has a linear dependence on the electric field strength which can be described as

$$P(t) = \chi^{(1)}E(t) \tag{6.1}$$

where the constant of proportionality χ is the linear optical susceptibility. When the electric field is significantly high, nonlinear interaction occurs and the observed nonlinear optical effects can be described by expressing the polarization P(t) as a power series in the field strength E(t) as

$$P(t) = \chi^{(1)} E(t) + \chi^{(2)} E^2(t) + \chi^{(3)} E^3(t) + \ldots\ldots\ldots \tag{6.2}$$

$$= P^1(t) + P^2(t) + P^3(t) + \ldots\ldots\ldots \tag{6.3}$$

where $\chi^{(1)}$, $\chi^{(2)}$ are the second and third order nonlinear optical susceptibilities respectively. The second and third order polarizations can be expressed as

$$P^2(t) = \chi^{(2)} E^2(t) \tag{6.4}$$

$$P^3(t) = \chi^{(3)} E^3(t) \tag{6.5}$$

The physical processes that occur due to second and third order polarizations are distinct from each other. Second order nonlinear effects occur only in noncentrosymmetric crystals. They are crystals which do not posses inversion symmetry. Liquids, gases, amorphous solids like glass and even many crystals display inversion symmetry and the $\chi^{(2)}$ value vanishes for such media and consequently they cannot exhibit second order nonlinear optical effects. On the other hand third order nonlinearity which is described by $\chi^{(3)}$ can occur both for centrosymmmetric and noncentrosymmetric media. Third order NLO effects are particularly interesting since

they have great technological relevance and these effects are present in varying measure of strength in all materials irrespective of symmetry of materials. The third order optical susceptibility is considered to be a complex quantity having both real and imaginary components. $\chi^{(3)} = \chi_R^{(3)} + \chi_I^{(3)}$. The real and imaginary parts are related to γ and β respectively where γ is the nonlinear refractive index in cm^2W^{-1} and β is the nonlinear absorption coefficient and is defined as $\alpha(I) = \alpha_0 + \beta I$. The nonlinear refractive index γ is one of the simplest quantities derived from $\chi^{(3)}$ and is a very complicated one in its most general form [2-4].

6.2 NLO properties of organic molecules

Since no symmetry requirement exists for the occurrence of third order nonlinear optical effects in materials, different kinds of materials like liquids, glasses, crystals and thin films exhibit these effects. Report of strong SHG in organic molecule led to intense effort to develop new organic materials for nonlinear effects. During the past two decades lots of investigations were done to develop materials with large third order nonlinearity and ultrafast response times for their potential applications in the area of science and engineering [4-7]. A variety of materials have been experimented for various NLO applications which include conjugated polymers, semiconductors, quantum dots, organic molecules, sol-gels, dye aggregates, guest-host systems, organic composites etc. During 1980s it became evident that organic materials can be a better choice for use in nonlinear optical applications. Organic chromophores generally exhibit extremely high and fast nonlinearities, much better than those exhibited by inorganic materials. Due to the versatility of organic synthesis, their nonlinear optical properties can be tailored depending on the desired applications.

In contrast to inorganic materials which consist of covalent or ionic bond of atoms, organic materials are based on independent molecules and characterized by

weak intermolecular interactions. The NLO property in these molecules is due to the virtual electron excitation occurring in the individual molecular or polymeric units. Organic dyes and polymeric materials possess lower dielectric constants and faster response time. The nature of π electron bonding sequence, the substitution of alternate atoms into the conjugate structure etc. affect the dipole moment and optical susceptibility. In organic materials large charge separation can be achieved through the easy delocalization of the π electron cloud, leading to very large and fast nonlinearity since it requires only electronic motion which could be in few femtoseconds. Moreover, these chromophores are easily amenable to structural modifications and possess tremendous applications [10]. The applications of organic molecules are related to two different nonlinear effects exhibited by the molecules. The optical limiting systems are related to the multiphoton absorption whereas signal processing applications rely upon the nonlinear refractive index change.

6.3 Nonlinear absorption (NLA)

The amount of light absorbed by any absorbing medium increases linearly with input intensity and is termed as linear absorption. But an intense monochromatic radiation from a laser can induce profound changes in the optical properties of the materials. While the linear absorption coefficient is expressed as a function of the excitation wavelength, at significantly high beam intensity, the absorption coefficient is expressed as function of wavelength and intensity as $\alpha(I,\lambda)$ and is termed as non linear absorption. At sufficiently high intensities the probability of a material absorbing more than one photon before relaxing to the ground state is greatly enhanced. Other than two or more photon absorption, many other complicated phenomena like population redistribution, complicated energy transitions in complex molecular systems and the generation of free carriers are accompanied by the intense

optical fields. The effects observed due to these phenomena are saturable absorption (SA) and reverse saturable absorption (RSA).

The nonlinear process associated with real energy level is the saturable absorption. In this process a light beam which is highly absorbed by the material when it is of low intensity, will pass through the medium without any absorption when it is highly intense. Here, the absorption cross section $\alpha(I)$ decreases with intensity. On the other hand, when the absorption cross section increases with intensity, the system will be less transmissive when excited. This gives the opposite effect of SA and the phenomenon is termed as reverse saturable absorption[1,12].

The two absorptive mechanisms resulting in RSA are the two or multiphoton absorption and the excited state absorption. Two photon or multiphoton absorption involves a transition from the ground state of a system to a higher lying state by the simultaneous absorption of two or more photons from an incident radiation. This process involves different selection rules than those of single photon absorption.

When the incident intensity is well above the saturation intensity , the excited state can become significantly populated. The excited electrons can rapidly make a transition to higher excited states before it eventually makes transition back to the ground state. In organic molecules, transitions are possible to higher energy singlet and triplet manifolds. Depending on the pulse duration, pump intensity and wavelength, the excited electrons from the first excited singlet state S_1 can make transition to higher excited singlet states S_n or from the T_1 to T_n states in the triplet manifold. This is known as the excited state absorption (ESA). When the cross section for TPA or ESA is greater than that of linear absorption, reverse saturable absorption occurs. It is observable when the incident beam intensity is sufficiently high to deplete the ground state significantly [1-3].

6.4 Open aperture Z-Scan to Study NLA

The Z-scan technique is a simple and sensitive single beam method to measure the sign and magnitude of both real and imaginary part of third order nonlinear susceptibility $\chi^{(3)}$. The experiment uses a Gaussian beam from a laser and the transmittance of the sample is measured as the sample is moved along the propagation direction of a focused beam. In an Z-scan measurement, it is assumed that the sample is thin and the sample length is much less than the Rayleigh's range z_0 which is given by

$$z_0 = \frac{k\omega_0^2}{2} \tag{6.6}$$

where k is the wave vector and ω_0 is the beam waist. This is essential to make sure that the beam profile does not vary appreciably inside the sample. The refractive nonlinearity is obtained by measuring the transmittance through a finite aperture in the far field as a function of the sample position z from the focal plane. This is the closed aperture Z-scan technique by which the sign and magnitude of nonlinear refractive index n_2 can be determined. In this method, the phase distortion suffered by the beam while propagating through the nonlinear medium is converted into corresponding amplitude variation [13-15].

The absorptive nonlinearities are determined by the open aperture Z-scan technique where the entire light is collected by removing the aperture from the experimental setup. Since Z-scan measurements are very sensitive to nonlinear refractive index effects that will spread the transmitted beam, care must be taken to collect the whole transmitted energy. Nonlinear absorption can produce thermal lensing in some cases which may also lead to strong defocusing of the beam. When the entire light is collected, the throughput is sensitive only to nonlinear absorption.

The Z-scan graphs are normalized to linear transmittance at large values of z. Thus the refractive and absorptive nonlinearities can be studied by performing the Z-scan measurements with and without an aperture [16-17]. Since the desired pump beam quality could not be achieved, we have carried out only the open aperture Z-scan measurements in the present case.

6.5 Theory of open aperture Z-scan technique

When the absorption coefficient of a medium has a nonlinear dependence on laser beam intensity, one can use the relation

$$\alpha(I) = \alpha_0 + \beta^{(2\omega)} I \tag{6.7}$$

where α_0 is the linear absorption coefficient and $\beta^{2\omega}$ is the two photon absorption coefficient of the medium. In the case of three photon absorption, the dependence of the absorption coefficient on the laser radiation intensity can be represented as

$$\alpha(I) = \alpha_0 + \beta^{(2\omega)} I + \beta^{(3\omega)} I^2 = \alpha_0 + \beta_{eff} I \tag{6.8}$$

where $\beta^{(3\omega)}$ is the three photon absorption coefficient and β_{eff} is the effective nonlinear absorption coefficient. For the measurement of nonlinear absorption coefficient, an open aperture Z-scan configuration is used. In the closed aperture Z-scan measurements, the sensitivity of the experiment to refractive nonlinearities is entirely due to the aperture. When the aperture is removed and the entire transmitted light is collected by the detector, it is sensitive only to the absorptive nonlinearities. The transmitted light is not sensitive to the phase variations. The intensity dependent nonlinear absorption coefficient $\alpha(I)$ can be written in terms of the linear absorption coefficient α and the effective nonlinear absorption coefficient β_{eff} due to TPA or ESA.

$$\alpha(I) = \alpha_0 + \beta_{eff} I \tag{6.9}$$

The irradiance at the exit surface of the sample can be written as

$$I_r(z,r,t) = \frac{I_{(z,r,t)} e^{-\alpha_0 l}}{1 + q(z,r,t)} \tag{6.10}$$

where $$q(z,r,t) = \beta_{eff} I(z,r,t) L_{eff} \tag{6.11}$$

L_{eff} is the effective length and is given in terms of sample length l and α_0 by the relation

$$L_{eff} = \frac{(1 - e^{\alpha_0 l})}{\alpha_0} \tag{6.12}$$

The total power transmitted P(z,t) is obtained by integrating equation 6.10 over z and r and is given by

$$P(z,t) = P_1(t) e^{-\alpha_0 l} \frac{\ln[1 + q_0(z,t)]}{q_0(z,t)} \tag{6.13}$$

$P_1(t)$ and $q_0(t)$ are given by the equations

$$P_1(t) = \frac{\pi \omega_0^2 I_0(t)}{2} \tag{6.14}$$

$$q_0(z,t) = \frac{\beta_{eff} I_0(t) L_{eff} z_0^2}{z^2 + z_0^2} \tag{6.15}$$

For a pulse of Gaussian temporal profile, equation 6.13 can be integrated to give the transmission as

$$T(z) = \frac{C}{q_0\sqrt{\pi}} \int_{-\infty}^{\infty} \ln(1 + q_0 e^{-t^2}) dt \qquad (6.16)$$

The nonlinear absorption coefficient is obtained by fitting the experimental data to equation 6.16.

6.6 Experimental setup

The experimental setup for the transmittance measurement as a function of incident intensity is shown in Fig.6.1. A Gaussian beam is employed for the measurements. Using a single beam in tight focus geometry, the transmittance of the nonlinear medium is collected as a function of the sample position z measured with respect to the focal plane. The excitation wavelength used is 590 nm taken from a Quanta Ray MOPO (MOPO 700) pumped by Q-switched Nd:YAG laser at 355 nm that emits pulses of 7 ns duration at a repetition rate of 10 Hz. Spatially filtered input beam is focused using an achromatic lens of focal length 20 cm. The lens produces a beam waist of $1/e^2$ radius of 47 μm at 590 nm. The corresponding Rayleigh range (z_0) is 11.75 mm. The sample is taken in a 1 mm cuvette to ensure that the thin lens approximation is satisfied where the beam dimension does not change at the entrance and exit side of the sample. While the input energy is kept constant the medium experiences a different incident field at different positions of z when it is scanned across the focus using a motorized translation stage. The ratio of the transmitted and incident energies is measured using energy ratio-meter (Laser probe Inc.) with RjP735 probes. The complete experimental setup is automated using Labview. It is assumed that the focus corresponds to sample position z = 0. The typical Z-scan data with fully open aperture is insensitive to nonlinear refraction; therefore the data is expected to be symmetric with respect to focus. For material with two photon absorption or ESA there is a minimum transmittance at the focus (valley) and for saturable absorption

there is a maximum transmittance at the focus (peak). The measured nonlinear transmittance is normalized with respect to the linear transmittance.

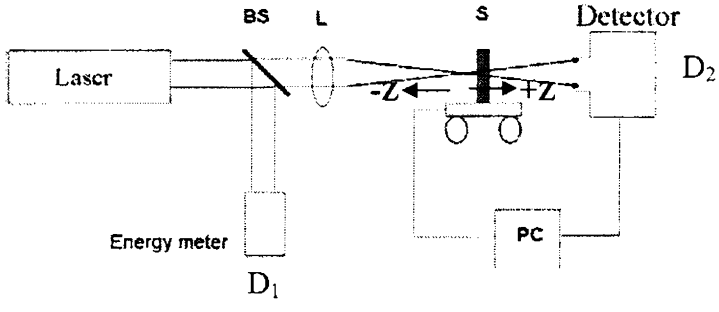

Fig.6.1 The Z-scan experimental setup in which the ratio D_2/D_1 is recorded as a function of the sample position Z

6.7 Nonlinear absorption in C 540 dye solution

The nonlinear absorption studies in C 540 dye solution is performed by taking the dye solution at a concentration of 2 x 10^{-4} M .The solution is taken in a 1 mm thick quartz cuvette. The open aperture Z-scan measurements are done to evaluate the nonlinear behavior of the dye solution. The excitation wavelengths chosen to study the non linear absorption in the dye doped samples are 590 nm corresponding to the two photon resonance of the absorption peak 295 nm and 650 nm which is at near resonance. At both these wavelengths the absorbance of the sample is less than 0.01(Fig.6.2). The dye in different solvents including polar, dipolar and nonpolar are tested for the nonlinear absorption but only toluene gives a good result which is a nonpolar one.

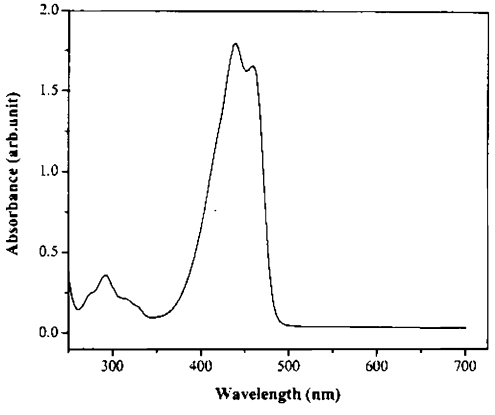

Fig.6.2 Absorption spectrum for C-540 dye in toluene

The open-aperture Z-scan measurements are done at various input fluences. The Z-scan plot exhibits a valley at the focal point due to the minimum transmittance which steadily increases on both sides of the focus. This behavior is typical of reverse saturable absorption. The large power density available at the focus induces nonlinear effects in the sample by which excited state absorption (ESA) occurs from S_1 to higher S_n states or a simultaneous absorption of two (TPA)or more photons. This nonlinear absorption results in a reduced transmittance. Typical open aperture Z-scan curves of the C-540 dye solution in toulene with normalized transmittance is shown in Fig.6.3. It shows the nonlinear absorption of the dye solution for different input fluences at a wavelength of 590 nm. The depth of the valley increases with increasing fluence level. No cross over from reverse saturable absorption to saturable absorption occurs with increase in input fluence as reported in the case of Rhodamine B dye [18-19].

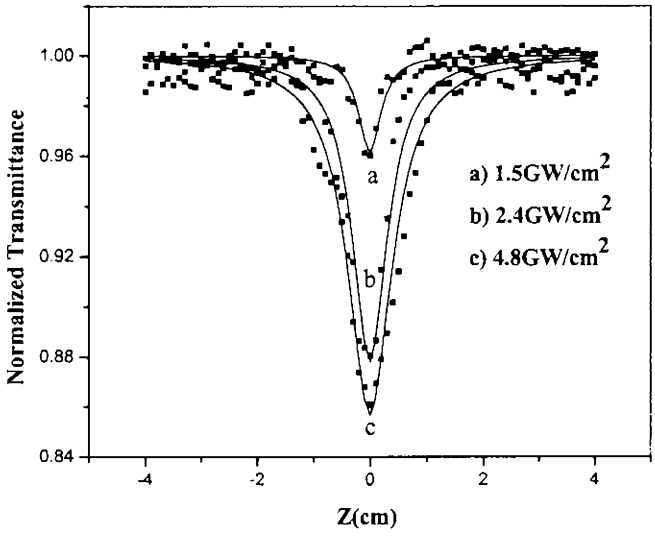

Fig.6.3 Open aperture Z-scan plots at different energy densities for C 540 dye in toluene .Excitation wavelength length 590 nm

Z-scan experiments are repeated at a wavelength of 650 nm which is the edge of the absorption band. No significant variation in the RSA behavior is observed. Fig.6.4 shows the plot for the dye solution at a wavelength of 650 nm. The nonlinear effects due to high power density can result in ESA or TPA. The predominance of any of these two absorption processes depends on many factors like the lifetime of various excited states of the molecule, the rate of intersystem crossing and pulse width of the laser source used.

The values of nonlinear absorption coefficient β_{eff} for the dye solution can be extracted by fitting the experimental open-aperture Z scan data to the equation 6.16. The constant q_0 is obtained as the fit parameter and knowing the values of I_0, z_0 and L_{eff} the nonlinear absorption coefficient can be evaluated. The experiments are done at various energy densities and the nonlinear absorption coefficient β_{eff} is evaluated for the dye solution for the two wavelengths of excitation. The calculated values of β_{eff} is

given in Table.6.1.Somewhat similar values are obtained for absorption coefficients corresponding to the two excitation wavelengths 590 nm and 650 nm. The observed RSA can be attributed to resonant two photon absorption along with some ESA effects.

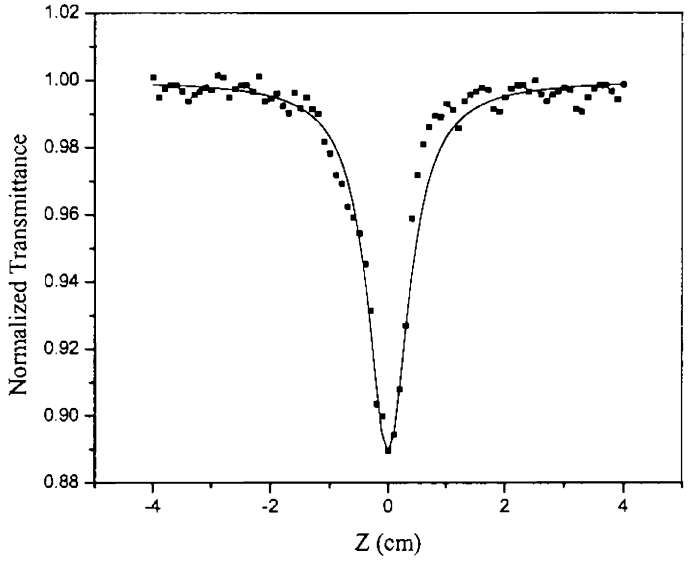

Fig.6.4 Open aperture Z-scan plots for C 540 dye in toluene . Excitation wavelength length 650 nm

Wavelength (nm)	Irradiance GW/cm^2	β_{eff} $cm\ GW^{-1}$
590	1.5	0.8
590	2.4	1.6
650	1.25	2.8

Table.6.1 Values of irradiance and β_{eff} for C 540 dye in toluene for two wavelengths.

6.8 Nonlinear absorption in Dye doped polymer films

The nonlinear absorption and Z-scan studies are carried out in dye doped polymer films as well. PMMA, polystyrene and PVC are used as the polymer matrices. The method of preparation is described in chapter 3. The concentration for the dye doped film prepared for Z-scan studies is $2x10^{-4}$ M. The thickness of the films used for the studies varied from 10 -150 microns. Since the variation of the excitation wavelength exhibited no significant change in the absorption coefficient for the dye solution, Z-scan studies are performed only at 590 nm. The Z-scan measurements are carried out at various fluence levels for the different dye doped polymer matrices. All of them exhibit the typical RSA behavior with a transmittance minimum at the focus. Fig 6.5 and 6.6 show the nonlinear absoption plots exhibited by the dye doped in PMMA and polystyrene solid matrices. For a better comparison of the nonlinearity of the dye doped polymer matrices, the nonlinear absorption coefficients are calculated by fitting the experimental data to the equation as in the case of the dye solution. The measured values of β_{eff} and irradiance I_0 for different dye doped polymer matrices are given in Table 6.2. From the table, it is clear that β_{eff} is higher for the dye doped polystyrene films compared to the other two polymer matrices.

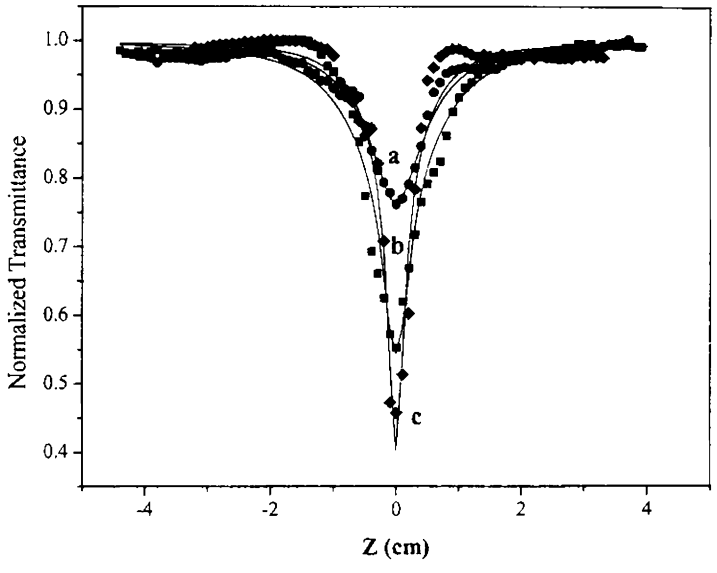

Fig.6.5 Open aperture Z scan curves for C 540 doped PMMA films at three different irradiances a)805 MW/cm^2 b)985 MW/cm^2 c)1850 MW/cm^2

Sample	**Thickness of film μ m**	**Irradiance MW/cm^2**	β_{eff} **cmMW^{-1}**
Dye doped PMMA	190	746	0.05
Dye doped Polystyrene	30	400	6.35
Dye doped PVC	14	573	2.17

Table.2 Values of irradiance and β_{eff} for different dye doped polymer matrices.

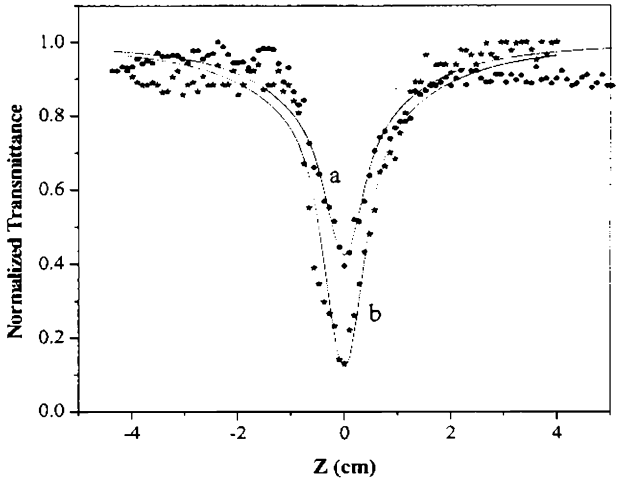

Fig.6.6 Open aperture Z scan curves for C 540 doped Polystyrene films at different irradiances a) 322MW/cm^2 b) 530 MW/cm^2

6.9 Optical limiting

Optical limiters are devices which make use of the nonlinear absorption properties of materials. They are widely used for optical sensor protection including human eyes from intense beam of laser light [20-22]. They display a decrease in transmittance with increase in intensity or fluence of light. There will be a linear transmittance upto a threshold value of incident intensity. Beyond this threshold value the optical limiters exhibit an abrupt change in transmittance and the output remains a constant in spite of increase in incident intensity. This critical value of the input intensity is termed as the threshold of the device. The optical limiting results from the absorptive nonlinearity of the material which can be due to TPA or ESA.

6.10 Optical limiting in dye doped polymer films

In order to understand the optical limiting behavior of the samples and to find the threshold value of optical limiting, one has to keep the sample in a fixed position and to measure the transmittance as a function of input fluence. The optical limiting properties of a material can also be estimated from its Z-scan plots for various input fluences. For this, the nonlinear transmission has to be plotted as a function of input fluence and such plots can be generated from the Z-scan measurements. From the value of fluence at the focus, fluence level at other sample positions can be calculated using the standard equation for Gaussian beam waist given by;

$$\omega^2(z) = \omega_0^2\left(1+\frac{z^2}{z_0^2}\right) \tag{6.17}$$

Fig.6.7 shows the nonlinear transmission for the different dye doped polymer samples. Generally it is found that the threshold value of optical limiting is not sharp for material [1]. One will be able to find an exact value for threshold from the Z-scan plot for the transmission in terms of input fluence. In Fig.6.7 the arrow indicates the approximate fluence level at which the transmission deviates from its linear behaviour which is considered as the threshold value of the optical limiter. The threshold values obtained for the polystyrene, PMMA and PVC dye doped polymer films are 0.85 Jcm^{-2}, 1.75 Jcm^{-2} and 4.37 Jcm^{-2} respectively. This shows that the polystyrene films exhibit a better optical limiting threshold compared to PMMA and PVC films.

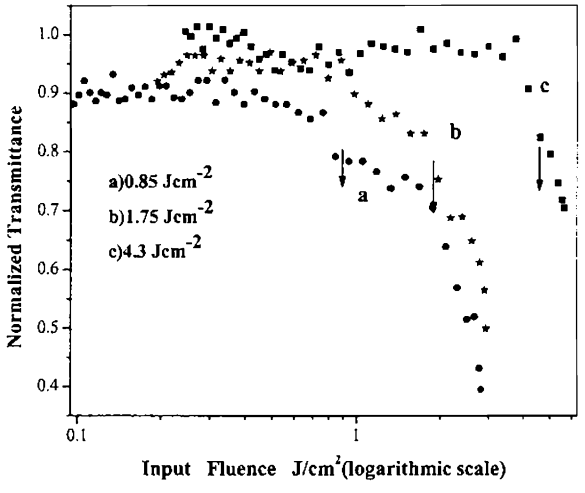

Fig.6.7 Non linear transmission in dye doped polymer films
a) polystyrene (b) PMMA c) PVC

6.11 Conclusion

The nonlinear absorption characteristics of C540 dye solution and dye doped polymer matrices are investigated using the open aperture Z-scan technique. The Z-scan plots are drawn for various pump fluences. For the dye solution, Z-scan plots are drawn for a two photon resonance wavelength as well as for a near two photon resonance wavelength and both exhibit typical reverse saturable absorption. The nonlinear absorption coefficient is determined for all the polymer matrices. The high nonlinear absorption and the observed RSA can attributed to resonant two photon absorption along with some ESA effects. Among the different polymer matrices, dye doped polystyrene matrices exhibits better nonlinearity. The optical limiting behavior of the polymer matrices is also studied.

References

1. R.L.Sutherland, *Hand book of nonlinear optics*, Marcel Dekker (1996)
2. Y.R.Shen,*The Principles of nonlinear optics*, John Wiley and sons, New York (1991)
3. E.G.Sauter, *Nonlinear optics*, John Wiley and sons Inc. New York (1996)
4. T.Kobayashi, *Nonlinear optics of organics and semiconductors*, T.Kobayashi, *Nonlinear optics*,1,Springer –Verlag,Berlin (1991)
5. R.A.Gannev, *nonlinear refraction and nonlinear absorption of various media*, J.Opt.A: pure and App.Opt , **7** (2005)717-733
6. J.S.Shirk, R.G.S.Pong ,F.J.Bartoli , A.W.Snow, *Optical limiter using a lead phthalocyanine* ,Appl.Phys.Lett. **63** (1993)1880
7. H.Ditlbacher ,J.R.Krenn, B.Lamprecht, A.Leitner ,F.R.Aussenegg, *Spectrally coded optical data storage by metal nanoparticles*,Opt.Lett, **25** (2000)563
8. A.Bhardwaj, P.O.Hedekvist, ,K.Vahala, All optical logic circuits based on polarization properties of nondegenerate four-wave mixing , J.Opt.Soc.Am.B.**18** (2001)657
9. H.Hashimoto, T.Nakashima, K.Hattori, T.Yamada , T.Mizoguchi, Y.Koyama, T.Kobayashi, Pure Appl.Chem.**71** (1999)2225
10. K.P.Unnikrishnan, *Z-scan and DFWM techniques in certain photonic materials* (Ph.D thesis),International school of Photonics,CUSAT,(2003)
11. J.D.Bhawalkar, G.S.He, P.N.Prasad, *Nonlinear multiphoton processes inorganic and polymeric materials*,Rep.Prog.Phys.**59** (1996) 1041-1070
12. B.B.Laud, *Lasers and Nonlinear optics*, Wiley Eastern Ltd.India (1993)
13. M.Sheik Bahae, A.A.Said, T.Wei, D.J.Hagan,E.W.Van Stryland ,*Sensitive measurements optical nonlinearities using a single beam* IEEE,**26** (1990)760-

780

14. W.Zang, J.Tian, Z.Liu, W.Zhou, F.Song, C.Zhang, J.Xu, *Accurate determination of nonlinear refraction and absorption by a single Z-scan method*, J.Opt.Soc.Am.B , **21**(2004)439-446

15. U.Tripathy, R.J Rajesh, P.B Bisht, A.Subrahamanyam, *Optical nonlinearity of organic dyes as studied by Z-scan and transient grating techniques*, proc,Indian Acad.Sci.(Chem.Sci) **114**(2002) 557-564

16. Q.Mohammed Ali, P.K.Palanisamy ,*Investigation of nonlinear optical properties of organic dye by Z-scan technique using He-Ne laser*,Optik,**116**(2005)515-520

17 E.W.Van Stryland , M.Sheik-Bahae, *Z.scan measurements of optical nonlinearities,*Marcel dekker.Inc.(1998) 655-692

18. N.K.M.Naga Srinivas, S.V.Rao, D.N.Rao, *Saturable and reverse saturable absorption of Rhodamine B in methanol and water* ,J.Opt.Soc.Am.B , **20** (2003)2470-2479

19. S.V.Rao, N.K.M.Naga Srinivas, D.N.Rao, *Nonlinear absorption and excited state dynamics in Rhodamine B studied using Z-scan and degenerate four wave mixing techniques,* Chem.Phys.Letts.**361** (2002) 439-445

20. G.S.He, Gen C.Xu, P.N.Prasad, B.A.Reinhardt , J.C.Bhatt, A.G.Dillard, *Two photon absorption and optical limiting properties of novel organic compounds*, Opt.Lett. **20**(1995)435-437

21. G.S.He, J.D.Bhawalkar ,C.F.Zhao, P.N.Prasad, *Optical limiting effect in a two-photon absorption dye doped solid matrix*, Appl.Phy.letts.**67** (1995) 2433-2435

Chapter 7

Conclusions and future prospects

7.1 General conclusions

Organic dyes are a class of materials with enormous potential which can be exploited in a variety of fields of science and technology. The almost unlimited number of dyes available and the ease with which the structure of organic compounds and their derivatives can be modified, make these materials still quite attractive in the area of research. Intense effort is going on to develop new organic materials and to tailor them to meet the current needs of the photonic world. The wide spectral range of their emission which covers the entire visible, near ultraviolet and near infrared makes them versatile laser sources. In addition to tunability, the unique level of high performance they provide in certain areas keep them quite promising among the variety of laser materials. Fluorescence spectroscopy is another major field where organic dyes are widely used for biological analysis, spectroscopic studies environmental analysis and diagnostics.

Nonlinear optics is an important branch of photonics with potential applications in the area of optical communication, optical data storage, optical limiting and optical switching. Among the variety of materials explored for good nonlinearity, the organic dyes have proved to be equally competitive with their promising third order nonlinearities. In the present work, photophysical, lasing and nonlinear characterization of certain laser dyes are carried out mainly focusing on Coumarin 540, a highly fluorescent dye in the green wavelength region.

For all applications of an organic dye, the photophysical, chemical and thermal characterization is of utmost importance. In order to explore the solvent environment effect on laser dyes, an exhaustive investigation is carried out in a good number of solvents. Since the polarity, refractive index and dielectric constants of the medium are decisive factors in the performance of a laser dye, investigations are carried out in polar protic, dipolar aprotic and nonpolar solvents. The different optical parameters such as the quantum yield, lifetime, Stoke's shift, relation of Stoke's shift with solvent polarity function, radiative and nonradiative decay constants are evaluated.

In one of the investigations of C 540 dye, taking the dye solution in a quartz cuvette, it is excited with 476 nm radiation after focusing by a cylindrical lens to form a stripe like excited region. This simple experimental arrangement resulted in laser emission with well resolved and equally spaced resonant modes. The resonant modes originate from the subcavities formed between the walls of the cuvette. The total emission spectral width and the number of modes exhibited by them present a correlation between the gain of the medium, the quantum yield and the refractive index of the solvent.

Solid matrices containing laser dyes are widely used to build practical tunable solid state dye lasers. Polymers are the most popular host materials with their good optical qualities, simple way of processing and low production cost. Dye doped polymers have also demonstrated high conversion efficiencies. In this context, we have compared the amplified spontaneous emission and laser emission from C 540 dye doped polymer films. Studies are carried out using the PMMA, polystyrene and PVC polymer host materials and dye doped polystyrene films exhibit comparatively high gain. We have carried out the investigation in free standing dye doped films which act as symmetric waveguides. These films exhibit significant enhancement in optical gain compared to dye doped thin films coated on substrates which act as

asymmetric waveguides. Gain studies are conducted by exciting the gain medium in a transverse direction focusing the pump beam using a cylindrical lens. At sufficiently high pump intensity and excitation length, laser emission is observed with equally spaced well resolved resonant modes. For dye doped polystyrene films laser emission is observed even from a short length of 1.25 mm at pump intensity of 760 kW/cm^2. The optical feedback due to the partial reflections from the well polished surfaces of the film generated the necessary gain for laser emission.

The highly sensitive and simple photacoustic technique is employed for the characterization of the photostability of the dye doped polymer films. The photostability of these samples are investigated under various conditions like different solvent medium, concentration of the dye, pump powers , excitation wavelengths and chopping frequencies.

Energy transfer studies in dye mixtures are carried out in different solvent environments by recording the ASE intensity under pulsed optical excitation. C 540 as donor and rhodamine 6G and rhodamone B as the acceptors are the different d-a pairs used for the investigations. Methanol, ethanol, DMF and MEK are the solvent media in which investigations are carried out. Efficient energy transfer is observed in these d-a pairs. The critical transfer distance obtained for the different d-a pairs and the good spectral overlap between the emission spectrum of donor and absorption spectrum of acceptor suggest the role of resonance energy transfer in these dye mixtures. For C 540-Rh6G d-a pairs in all the four solvents, the donor ASE gradually dies out with a corresponding enhancement in acceptor ASE intensity. In contrast, for the C 540-RhB d-a pairs in DMF and MEK, the donor ASE is gradually quenched without any transfer of ASE to the acceptor side. This dark quenching without any acceptor emission may be due the formation of some nonfluorescent complexes in the excited state of the donor. This is of great importance in biological analysis due to the absence of any background fluorescence.

T388

Organic dyes nowadays acquired a renewed demand in the photonics field with its nonlinear optical properties. They are attractive materials mainly due to their third order nonlinearities. We have carried out the nonlinear absorption characterization of the C 540 dye, both in solution and dye doped polymer films using the open aperture Z-scan technique. Typical reverse saturable absorption (RSA) behaviour is observed in both these cases. The nonlinear absorption coefficient and the irradiance level for nonlinearity are estimated. The performance of the dye doped polymer films as an optical power limiter is also studied.

7.2 Future prospects

Many of the studies performed in the present thesis work leave space for future investigations. The significant enhancement in optical gain observed in free standing dye doped films with micrometer thickness can be explored in detail. This could be of considerable application in the design of active optical integrated circuits. Among the different dye doped polymer films studied, dye doped polystyrene films exhibit comparatively high gain and better photostability. The choice of solvents and the weight percentage of polystyrene are critical parameters which have to be tailored to get the optimum conditions for the fabrication of good quality films. We have adopted free cast evaporation methods for the formation of thin films. Tape casting technique can be employed to achieve better quality films of desired thickness. Regarding the energy transfer studies, the C540-RhB d-a pairs have to be extensively studied to understand the quenching mechanism in detail. Lifetime measurements can throw more light into the different energy transfer mechanisms possible in the d-a pairs. Another area for further investigations is the nonlinear studies on the dye doped polymer films. Closed aperture Z-scan measurements can be employed to investigate the nonlinearity in refractive index.